

GEOCHEMISTRY AND PETROGENESIS OF THE ETENDEKA VOLCANIC ROCKS FROM SWA/NAMIBIA

by

A.J. ERLANK, J.S. MARSH, A.R. DUNCAN, R.McG. MILLER, C.J. HAWKESWORTH,
P.J. BETTON and D.C. REX

ABSTRACT

The volcanic rocks of the Etendeka Formation from north-west SWA/Namibia have a present-day coverage of 78,000 km² and comprise a series of interbedded basalts, latites and quartz latites, together with four varieties of intrusive dolerite. Apart from one group of dolerites (regional dolerites) which have mineralogical and geochemical similarities to the Lesotho Formation lavas from the Central area, the Etendeka volcanics differ from all other Karoo volcanics by virtue of their Cretaceous age, stratigraphy, mineralogy, geochemistry, and range in mineralogical, elemental and isotopic compositions for the basaltic rocks. Thus the most voluminous basic rocks (Tafelberg basalt type) consist of basalts and dolerites with SiO₂ = 48.9–57.8%, Mg-number = 68–28, and initial ⁸⁷Sr/⁸⁶Sr = 0.7078–0.7135.

The interbedded basalt–latite–quartz latite sequence exhibits many regular and rational compositional variations for major and trace elements, as well as incompatible inter-element and Sr- and Nd- isotopic ratios. These relationships preclude the derivation of these three rock types by any simple melting or fractional crystallization process involving a homogeneous source or parental magma. Consideration of certain critical inter-element and isotopic ratio inter-relationships also rules out any magma mixing model, whether by simple mixing, or by mixing and subsequent fractional crystallization, that might seek to derive the more evolved basaltic rocks by magma mixing of any of the less evolved basic magmas with either latite or quartz latite. Detailed assimilation–fractional crystallization (AFC) modelling, using a variety of actual and putative rock compositions, either as starting materials or as contaminants, cannot consistently explain inter-element and isotopic ratio variations in either the less evolved or more evolved basaltic rocks. The former have variable initial ⁸⁷Sr/⁸⁶Sr ratios that almost encompass the range shown by the latter and it is postulated that the evolved basic magmas have been derived by crystal fractionation from less evolved basic magmas which had a range in isotopic compositions. This is supported by quantitative major and trace element modelling across the basaltic spectrum. The majority of the parental basic magmas are considered to be derived from heterogeneously enriched lithospheric mantle, evidence for which is provided by metasomatized mantle-derived nodules contained in kimberlite. Although these basic magmas have “calc-alkaline” affinities there is no compelling evidence for the operation of subduction-related enrichment processes, which would be of Proterozoic age because of Sr- and Nd- model age considerations, in the mantle source areas of these magmas. Instead, the majority of the basic rock types are considered to be continental flood basalts with their own distinctive lithospheric mantle sources, the only exception being late-stage MORB-like intrusives (Horingbaai dolerites) which are thought to be asthenospheric melts emplaced during an advanced stage of rifting and crustal thinning.

The overall compositional relationships of the latites and quartz latites suggests that they are crustal melts, probably of Damaran rocks in view of isotopic relationships. The Etendeka basic volcanics are considered to mark the surface expression of a distinct thermal and geochemical anomaly in the sub-continental lithosphere. The interbedded nature of the basaltic and acidic volcanics indicates that asthenospheric material (Tristan da Cunha plume?) penetrated lithospheric mantle to or near the base of the continental crust in order that lithospheric mantle and crust could melt simultaneously. It is suggested that whereas the direction and alignment of Gondwana rifting and breakup was crustally controlled, the question of where rifting actually occurred was ultimately controlled by the distribution of highly enriched domains in the sub-continental lithosphere.

CONTENTS

	<i>Page</i>
I. INTRODUCTION	196
II. KAROO SEDIMENTARY SEQUENCE: STRATIGRAPHY AND STRUCTURAL RELATIONSHIPS	197
III. ETENDEKA FORMATION LAVAS AND DOLERITES: DISTRIBUTION, STRATIGRAPHY AND CLASSIFICATION	201
A. Introduction	201
B. Etendeka Formation Lavas	201
C. Intrusive Sills and Dykes	202
D. Classification of Lavas and Intrusives	202
IV. AGE RELATIONSHIPS	203
A. Previous Work	203
B. New Age Determinations	204
V. PETROGRAPHY	207
A. Tafelberg Basic Lavas	207
B. Albin Basic Lavas	207
C. Dolerites	209
D. Tafelberg Latites	211
E. Tafelberg Quartz Latites	211
VI. CORRESPONDENCE BETWEEN ROCK AND MAGMA COMPOSITIONS	211
A. Zeolite and Calcite Formation	211
B. Other Alteration Effects	212

VII. DESCRIPTIVE GEOCHEMISTRY OF ETENDEKA FORMATION	
MAGMA TYPES	213
A. Basic Magma Types	216
1. Tafelberg basalts and dolerites	216
2. Albin basalts	218
3. Horingbaai dolerites	219
4. Regional dolerites	219
B. Tafelberg Latites	220
C. Tafelberg Quartz Latites	220
VIII. PETROGENESIS—I. INTER-RELATIONSHIPS BETWEEN BASALTIC ROCKS, LATITES AND QUARTZ LATITES	220
A. Introduction	220
B. Simple Mixing and Fractional Crystallization	221
C. Combined Magma Mixing and Fractional Crystallization Processes	222
1. Isotopic constraints	223
2. Inter-element constraints	223
3. Constraints imposed by combined use of initial Sr-isotope ratios and elemental data	224
4. Other possibilities involving magma mixing	225
IX. PETROGENESIS—II. DERIVATION OF MAJOR ROCK TYPES	226
A. Tafelberg Basaltic Rocks	226
1. Derivation of evolved rocks	227
(a) Fractional crystallization	227
(b) Crustal contamination	230
2. Derivation of less evolved rocks	231
(a) Crustal contamination	231
(b) Mantle enrichment	233
B. Other Basaltic Rocks	234
C. Source Area Characteristics of Basic Magma Types	236
D. Tafelberg Latites	238
E. Tafelberg Quartz Latites	239
X. GEODYNAMIC IMPLICATIONS	239
XI. CONCLUSIONS	241
ACKNOWLEDGMENTS	242
REFERENCES	242

I. INTRODUCTION

In SWA/Namibia (hereafter referred to simply as Namibia) mafic, intermediate and felsic lavas and associated dykes and sills of Mesozoic age occur in the vicinity of Mariental (17°56'E; 24°37'S) in the area between Brandberg (14°35'E; 21°08'S) and Cape Cross (13°55'E; 21°47'S) in Damaraland, to the north-east, east and south-east of Grootfontein (18°10'E; 19°35'S) and at various localities in the coastal area between the Kunene River and latitude 21°S (Fig. 1). In the latter region is the Etendeka (from the Ovahimba meaning an area of flat-topped hills) where the largest remnant of these lavas is found outcropping continuously over an area of 15,000 km² between latitudes 19° and 21°S. Between Cape Cross and Grootfontein a broad belt of subvolcanic plutons and ring complexes built of alkaline, tholeiitic and carbonatitic rocks is associated with the volcanics. These constitute the Damaraland Province intrusive igneous suite (Martin *et al.*, 1960).

The lava outcrops are erosional remnants of once extensive flood lava fields and, in general, they follow conformably on sedimentary formations of the Karoo Sequence. On the basis of this stratigraphic relationship, the lavas and the intrusive dykes (including some spectacular dyke swarms), sills and ring complexes have traditionally been correlated with the Karoo igneous suite in the Central area in South Africa.

Subsequent age studies by McDougall (1963) and Fitch and Miller (1971, 1984) on Central area basalts and dolerites and by Siedner and Miller (1968), Gidskehaug *et al.* (1975) and Siedner and Mitchell (1976) on Namibian occurrences have shown that this general correlation is not correct. The Central area igneous suite is largely early to middle Jurassic in age, as are the dolerites from southern Namibia and the Kalkrand basalts north of Mariental. It is on this basis, as well as on compositional similarities, that these occurrences have been grouped together as constituting the Central area volcanic suite (Marsh and Eales, 1984). In contrast, the lavas of the Etendeka and

those near Cape Cross were found to be late Jurassic to early Cretaceous in age and therefore represent a distinctly younger manifestation of Karoo igneous activity. Siedner and Miller (1968) therefore propose the term "Kaoko" lavas to distinguish them from the older Karoo lavas of the Central area. These lavas are now grouped into an Etendeka Formation (SACS, 1980) and the term "Kaoko" has fallen into disuse. Associated dolerites were found to give a spectrum of ages from early Jurassic to early Cretaceous. However, rather than indicating continuous activity, Siedner and Mitchell (1976) suggested that the age data were consistent with episodic activity over a 60 m.y. period. Available data for the Damaraland complexes indicates that they are broadly contemporaneous with the late Jurassic-early Cretaceous regional volcanism.

Although questions of contemporaneity have only been resolved in the last 15 years, the differences in compositional character between the Etendeka and Central area lavas have been known for far longer. In the earliest comprehensive account of the Etendeka suite, Reuning (1929) described the sequence as consisting of basic melaphyres, glassy intermediate rocks and 600 m of orthoclase porphyries. He listed chemical analyses indicating that the latter contain 65–68% SiO₂ whereas the basic and intermediate lavas have between 46 and 56% SiO₂. Subsequent descriptions of the Etendeka sequence have mentioned "600 m of phyrlic andesite" and that the "uppermost extrusives are rhyolitic" (Korn and Martin, 1954), or "amygdaloidal basalt and andesites (150–220 metres) followed by andesites with intercalated more felsic layers and a capping of rhyolite composition (600 metres)" (Martin *et al.*, 1960). On the other hand Siedner and Miller (1968) report "predominantly basalts with major quantities of intermediate and acidic lavas" in the suite.

Despite the inconsistencies in these descriptions it is clear that significant proportions of evolved rock types in the Etendeka sequences have been known since the earliest investigations. This contrasts strongly with the overwhelmingly monotonous basaltic character of the

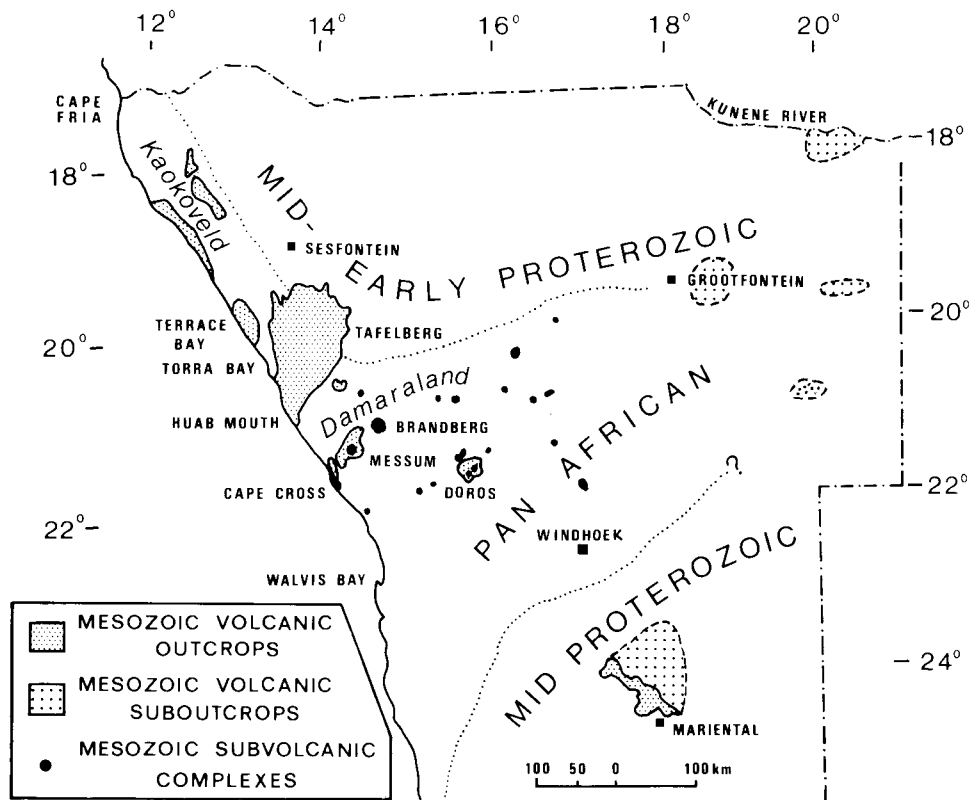


Figure 1

Generalized map of Namibia showing distribution of Karoo lavas and sub-volcanic complexes, together with basement age/tectonic provinces. The southernmost lavas (Kalkrand Formation) near Mariental are Jurassic in age, while the other lavas to the north (Etendeka Formation) are of Cretaceous age.

preserved lava sequence in the Central area. In this respect the Etendeka suite is more akin to the Lebombo volcanics which comprise substantial proportions of acid material (see Cleverly *et al.*, 1984). More detailed comparisons of these two sites can be found in the account of Duncan *et al.* (1984).

The outcrop area of Etendeka volcanics close to the coastline of Namibia has invited comparisons with the extensive Serra Geral volcanics in the Paraná basin of South America. Such comparisons were used by early proponents of the Continental Drift hypothesis (Du Toit, 1937; Martin, 1961) to demonstrate that the eastern and western seabords of South America and Africa respectively, must once have been juxtaposed. The general contemporaneity of these volcanic suites has only been well established since the age studies mentioned above and those in South America reported by Amaral *et al.* (1966, 1967) and Melfi (1967) were published. Likewise, the overall petrological and geochemical similarity of the Etendeka and Paraná (Serra Geral) suites has only become apparent with this study on the Namibian rocks and those of Ruegg (1976) on the Paraná volcanics.

The general acceptance of the sea floor spreading hypothesis has allowed these volcanics to be viewed in a new light. No longer is their significance confined to demonstrating the juxtaposition of South America and Africa. Instead, with independent evidence from the sea floor on the possible age of the South America–Africa rift (summarized by Duncan *et al.*, 1984) the Etendeka suite can be evaluated in the context of a developing continental rift that evolved into an ocean.

This study presents major, trace element and Ar-, Sr-, Nd- and Pb-isotopic data for a variety of mafic and felsic volcanics belonging to the Etendeka Formation. We emphasize the integrated nature of this investigation but note that while this is the first comprehensive account of

these volcanic rocks, additional field and laboratory studies are required to understand more fully this complicated and interesting area.

II. KAROO SEDIMENTARY SEQUENCE: STRATIGRAPHY AND STRUCTURAL RELATIONSHIPS

The sedimentary sequence correlated with the Karoo Sequence occurs in scattered outcrops throughout the Kaokoveld and north-west Damaraland. These Karoo sediments have been described by Reuning and Martin (1957), Frets (1969) and Hodgson and Botha (1975). In the vicinity of the Etendeka representatives of the Dwyka (oldest), Prince Albert, Gai-As and Etjo (youngest) Formations (SACS, 1980) are present. However, the overall succession in many localities is incomplete with thicknesses and actual stratigraphic sequences having been profoundly influenced by considerable pre-Karoo topography, particularly pre-Dwyka glacial valleys (Martin, 1975) and, in the coastal region, by the occurrence of syn-sedimentary faulting.

The Karoo sedimentary formations and the overlying lavas are underlain by folded and metamorphosed basement rocks of varying ages (Fig. 1). In the coastal region the basement rocks are schists belonging to the Damara Sequence of Pan-African age. These schists are intruded by syn- and post-tectonic granites and granodiorites. To the east of the Etendeka lies the pre-Damara Huab massif comprising paragneisses and intrusive granites with ages in the range 1.9–1.7 b.y., while to the north lies the early Proterozoic Epupa crustal segment overlain in places by low-grade metamorphic rocks of the Damara Sequence.

Varicoloured shales of the Prince Albert Formation usually form the base of the Karoo succession around the southern margin of the Etendeka, but in places they may be

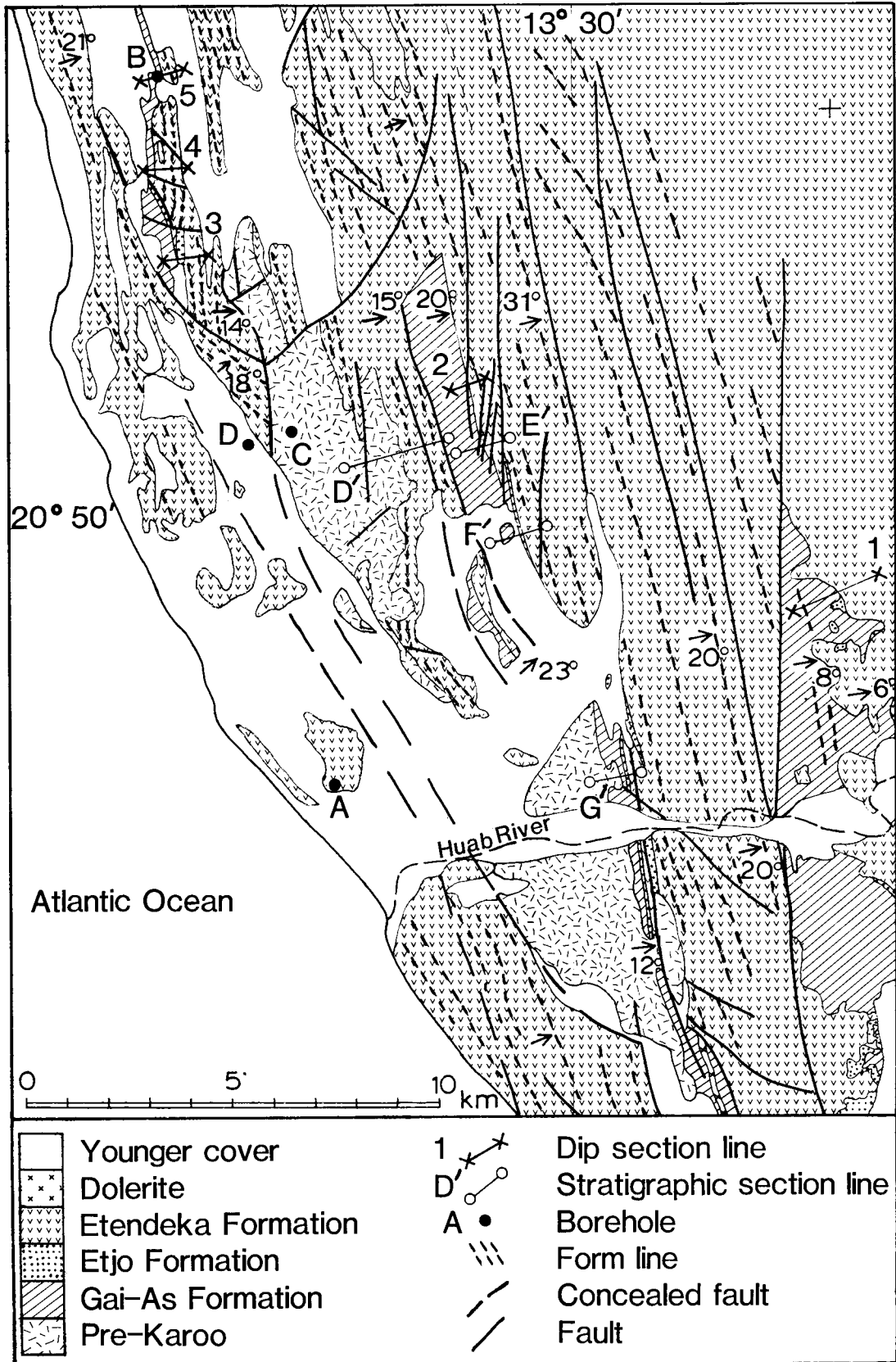


Figure 2
 Geological map of the area around the mouth of the Huab River. Location of area shown on Fig. 5. After Miller (1973; unpubl. data).

underlain by small patches of Dwyka tillite up to 7 m thick. The Prince Albert Formation is tentatively correlated with the lower part of the Ecca Group in the Central Karoo basin. The overlying red beds of the Gai-As Formation and the aeolian sandstones of the Etjo Formation are possible equivalents of the Molteno and Clarens Formations of the Central area. The Etjo sandstones are interbedded with the lowermost lava flows of the volcanic sequence.

Generally, the Prince Albert and Gai-As Formations thicken from a cumulative thickness of about 130 m south-east of the Etendeka to about 340 m in the west at the mouth of the Huab River. The Etjo Formation has a maximum thickness of about 100 m near Doros (Fig. 1). All three formations pinch out to the north and south; the Etjo sandstones overstep the lower formations around the

eastern edge of the Etendeka and are in turn overstepped by the lavas. Although thin lenses of sandstone a few metres thick may intervene between the volcanics and the basement in places, the lava sequence north of the Tafelberg beacon mostly lies directly on the basement.

Further north towards the Kunene River the lavas are usually underlain by representatives of all the Karoo sedimentary formations. The Dwyka glaciogenic sediments are particularly well developed occurring in many areas where no volcanics are present and show local thickening in a number of pre-Dwyka valleys.

In the coastal region there is considerable variation in the stratigraphic sequence and in the thicknesses of the different formations due to the occurrence of syn-sedimentary coast-parallel faulting. This has been revealed by detailed measurements of 2 borehole cores and several stratigraphic sections measured in the vicinity of the Huab River mouth. A similar development may be inferred for much of the coastal area as coast-parallel faults are common within 30 km of the coast line although detailed mapping of this area is lacking.

Relationships at the Huab mouth are illustrated in Figs. 2 and 3 which show the location and character of a number of measured sections. It appears that the full stratigraphic succession is preserved in down-faulted blocks, but in an adjacent horst structure certain stratigraphic units may be missing. The marked variations in the thicknesses of some formations over short distances and the absence of some or all members of the sedimentary succession suggests that faulting occurred periodically both during and after sedimentation. There are no significant differences in the dips of different formations in the fault blocks and this indicates that no rotation of fault blocks occurred during the syn-sedimentary movements. The observed dips of 15–30° to the east in the lavas and sediments are probably a result of post-extrusion rejuvenation of the faults. In the north-western Kaokoveld the Karoo sediments and lavas are frequently down-faulted to the west against the basement.

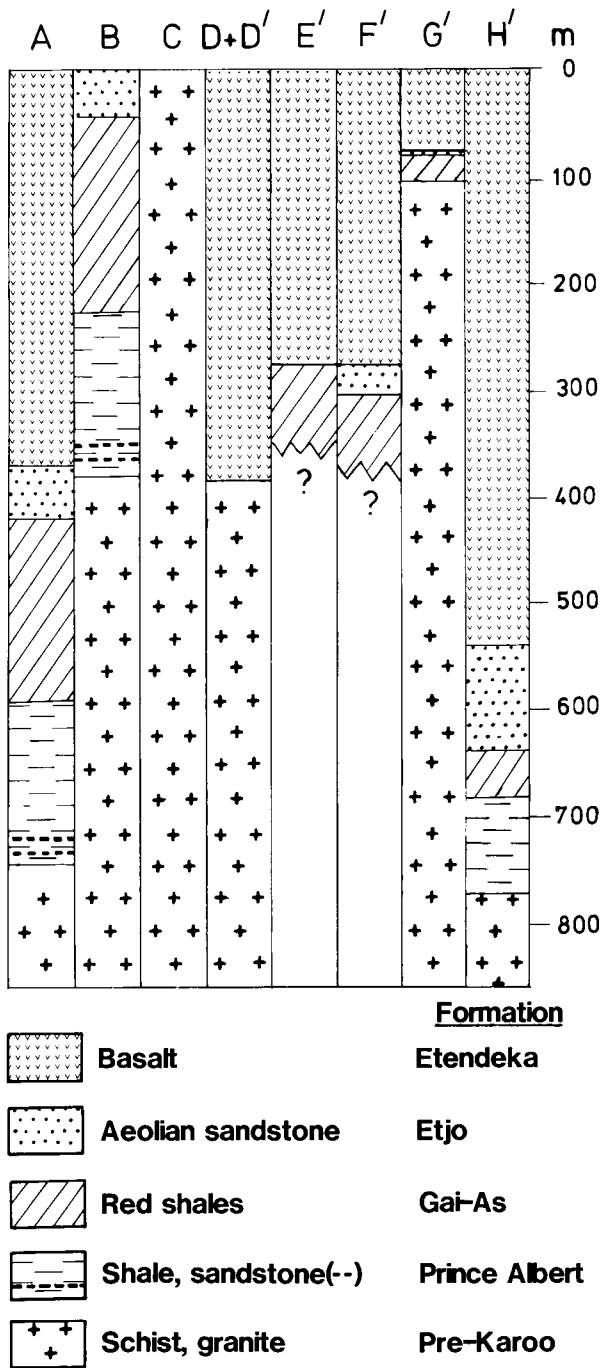


Figure 3

Stratigraphic sections of the Karoo Sequence in the Huab River region. Location of sections A–D (boreholes) and D'–G' (surface sections) shown on Fig. 2. Location of surface section H' shown on Fig. 5.

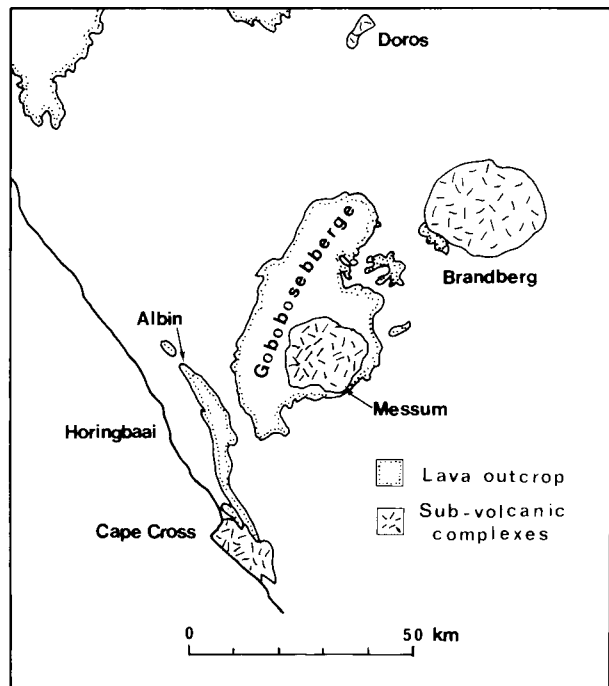


Figure 4

Simplified map of area near Cape Cross showing type locality of the Albin plagioclase-phyric basaltic lavas and intrusive Horingbaai dolerite dykes and sills, together with the Messum Igneous Complex, dated at 132 ± 2.2 m.y., which is intrusive into the Gobobosebberge.

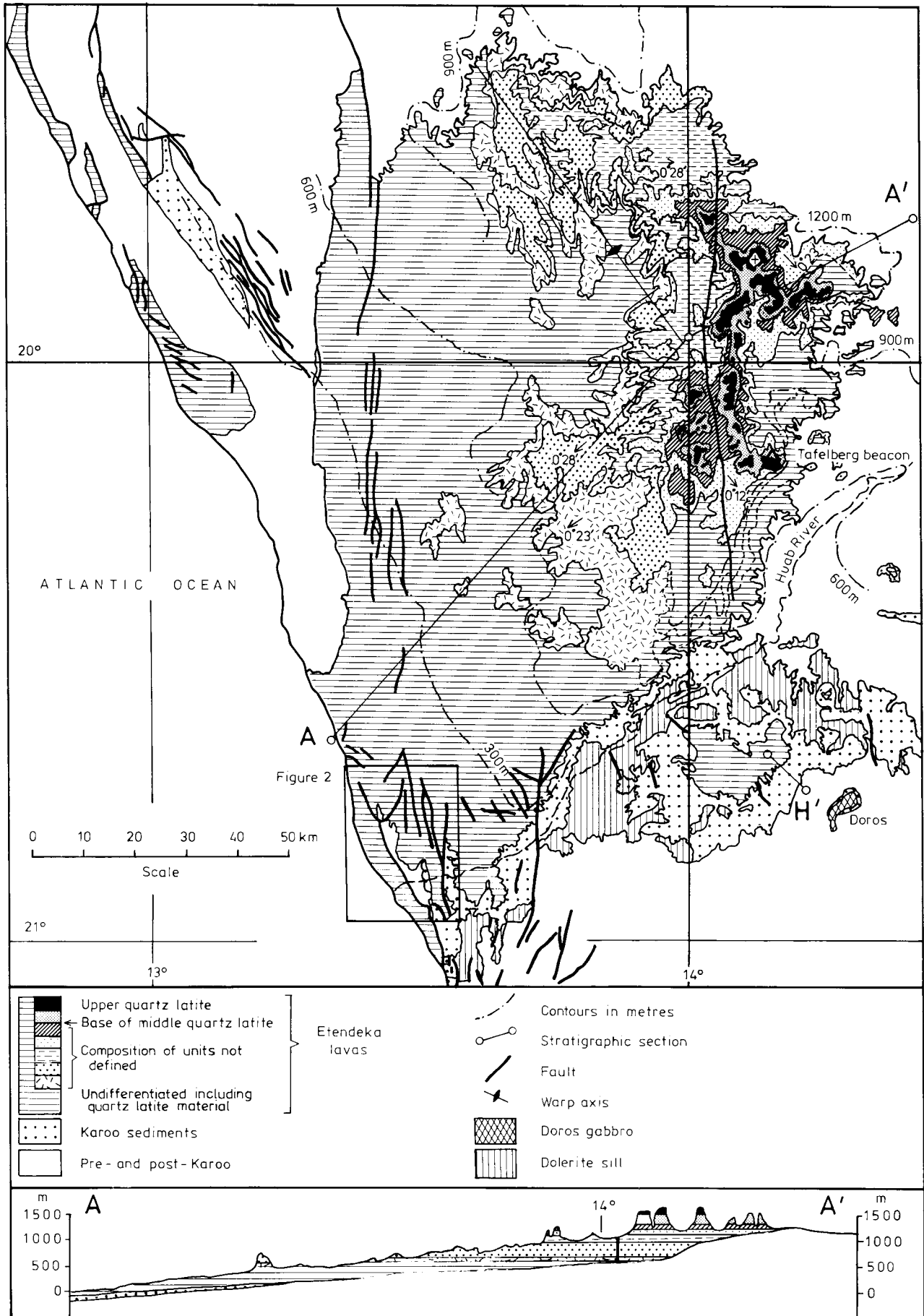


Figure 5

Geological map of the Karoo Sequence in the Huab River-Doros-Tafelberg area. Distribution of prominent lava units inferred from field studies and photogeological interpretation (Miller, unpubl. data). Note that dips are given in minutes.

III. ETENDEKA FORMATION LAVAS AND DOLERITES: DISTRIBUTION, STRATIGRAPHY AND CLASSIFICATION

A. Introduction

The dolerite and lava samples constituting the igneous suite which is the basis of this investigation come from various collections made over a number of years. The most comprehensive sampling of the volcanic sequence has been carried out at Tafelberg (14°09'E; 20°10'S) on the eastern edge of the Etendeka where the maximum preserved thickness of lavas (about 900 m) is found. Additional samples from the Etendeka come from widely separated localities—Terrace Bay (13°03'E; 20°00'S), Torra Bay (13°10'E; 20°13'S), the northernmost edge of the lava field to the south of Sesfontein (13°37'E; 19°07'S), the coastal area north of the Huab River mouth and from the scattered outliers between Tafelberg and Khorixas (14°58'E; 20°23'S)—see Fig. 1. A second stratigraphic suite was collected from the lava outcrops 35 km north of Cape Cross, in the vicinity of the trigonometrical beacon "Albin". These lavas are outliers of the Gobobosebberge lava field surrounding the Messum Complex, and have been supplemented by a suite of samples from the Gobobosebberge (Fig. 4). No samples have been obtained from outcrops in the north-western Kaokoveld nor from the suboutcrops north-east of Grootfontein. Intrusive dolerites have been sampled from widespread localities between 20° and 23°S and between the coast and longitude 15°30'E. Details of sample localities may be found in Microfiche Card 1 attached to this volume.

B. Etendeka Formation Lavas

The remnants of Etendeka Formation lavas are scattered over an area of 78,000 km² and Reuning and Martin (1957) have argued that the original thickness must once have exceeded 2 km. At present the maximum preserved thickness of about 900 m appears to be at Tafelberg. In the Gobobosebberge Korn and Martin (1954) report a maximum thickness of about 350 m. The lavas have a horizontal attitude over much of their outcrop area but in the strongly faulted coastal belt they exhibit variable shallow dips to the east. In the vicinity of the Huab River and the Doros Complex there is evidence of slight intra-lava warping and tilting. Flows in the lower part of the sequence dip at very shallow angles (~0.5°) to the south and east whereas the uppermost flows are horizontal.

Where underlain by Karoo sedimentary strata the lavas follow on the latter with apparent conformity. In many places the lowermost flows are interbedded with Etjo sandstones. Stratigraphically the lowermost lavas in the succession crop out in the coastal region, possibly near the mouth of the Huab River, and these are progressively overstepped by flows higher in the sequence as one moves north-east (Fig. 5). As a unit the Etendeka Formation oversteps the underlying sedimentary formations, and over large areas around the eastern and northern edges of the Etendeka the lavas lie directly on the basement.

Thus at Tafelberg (Fig. 5) the 900 m thick sequence does not include the lowermost lavas and an unknown thickness of the upper lavas has been lost to erosion. The stratigraphic succession comprises basalts and evolved basalts interbedded with two thick units of quartz latite and one thinner unit of latite (Fig. 6). The thickness proportions of the different lithological types in this section are: basalt-to-intermediate lavas—70%; quartz latite—25%; latite—5%. The basalts and evolved basalts occur in thick flows and are fine- to medium-grained aphyric rocks with an intergranular texture. We propose to call these lavas the *Tafelberg basalt type*. This type is overwhelmingly dominant in all the exposed lava remnants we have examined. We shall also likewise refer to the other two rock units as the *Tafelberg latites* and *Tafelberg quartz latites* (see subsequent section for classification used).

To date the latites have been encountered in the Tafelberg section only, where their outcrop forms a prominent scarp which can be observed to extend for several kilometres to the south and north. However, no attempt has been made to map out the latites and their true extent must await the results of a detailed mapping programme. Quartz latites cap many of the high table-topped mountains between Tafelberg and the coast (Fig. 5). South of Torra Bay a thick sequence of easterly dipping quartz latite flows occurs in a linear belt extending for

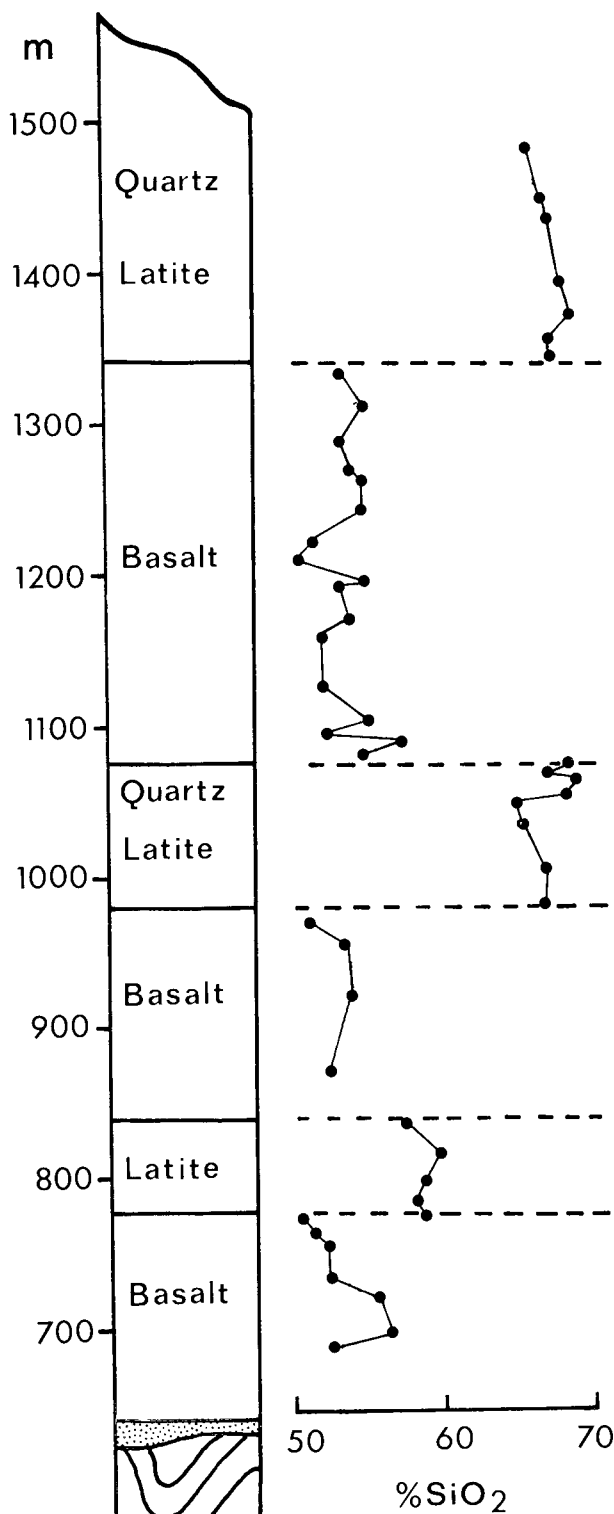


Figure 6

Stratigraphic section of the Etendeka lavas at Tafelberg (Fig. 5) together with the distribution of SiO₂ content with height in the sequence.

70 km. Poor exposures and the possible presence of coast-parallel faulting has not allowed us to correlate this sequence with either of the two units exposed at Tafelberg. As with the latites, the true distribution and stratigraphic relationships of the quartz latites await the results of detailed mapping currently in progress. Our current investigation suggests that they are, at present erosion levels, mainly confined to the Etendeka and the outliers north-west of Doros. However, reconnaissance work has shown the presence of a thick quartz latite unit interbedded with basalts south-east of the Albin beacon and of thin quartz latite units in the Gobobosebberge just north-west of the Messum Complex. A single sample of quartz latite has also been obtained from the lava xenoliths at the top of the Brandberg Complex. Also, although we have no evidence of quartz latites occurring in the strip-like outliers between the Etendeka and the Kunene River, a single sample of quartz latite has been obtained from near the Kunene at Cape Fria. These latter samples have not been analysed in the present study.

At the base of the volcanic succession nearly everywhere in the coastal region a sequence of thin flows of plagioclase-phyric basalts occurs overlying Karoo sediments. These basalts have their thickest development (~200 m) in the vicinity of the trigonometrical beacon "Albin" on the coastal hills north-east of Cape Cross as well as on the western edge of the Gobobosebberge. These plagioclase-phyric basalts are texturally distinct from the Tafelberg type and are hereafter referred to as the *Albin basalt type*. The Albin basalts may be interbedded with Etjo sandstones as can be seen at several places north of the Huab mouth and at Terrace Bay. They are followed conformably by the Tafelberg basalts with some interfingering of the two types in some areas. The full extent of the Albin basalts to the north and east is at present unknown but they are minor in volume compared to the Tafelberg type.

Throughout the Etendeka and in the Gobobosebberge each unit of the different magma types comprises a number of flows. Flows of basic lavas are generally thick, frequently in excess of 5 m. Amygdaloidal flow tops are ubiquitous. The laterally persistent sheet-like nature of the quartz latite units throughout much of the Etendeka (Fig. 5) suggests they are ignimbrites. Final conclusions regarding the volcanological character of these sheets must await completion of a detailed field and petrographic study that has recently commenced. Preliminary results from this study do, however, indicate that the quartz latite sheets have internal features similar to those displayed by Karoo rhyolites of the Lebombo (Bristow and Cleverly, 1979).

C. Intrusive Sills and Dykes

Intrusive sheets, sills and dykes, overwhelmingly basaltic in composition, are widespread throughout Damaraland and the Kaokoveld. Minor quantities of lamprophyre are also encountered and appear to be related to the alkaline phase of the subvolcanic complexes. The dolerites intrude basement rocks, Karoo sedimentary strata and the overlying lavas. Dense swarms occur locally between the Huab River and Walvis Bay (Fig. 7) and part of one of these swarms has been described by Botha and Hodgson (1976). No intrusives of latite or quartz latite have been encountered.

The comparison of data for the intrusives with that of the lavas is complicated by the fact that the intrusives seem to cover a span of ages (Siedner and Mitchell, 1976; Table II) and unambiguous ages are available only for a few of our suite of intrusive samples. Moreover, a wide variety of textural types exist and we have, in general, found no consistent relationship between texture, chemical composition and age.

In the sections that follow we discuss the data of only some of our intrusive samples, namely those that definitely

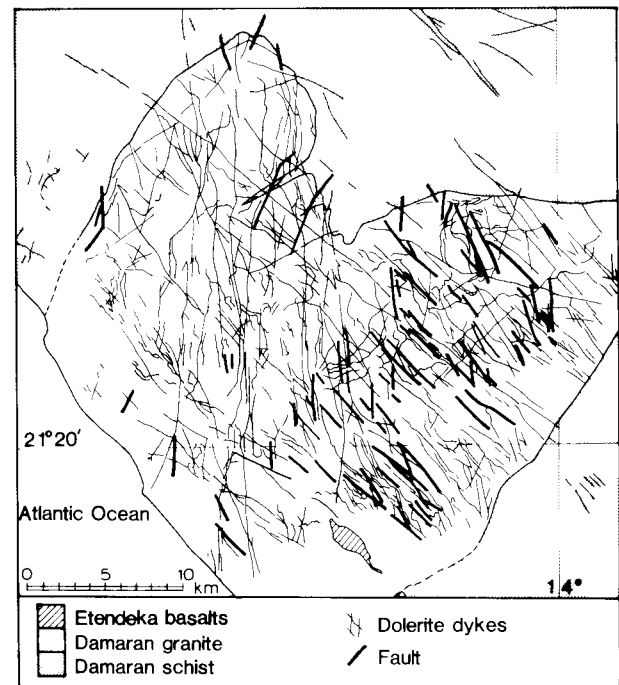


Figure 7

Distribution of dolerite dykes and faults in pre-Karoo Damaran rocks south-east of the mouth of the Ugab River (Miller, unpubl. data).

intrude Karoo sedimentary strata or the overlying lavas. Amongst these we recognize several groups. Firstly, there are dykes and sills cutting Tafelberg-type lavas. Some of these (KLS16, 20, 152, 155, 156) cannot be distinguished texturally or chemically from these lavas. Others have ophitic textures (KLS38, 48, 100, 186) and although they differ slightly in their chemistry from the Tafelberg lavas are believed to be of the same magma type. Both the above types are referred to as *Tafelberg intrusives*. Secondly, there are a group of dykes and sills found only in the coastal region and which are texturally very similar to the Albin-type basic lavas. These are provisionally named as the *Albin intrusives* although none have been analysed to date. Thirdly, there are a group of narrow (usually <1 m in thickness) fine-grained basaltic dykes and sills which intrude Albin-type lavas in the type section (Fig. 4). They have a distinctive "depleted" chemical composition and we propose to refer to them as the *Horingbaai intrusives*. Finally, there are two sills intruding Prince Albert Formation sedimentary strata (KLS43 and KLS44) which have ophitic textures and ambiguous ages (see below). They may be representatives of early Jurassic intrusive activity since their chemistry is similar to that of the widespread Lesotho Formation basalts and dolerites of the Central area (Marsh and Eales, 1984). For want of a better name we shall call them *regional intrusives*, although in many cases we shall simply refer to them by sample number. No other representatives of this type appear to cut the lavas, i.e. those intrusives which have ophitic textures and which cut the lavas belong to the first group mentioned above.

There are also a great many dolerites which intrude pre-Karoo rocks (Fig. 7) which could be classified as regional dolerites. However, in view of uncertainty with regard to their ages (Section IV) and since we have not studied these rocks in any detail, they are not discussed in this study, except with respect to their ages. Their geodynamic significance should not, however, be ignored.

D. Classification of Lavas and Intrusives

Table I presents averages or analyses of individual rocks which indicate ranges for the four lava types, together with

TABLE I
Average and Individual Analyses for Etendeka Formation Volcanic Rocks

%	Tafelberg Basic Rocks			Albin Basic Lavas		Horingbaai Dolerites		Regional Dolerite	Tafelberg		
	1	2	3	4	5	6	7		Latite	Quartz Latite	High-K Dacite
SiO ₂	49.81	51.82	57.81	51.21	55.41	47.13	46.53	49.01	59.23	68.00	68.62
TiO ₂	1.13	1.00	1.81	1.12	1.22	1.26	1.64	0.99	2.29	0.95	0.91
Al ₂ O ₃	15.84	14.83	12.66	16.19	14.88	15.28	15.21	16.41	13.87	12.89	13.30
Fe ₂ O ₃	12.15	11.82	13.94	10.34	11.24	12.61	14.16	10.42	11.21	6.61	6.14
MnO	0.17	0.18	0.20	0.15	0.17	0.19	0.21	0.15	0.13	0.10	0.10
MgO	7.23	6.78	2.30	7.29	4.64	8.68	7.00	8.89	1.70	1.26	1.25
CaO	10.58	10.50	6.07	11.28	8.98	12.68	11.89	11.45	4.23	2.74	3.54
Na ₂ O	2.17	2.11	2.26	1.55	1.83	1.92	2.63	2.13	2.48	2.69	3.28
K ₂ O	0.81	0.83	2.69	0.68	1.44	0.13	0.58	0.45	4.42	4.46	2.57
P ₂ O ₅	0.11	0.12	0.26	0.19	0.19	0.11	0.15	0.10	0.44	0.29	0.28
ppm											
Rb	20	19	96	16	43	2.3	23	10	154	175	177
Ba	188	217	496	238	338	50	228	130	100	627	634
Sr	244	216	188	274	244	196	362	278	215	131	194
Zr	102	114	238	122	188	68	100	83	457	279	292
Nb	4.8	7.5	16	12	12	3.8	13	4.3	26	22	25
Cr	104	73	9.4	154	40	232	74	226	16	10	7.5
V	226	264	372	231	232	342	338	269	62	53	50
Sc	30	42	37	35	37	36	30		20	20	19
Ni	49	63	5.1	129	65	167	107	180	6.1	4.5	1.8
Co	55	55	43	50	48	61	58	67	24	13	11
Zn	98	89	104	82	78	65	77	71	147	78	83
Cu	28	98	71	70	83	173	197	80	21	42	24
La	11	14	33	14	29	5.2	15	10	73	47	48
Ce	26	32	73	39	64	14.2	38	25	149	93	100
Nd	17	19	39	21	31	10.1	21	15	74	46	47
Y	25	24	39	20	28	20	23	20	57	37	37
Mg#	57.7	56.8	27.5	61.8	48.7	61.2	53.1	66.2	25.8	30.7	31.9

All data from Microfiche Card 2, normalized to 100% on a volatile-free basis. Total Fe as Fe₂O₃. Mg# is the Mg-number, or atomic ratio of Mg/(Mg + Fe²⁺) based on a whole rock ratio of FeO/(FeO + Fe₂O₃) of 0.85. Number of samples used for individual element averages (columns 9, 10, 11), together with other averages, may be found in Duncan *et al.* (1984). Column numbers refer to following samples or averages:

- | | | | |
|------------------------------|----------------------------|-----------------------------|----------------------------|
| 1. KLS100, olivine dolerite. | 4. KLS134, basalt. | 7. KLS157, olivine basalt. | 10. Average quartz latite. |
| 2. KLS24, basalt. | 5. KLS144, evolved basalt. | 8. KLS43, olivine dolerite. | 11. Average high-K dacite. |
| 3. KLS42, evolved basalt. | 6. KLS145, olivine basalt. | 9. Average latite. | |

analyses of dolerite intrusives, found in the Etendeka Formation. In addition Fig. 8 illustrates the K₂O–SiO₂ compositions of the *lavas* in relation to two commonly used classification schemes for calc-alkaline volcanics. The Tafelberg basic lavas exhibit a continuum in chemical composition from 52 to 58% SiO₂. The silica-poor members of this suite are undoubtedly basalts and in view of the disposition of the composition points for the more silica-rich specimens in Fig. 8 one might be tempted to refer to them as “basaltic andesites” or “andesites”. We prefer not to use separate names like these for two reasons: firstly, we wish to avoid the tectonic or petrological implications of using the name andesite; and secondly, we want to emphasize the continuous nature of the chemical, petrographic and mineralogical features of the suite. We therefore propose to refer to this suite as consisting of “basic lavas” and in a general way to refer to the low- and high-SiO₂ subsets in the suite as *basalts* and *evolved basalts* respectively. Similarly comments can be made for the Albin basic lavas, although they do not show as wide a range of composition as the Tafelberg lavas.

The *latites* are mineralogically unlike rocks usually called latite. However, we note from Johannsen (1937) that the term “latite” was originally defined in terms of chemical composition and it is in this sense that the name is applied here. Fig. 8 illustrates that the Tafelberg rocks plot in the appropriate field in both classification schemes and close to the average composition of three latites listed in Iddings (1913). The Tafelberg rocks with highest SiO₂ contents exhibit a wide range in K₂O content which for most

specimens is beyond the range considered typical of dacites, but note that there are substantial differences in the dacite field boundaries between the classifications of Peccerillo and Taylor (1976) and MacKenzie and Chappell (1972).

Again we wish to avoid using the term dacite and propose the name *quartz latite* for all these rocks with the exception of three samples with <3% K₂O which, for want of a better name, are referred to as *high-K dacites*. This distinction has been made in our sample data-base (Microfiche Card 1) but in the ensuing discussions we shall generally refer to both of these groups of rocks simply as quartz latites. Note that in the Tafelberg region the high-K dacites are confined to the lower quartz latite unit.

The intrusive rocks all have compositions within the range for the basic lavas with several of the olivine-bearing varieties extending to more SiO₂-poor compositions (not shown in Fig. 8). We propose to use the term *dolerite* for all these rocks.

IV. AGE RELATIONSHIPS

A. Previous Work

The eruptive age of the lavas is important in understanding the relationship between volcanism and rifting and a considerable number of ages have been published or are available from this investigation on the rocks in question.

Siedner and Miller (1968) reported a range of 114–132 m.y. for four whole rock basalt samples from the Etendeka Formation—two specimens from near the top and bottom of the sequence at Tafelberg, one from near

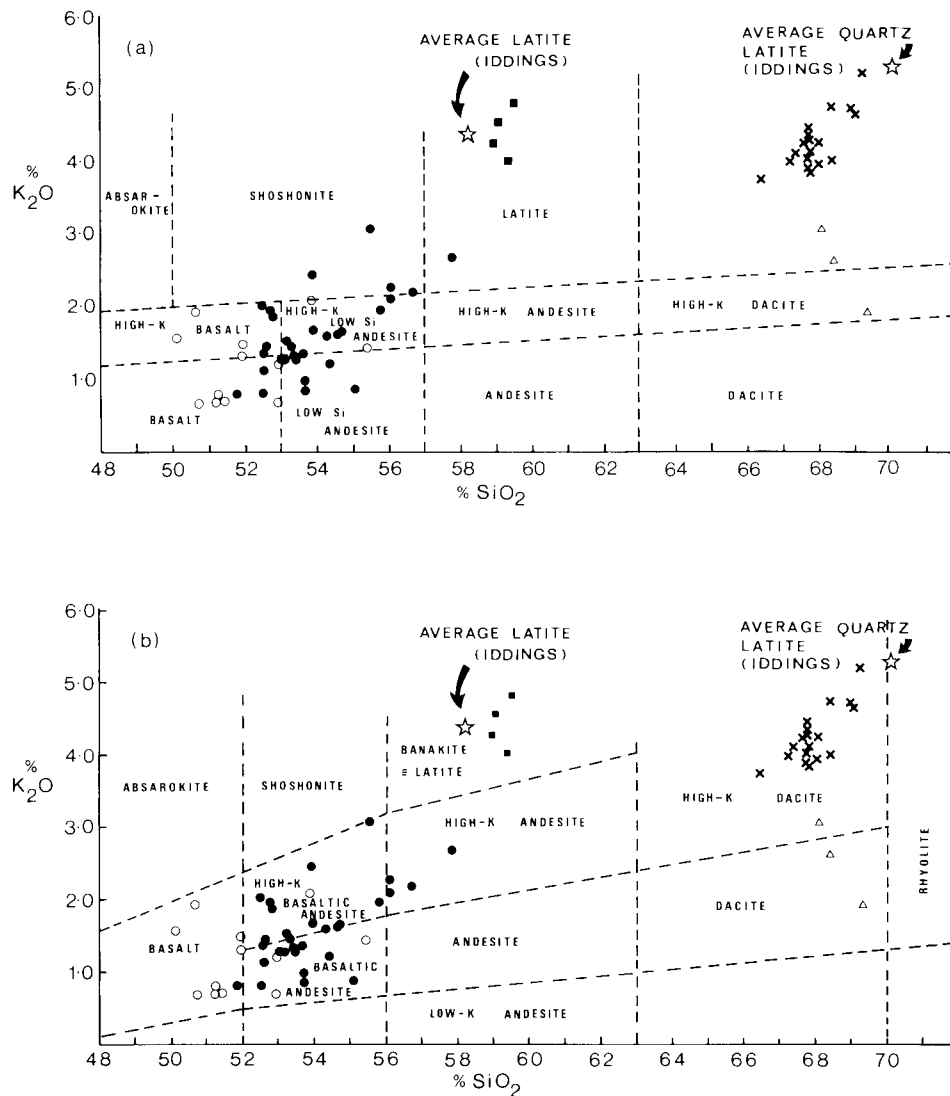


Figure 8

K_2O - SiO_2 variations and classification schemes used for Etendeka lavas (dolerites not shown). Closed circles, Tafelberg basaltic rocks; open circles, Albin basaltic rocks. (a) After Mackenzie and Chappell (1972); (b) after Peccerillo and Taylor (1976). Data plotted are recalculated to 100% on a volatile-free basis.

Cape Cross and one from the Gobobosebberge near the Messum Complex. Nine samples of regional intrusives cutting the basement yielded ages in the range 115–196 m.y. In a separate study Gidskehaug *et al.* (1975) found a range of 108–124 m.y. for four lava samples from near Tafelberg, one sample with very high K_2O being a quartz latite. They also obtained an age of 93 ± 3 m.y. for a sill cutting the lava pile. Subsequently, Siedner and Mitchell (1976) reinterpreted these conventional K-Ar ages in terms of $^{40}Ar/^{36}Ar$ - $^{40}K/^{36}Ar$ isochrons and found that the eight lava samples and two of the regional intrusives defined a well constrained isochron age of 121 ± 2 m.y. Five of the remaining regional intrusives together with specimens from the Doros Complex (Fig. 4) and two previously unreported dolerites gave an isochron age of 134 ± 1 m.y. The other two regional intrusives together with dolerites from southern Namibia which are correlated with the Central Karoo Lesotho-type dolerites yielded an isochron age of 184 ± 4 m.y. The sill cutting the Tafelberg lavas, sample AG13-2 (Gidskehaug *et al.*, 1975), was not included in the isochron treatment. Finally in the appendix to their paper, Siedner and Miller (1968) reported that three regional dolerites from widely separated localities yielded Palaeozoic ages in the range 303–468 m.y. and it was suggested that this could have resulted through crustal contamination.

B. New Age Determinations

In view of what is reported above it appeared desirable to document more precisely the time span involved in the Karoo volcanicity of the Etendeka region, and several approaches have been adopted to achieve this.

New conventional K-Ar whole rock data for 17 samples are presented in Table II. For these samples K was determined in triplicate using a Corning-Eel 450 Li standard flame photometer. Argon analyses were performed as described in Briden *et al.* (1979). Taken together, the data for the Tafelberg basalts and quartz latites, and the dolerites intruding these lavas correspond to the ages obtained in the earlier studies, although one sample (KLS197) has a distinctly higher age than the 121 m.y. age adopted by Siedner and Mitchell (1976) for these lavas. Of these samples only one is very fresh (KLS51), yet it has the lowest age, probably because of its glassy nature which has resulted in argon loss. The Albin basalts, which are interbedded with and underlie the Tafelberg basalts north of the Huab River mouth have anomalously high conventional K-Ar ages (307–377 m.y.) which conflict with their stratigraphic relationships since they overlie and are frequently interbedded with Jurassic Etjo sandstones. Similar anomalously high K-Ar ages (271–360 m.y.) are also found for the Horingbaai dolerites

TABLE II
K-Ar Age Determinations on Etendeka Volcanics

Sample No.	Rock Type	% K	Vol. ⁴⁰ Ar radiogenic scc/g × 10 ⁻⁵	% ⁴⁰ Ar radio- genic	Age m.y.
Tafelberg lavas					
KLS22	basalt	0.725	0.3193	68.8	110 ± 4
KLS197	basalt	1.21	0.7301	70.8	148 ± 5
			0.7265	65.9	
KLS51	qtz. latite	2.20	0.7682	78.2	88 ± 3
KLS102	qtz. latite	3.36	1.5103	89.6	112 ± 4
Albin lavas					
KLS112	basalt	0.898	1.4628	83.1	377 ± 15
KLS129	basalt	0.582	0.8121	80.4	327 ± 13
KLS196	basalt	1.04	1.3619	76.0	307 ± 12
			1.3387	76.4	
Horingbaai dolerites (intrude Albin lavas)					
KLS122	dolerite	0.174	0.2693	68.0	360 ± 14
KLS126	dolerite	0.289	0.3608	72.1	296 ± 12
KLS145	dolerite	0.117	0.1327	63.4	271 ± 11
Dolerites intrusive into Tafelberg lavas					
KLS48	dolerite	0.701	0.3591	56.2	127 ± 5
KLS152	dolerite	2.15	1.0646	77.2	123 ± 5
Regional dolerites					
KLS44	dolerite*	0.420	0.4867	64.3	276 ± 11
KLS151	dolerite†	0.666	0.3735	69.3	139 ± 5
KLS159	dolerite†	0.447	0.2914	55.3	160 ± 6
KLS161	dolerite†	1.00	0.5045	72.2	125 ± 5
KLS162	dolerite†	0.673	1.9386	86.0	622 ± 25
			1.9480	89.6	

* Intrusive into Karoo sediments; † Intrusive into pre-Karoo rocks.

intruding the Albin basalts. The same observation holds for two of the regional dolerites analysed, since sample KLS44 (276 m.y.) intrudes Karoo sediments while sample KLS162 intrudes Damaran granitic rocks which are younger than the 620 m.y. age obtained. To what extent the results from the remaining three samples (125, 139 and 160 m.y.) reflect true ages is unknown, since all three intrude pre-Karoo rocks.

The anomalously high K-Ar ages reported in Table II are suggestive of the presence of excess radiogenic argon. The volcanics concerned may well have acquired such excess argon by interaction with Damaran (and older?) basement rocks en route to the surface along the lines suggested by Dooley and Wampler (1978), or even by degassing of the immediately underlying Damaran mica-rich schists due to heat supplied by the lava pile. It was therefore decided to analyse minerals from two fresh Horingbaai dolerites, KLS122 and 145 (the Albin lavas are all altered to varying degrees), by the ⁴⁰Ar/³⁹Ar step-heating technique in order to test this supposition. Plagioclase and pyroxene separates from these two samples and aliquots of a monitor were sealed in silica phials and irradiated in the core of the Herald Reactor AWRE Aldermaston where they received a dose of about 1.6×10^{18} neutron/cm². Gas extraction and data processing techniques are given in Roddick *et al.* (1980). Results for the two samples concerned are shown in Tables III and IV and Figs. 9 and 10. Although only limited data were obtained from the pyroxenes it is apparent that both contain excess argon. The plagioclase separates also contain excess argon but they yield much more useful information. Age spectra for the latter plot as saddle-shaped curves (Figs. 9 and 10) which is an indication of excess argon. However, according to Lanphere and Dalrymple (1977), the true age is approached by the saddle in the curves. Thus for KLS122 the apparent true age is well defined at about 125 m.y. while for KLS145 an age of 125–130 m.y. may be inferred. These ages are somewhat higher than the 121 m.y. isochron age derived by Siedner and Mitchell (1976), but demonstrate clearly that the anomalously high ages given in Table II are due to excess argon.

In addition to the K-Ar and ⁴⁰Ar/³⁹Ar ages discussed above Rb-Sr age studies have also been carried out on certain rock types. An attempt to date the quartz latites directly yielded an errorchron with an age of 154 ± 21 m.y. (Allsopp *et al.*, 1984b), considerably older than the K-Ar isochron and ³⁹Ar/⁴⁰Ar ages discussed above. Two zeolite-host rock tie lines for the quartz latites have slopes indicating an age of about 150 m.y. suggesting that the presence of zeolite (with lower ⁸⁷Sr/⁸⁶Sr and very low Rb/Sr ratios) in some of the quartz latites could be partly responsible for the older Rb/Sr errorchron age. However, the disposition of some very fresh samples, which do not contain zeolites, on the isochron plot suggests that a heterogeneous crustal source, in view of the high initial

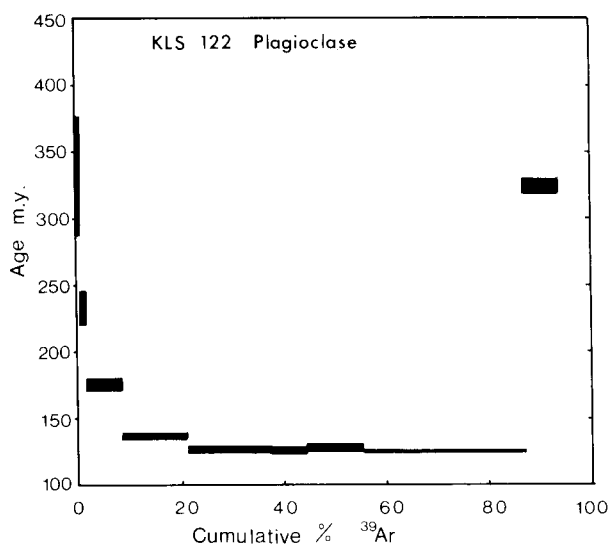


Figure 9
⁴⁰Ar/³⁹Ar spectra for plagioclase from Horingbaai dolerite KLS122. The saddle in the U-shaped pattern at approximately 125 m.y. is considered to reflect the true age of intrusion. Note excess argon as reflected also by conventional K-Ar age in Table II.

$^{87}\text{Sr}/^{86}\text{Sr}$ ratio of 0.718, could be a further complicating factor. An additional Rb-Sr study on biotite micro-gabbros from the sub-volcanic Messum Igneous Complex, which is considered to intrude the Etendeka lavas in the Gobobosebberge, was more successful (Allsopp *et al.*, 1984a). Three mica separates, a plagioclase separate and a whole rock define an isochron with an age of 132 ± 2.2 m.y. However, in contrast Fitch and Miller (1984) report an age of 149 ± 1 m.y. for one of these micas using the $^{39}\text{Ar}/^{40}\text{Ar}$ step heating technique. It should also be noted that Manton and Siedner (1967) obtained a Rb-Sr age (recalculated to $1.42 \times 10^{-11}\text{yr}^{-1}$) for the Paresis Complex (another sub-volcanic

ring complex in this area) which is identical to the Rb-Sr age of the Messum Complex reported above.

In conclusion, the results of this study confirm the early Cretaceous-late Jurassic ages of the main bulk of Etendeka Formation volcanics. However, the discovery of excess argon ages for many of our samples, coupled with clear argon loss for others, has confused rather than clarified many important aspects of the ages of lavas and intrusives—particularly the suggestions, made by previous studies, of a long history of continuous or periodic igneous activity. Of importance in this regard are the ages of the regional dolerites intruding basement and some, like

TABLE III
Argon Step Heating Data for Horingbaai Dolerite KLS122

Temp. (°C)	$^{36}\text{Ar}_{\text{Tr}}$ ($\times 10^{-9}\text{cm}^3\text{STP}$) ^a	$^{37}\text{Ar}_{\text{Ca}}$	$^{38}\text{Ar}_{\text{Cl}}$	$^{39}\text{Ar}_{\text{K}}$	^{40}Ar	Apparent Age ^b m.y. $\pm 2\delta$	^{39}Ar (%)
KLS122 Plagioclase (108.3 mg.)							
Blank ^c	0.0003				0.10		
450	0.009	0.500	0.009	0.090	4.71	331.1 \pm 44.7	0.7
500	0.004	1.091	0.004	0.150	3.50	232.5 \pm 12.5	1.2
600	0.015	16.502	0.011	0.880	14.91	175.4 \pm 4.4	6.9
700	0.034	77.647	0.013	1.596	24.62	136.5 \pm 2.1	12.5
785	0.014	80.157	0.005	2.105	21.99	126.4 \pm 1.9	16.5
825	0.004	14.890	0.001	0.862	8.40	125.7 \pm 2.1	6.8
855	0.004	16.238	0.004	1.411	13.08	127.9 \pm 2.5	11.1
965	0.015	33.816	0.007	3.960	37.45	125.3 \pm 0.5	31.1
1060	0.012	24.981	0.010	0.875	23.45	324.1 \pm 5.3	6.9
1150	0.012	35.775	0.011	0.320	21.39	703.0 \pm 4.3	2.5
1270	0.020	21.479	0.010	0.195	17.72	752.8 \pm 8.9	1.5
1425	0.015	32.497	0.013	0.276	18.14	645.9 \pm 4.6	2.2
Total ^d	0.16	355.57	0.09	12.72	209.4	188.7 \pm 2.0	
Conc.(/g)	1.5	3283.21	0.80	117.45	1933		
KLS122 Pyroxene (29.4 mg.)							
Blank	0.0020				0.60		
700	0.044	4.118	0.029	0.107	18.01	600.3 \pm 32.6	34.6
1415	0.039	113.802	0.027	0.203	22.23	675.2 \pm 16.6	65.4
Total ^d	0.08	117.92	0.06	0.31	40.2	649.7 \pm 16.5	
Conc.(/g)	2.8	4010.89	1.93	10.55	1369		

a — All gas quantities corrected for decay, minor products of neutron reactions on major isotope produced, and blanks; Tr = trapped; ^{40}Ar = trapped plus radiogenic.

b — Errors for steps are analytic only and do not include error in irradiation parameters, J. Ages calculated using decay constants and isotope ratios recommended by Steiger and Jäger (1977).

c — Blanks are for all steps except fusion which may be up to ten times larger.

d — Includes integrated age. Uncertainty in J (0.5 %) included in error.

TABLE IV
Argon Step Heating Data for Horingbaai Dolerite KLS145

Temp. (°C)	$^{36}\text{Ar}_{\text{Tr}}$ ($\times 10^{-9}\text{cm}^3\text{STP}$) ^a	$^{37}\text{Ar}_{\text{Ca}}$	$^{38}\text{Ar}_{\text{Cl}}$	$^{39}\text{Ar}_{\text{K}}$	^{40}Ar	Apparent Age ^b m.y. $\pm 2\delta$	^{39}Ar (%)
KLS145 Plagioclase (93.4 mg)							
Blank ^c	0.0007				0.20		
400	0.008	0.302	0.009	0.020	2.52	58.6 \pm 130.0	0.5
450	0.004	0.785	0.005	0.032	1.55	210.9 \pm 113.6	0.8
500	0.003	1.481	0.004	0.050	1.88	292.2 \pm 35.3	1.2
600	0.014	29.105	0.008	0.373	8.24	166.7 \pm 3.0	8.8
700	0.018	66.973	0.007	0.654	11.77	148.1 \pm 0.9	15.4
785	0.010	43.169	0.005	0.723	9.78	138.6 \pm 3.9	17.1
830	0.009	18.605	0.001	0.532	7.22	131.8 \pm 7.9	12.6
870	0.005	10.391	0.004	0.434	5.40	139.8 \pm 3.2	10.2
980	0.007	12.084	0.005	0.446	6.36	147.1 \pm 11.7	10.5
1070	0.009	18.428	0.010	0.248	8.44	326.7 \pm 8.7	5.9
1175	0.003	26.339	0.010	0.239	9.19	400.9 \pm 15.5	5.6
1275	0.005	13.142	0.002	0.097	4.38	422.2 \pm 24.8	2.3
1415	0.048	62.802	0.015	0.388	24.76	379.6 \pm 10.9	9.2
Total ^d	0.15	303.61	0.09	4.24	101.5	201.9 \pm 2.7	
Conc.(/g)	1.6	3250.61	0.93	45.36	1087		
KLS145 Pyroxene (25.0 mg)							
Blank ^c	0.0020				0.60		
700	0.023	6.042	0.034	0.385	10.94	158.5 \pm 10.1	59.7
1425	0.033	86.387	0.015	0.260	15.42	305.9 \pm 14.3	40.3
Total ^d	0.06	92.43	0.05	0.64	26.4	219.3 \pm 8.6	
Conc.(/g)	2.3	3697.18	1.95	25.79	1054		

Legend same as for Table III.

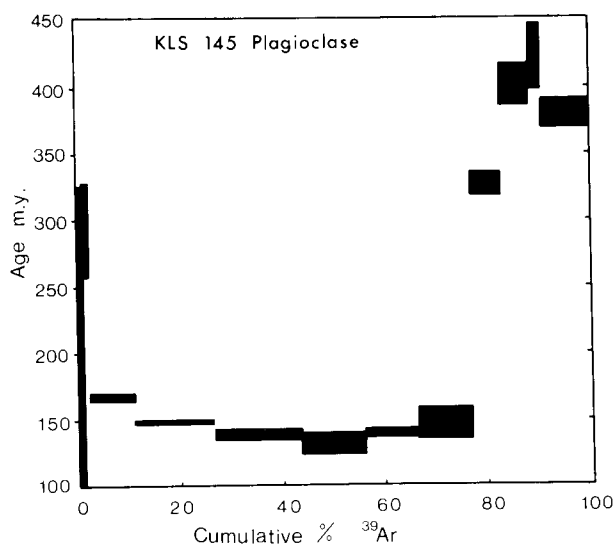


Figure 10

⁴⁰Ar/³⁹Ar age spectra for plagioclase from Horingbaai dolerite KLS145. The saddle in the U-shaped pattern at approximately 130 m.y. is considered to reflect the true age of intrusion, but is not as well developed as in Fig. 9. Note excess argon as reflected also by conventional K-Ar age in Table II.

KLS44, which intrude Karoo sedimentary strata as these dolerites have compositions very similar to the widespread early Jurassic Lesotho-type basalts and dolerites of the Central area. An intensive age study of these rocks is clearly necessary before any conclusion can be reached regarding the timing of volcanism in relation to rifting. Nevertheless, in view of the fact that both the Horingbaai dolerites and Messum Igneous Complex are intrusive into the Albin and Tafelberg basalts, the data presented above suggests that the minimum age for these lavas may be of the order of 130 m.y. This is somewhat older than the Siedner and Mitchell (1976) K-Ar isochron age of 121 m.y., and slightly older than the oldest magnetic anomalies on the adjacent sea floor (see summary by Duncan *et al.*, 1984).

The implications of this will be discussed in a later section, but the reader should note that in the ensuing geochemical sections an age of 121 m.y. has been retained when making age corrections for the isotopic data. Use of an older age of 130 m.y. would not alter the arguments that follow in these sections.

V. PETROGRAPHY

Detailed mineralogical studies on the Etendeka volcanics are continuing and preliminary compositional data on selected specimens are reported below. The petrographic descriptions, however, relate to a large number of samples. There are no published detailed petrographic descriptions of Etendeka volcanics although Botha and Hodgson (1976) have described some of the regional dolerites. Gidskehaug (1975) has reported on a detailed investigation of Fe-Ti oxides in 7 specimens of Etendeka lavas but unfortunately did not identify the petrological nature of the rocks. The electron microprobe technique used in this study, and the complete mineral analyses obtained, are contained in Appendix 1 to this volume and Microfiche Card 3 respectively.

A. Tafelberg Basic Lavas

These lavas have a range in composition from 51 to 58 % SiO₂ (volatile-free basis) and consequently exhibit variable mineralogical characteristics although texturally most rocks in the suite are remarkably uniform. The lavas are hypo- to holo-crystalline fine-grained rocks with intersertal or intergranular textures (Fig. 11a). Most specimens are equigranular with average grain sizes in the range 0.1 to

0.5 mm. In some thick flows, zones of medium- to coarse-grained equigranular basalt occur. Occasional specimens are sparsely porphyritic with phenocrysts of plagioclase or pseudomorphed olivine and, more rarely, clinopyroxene up to 1.5 mm in dimension.

Euhedral, zoned plagioclase laths form an interlocking framework packed with granular augite and pigeonite and, in the more evolved types, with interstitial glass or quartz and alkali feldspar intergrowths, although interstitial glass is also present in some of the less evolved varieties. Pigeonite commonly occurs as discrete subhedral laths or granules which may form up to half the pyroxene population. Their gin-clear irregularly cracked appearance and larger grain size distinguishes them from augite. Anhedral Ti-magnetite occurs as equant grains with extensively embayed margins and displays various types of exsolution intergrowth with ilmenite, although electron microprobe investigations have revealed the presence of single-phase grains in some specimens. Tiny granules of pyrite are also present although they are rare. In some of the least evolved basalts from the lower part of the succession sparsely distributed pale green to brown euhedral pseudomorphs of serpentine or carbonate, traversed by irregular cracks lined with magnetite, are observed. These are interpreted as pseudomorphs after olivine phenocrysts, since reasonably fresh olivine has been identified in one specimen of these lavas. In the more evolved lavas irregular patches of microlite-charged glass in various stages of divitrification occurs interstitially between plagioclase and pyroxene grains. In some evolved specimens with high SiO₂ contents interstitial "clots" of quartz and alkali feldspar occur. These samples usually have a higher plagioclase/pyroxene ratio and a higher abundance of Ti-magnetite compared to the least evolved basalts.

Preliminary compositional data for the major phases are summarized in Fig. 12a. The compositions of plagioclase from the least and most evolved specimens overlap considerably within the range An₆₈ to An₃₀. Normal zoning is common and of the order of less than 15 mole % An although reversed zoning of a similar magnitude is present in some grains in several specimens. Pigeonite shows marked Fe-enrichment from Ca₉Mg₆₈Fe₂₃ to Ca₁₀Mg₃₆Fe₅₄, the complete range sometimes being exhibited within a single specimen (KLS292). Augite exhibits a similar Fe-enrichment from Ca₄₀Mg₅₁Fe₉ in the least evolved basalts to Ca₃₃Mg₃₀Fe₃₇ in the most evolved rocks. Within individual samples augite shows considerable compositional zoning and, as with plagioclase, this zoning may be reversed in the case of some crystals in a sample. Single-phase Ti-magnetites range in composition from Usp₆₆ to Usp₅₀.

Most specimens show varying degrees of oxidation and alteration which imparts a reddish colour to the rocks in hand specimen. In the least oxidized specimens a slight red stain may be confined to grain boundaries in the immediate vicinity of the Ti-magnetites but in extensively oxidized specimens the reddish stain penetrates all grain boundaries and the pyroxenes and magnetites exhibit thick rims of a dark red-brown isotropic material.

B. Albin Basic Lavas

These basalts occur in the lowermost parts of the volcanic sequence in the coastal region where they are interbedded with typical Tafelberg type basalts. Available chemical analyses indicate that they are compositionally similar to the Tafelberg basalts although petrographically they are strikingly different, being characterized by distinctive porphyritic textures are shown in Fig. 11b. No mineral compositional data are available at present and nearly all samples show strong alteration in thin section despite being hard, compact and apparently fresh in hand specimen.

Albin-type basalts are fine- to medium-grained

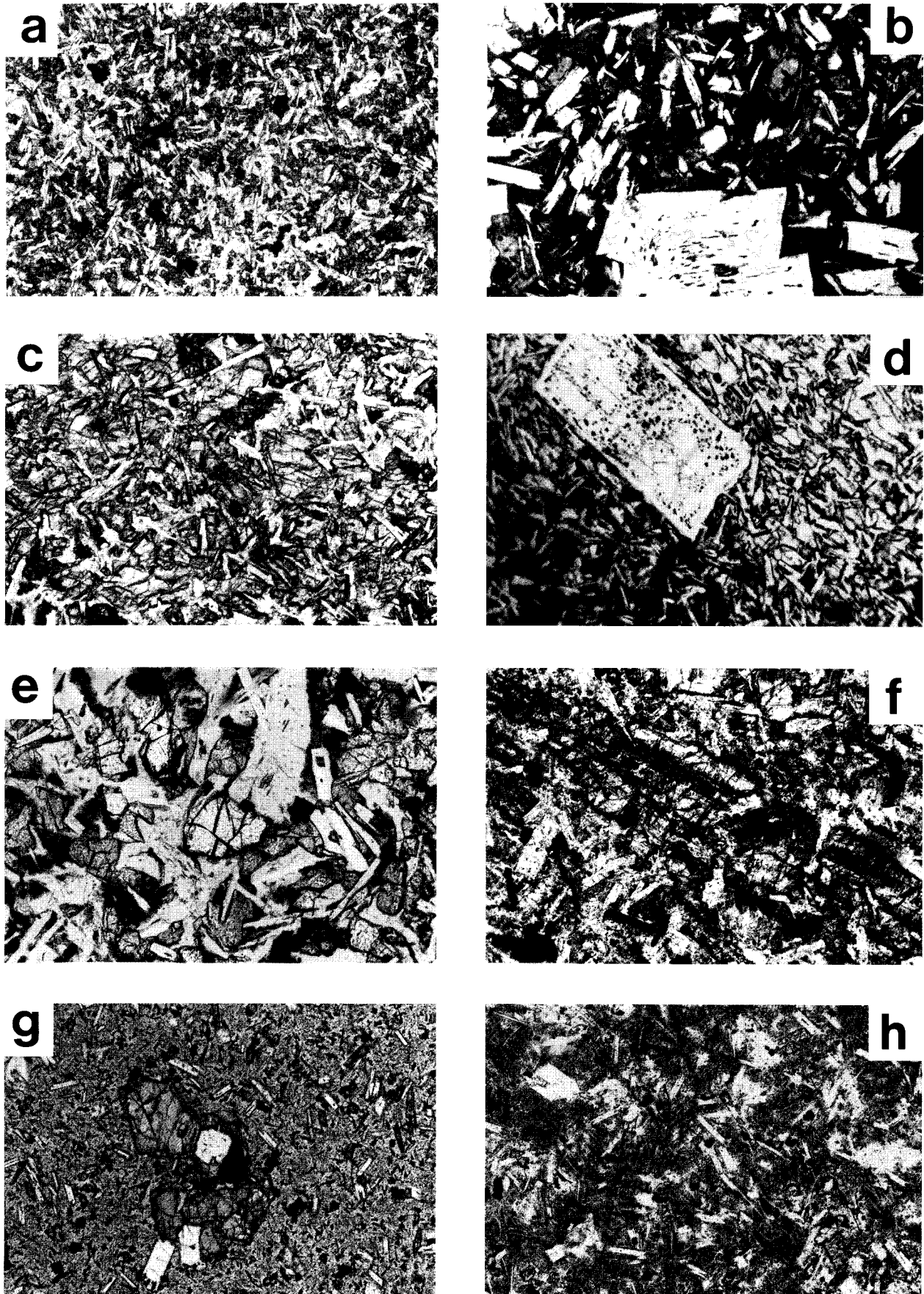


Figure 11 (caption opposite)

Figure 11

Photomicrographs of Etendeka volcanic rocks, all in plane polarized light. (a) Typical aphyric intergranular-textured Tafelberg basalt (KLS22) with plagioclase laths, granular clinopyroxene and interstitial clots of Fe-Ti oxides and minor glass. Field of view 2.5 mm. (b) Albin basalt (KLS141) with plagioclase phenocrysts in a groundmass of plagioclase, altered mafic minerals (largely pyroxene with minor olivine) and interstitial glass. Field of view 2.5 mm. (c) Ophitic regional dolerite (KLS44) with scattered grains of partially serpentinized olivine and laths of plagioclase enclosed by an augite oikocryst. Field of view 2.5 mm. (d) Poikilophitic Tafelberg dolerite KLS100. To the left of the large plagioclase grain is an augite oikocryst enclosing laths of plagioclase, partially serpentinized olivine and opaque oxides. The intergranular portion to the right of the large plagioclase grain mainly contains plagioclase laths, with minor olivine and orthopyroxene. The large euhedral plagioclase grain has a core of An_{56-53} similar to small plagioclase laths in the intergranular portion, but is mantled by a thin rim with a composition (An_{73-66}) analogous to that of the plagioclase laths (An_{73-65}) in the oikocrysts. The plagioclase relationships are interpreted as magma mixing between less evolved and more evolved basaltic magmas. This rock is also unusual in having enriched Sr- and Nd-, but unradiogenic Pb-isotopic compositions (Figs. 18, 19 and 20). Field of view 2.5 mm. (e) Horingbaai dolerite KLS145. Intergranular textured dolerite comprising plagioclase, augite, opaque oxides and unaltered olivine (in centre of photograph). This rock has the most unradiogenic Sr-, Nd- and Pb-isotopic compositions encountered in this study. Field of view 1.0 mm. (f) Tafelberg latite (KLS71) showing part of an elongated sub-calcic augite (top left to bottom right) displaying fine exsolution lamellae, laths of alkali feldspar and elongated grains of Ti-magnetite. Plagioclase is not present in this rock, and is only found as presumed xenocrysts of virtually pure albite in two other specimens. Field of view 1.0 mm. (g) An aggregate of orthopyroxene, plagioclase and Ti-magnetite phenocrysts from interbedded quartz latite (high-K dacite) KLS51. A rim of pigeonite is clearly developed on the orthopyroxene. The partially devitrified glassy groundmass encloses microphenocrysts of plagioclase, clinopyroxene and magnetite. Field of view 2.5 mm. (h) A devitrified, hypocrySTALLINE aphyric quartz latite KLS101 from the upper unit at Tafelberg (Fig. 6). White laths are plagioclase. Field of view 1.0 mm. Mineral compositions for some of these rocks may be found in Microfiche Card 3 and Figs. 12 and 13.

porphyritic rocks and both holo- and hypo-crystalline varieties are found. The dominant phenocryst phase is plagioclase which frequently occurs as glomero-porphyritic aggregates up to 7 mm across. Clinopyroxene, usually augite with pigeonite cores, is less frequently a phenocryst. Serpentine/chlorite/carbonate pseudomorphs of a phenocryst phase, presumably olivine, also occur in some specimens. Groundmass phases include subhedral plagioclase and augite, euhedral Ti-magnetite and varying amounts of devitrified glass. The groundmass phases are frequently strongly altered with sericitization of feldspar and serpentinization of mafic silicate phases. Secondary calcite, sometimes in abundance, has a patchy distribution in these highly altered rocks, where it apparently replaces the groundmass.

C. Dolerites

A wide range in chemical and petrographic types has been identified in our sample collection of dolerites. These will be discussed according to the terminology used in Section III-C although for petrographic purposes it is convenient to adopt a slightly different grouping, as discussed below.

(a) Some dolerites which intrude the Tafelberg and Albin basic lavas and which are compositionally similar to these magma types respectively also exhibit similar petrographic characteristics to the Tafelberg and Albin lavas as documented above. Further petrographic description is thus unnecessary except to note that both types of dolerite are usually fresher than the corresponding lavas. Only one of these dolerites, KLS152, belonging to the Tafelberg magma type, has been subjected to microprobe analysis. Plagioclase compositions range from An_{55} to An_{44} while the augites exhibit marked zoning in the Wo component with only a slight increase in Mg/Fe (composition range $Ca_{39}Mg_{38}Fe_{23}$ to $Ca_{24}Mg_{48}Fe_{27}$).

(b) A second group of dolerites includes those which have similar petrographic characteristics but different chemical relationships, but which nevertheless are associated with the Etendeka volcanic episode. These include KLS44, a regional dolerite intruding Karoo sediments, and three samples which intrude the Etendeka lavas. The latter have different textures from the Tafelberg dolerites described in (a) above but nevertheless have been classified as belonging to the Tafelberg magma type on the basis of their chemistry. Photomicrographs of two of the above group (KLS44 and KLS100) are shown in Fig. 11c and 11d.

This group of dolerites comprises holocrystalline medium-grained rocks with well-developed poikilophitic textures. Olivine is fresh or only partially serpentinized and together with plagioclase and minor augite and opaque oxides forms intergranular aggregates around the large (up to 5 mm) augite oikocrysts. In some specimens there is minor interstitial glass with abundant microlites. Ilmenite and magnetite occur as discrete phases in the poikilophitic dolerites. Tiny grains of pyrite are also observed in all specimens but are rare. Biotite occurs as narrow rims on magnetite in KLS38.

Fig. 12b summarizes the mineral composition data available for these dolerites including KLS100, which occurs high up in the Tafelberg succession and is inferred to be an intrusive sill although field relationships are obscured. This sample exhibits several unusual chemical and mineralogical features as discussed below and in later sections. However, the analysed compositions of the phases in KLS100 lie within the range of other dolerites described

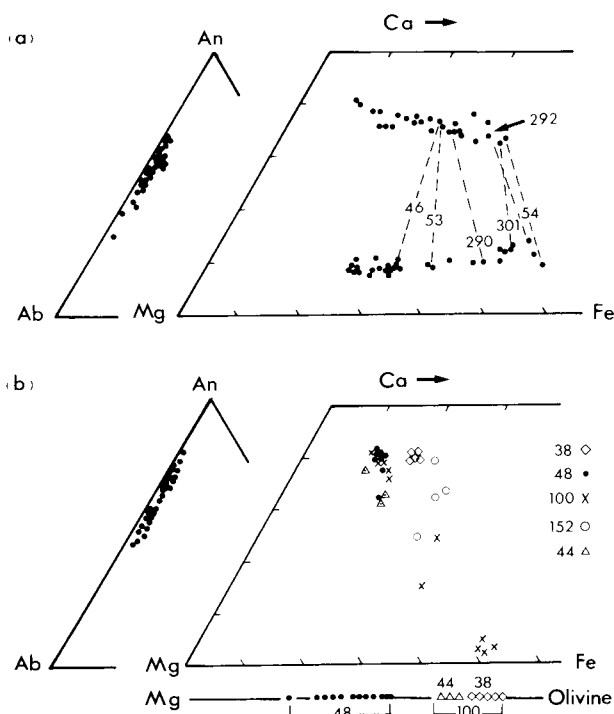


Figure 12

Plagioclase, pyroxene and olivine compositions in Etendeka basaltic rocks. Numbers refer to sample numbers, all prefixed KLS. (a) Tafelberg basalts and evolved basalts. Tie-lines denote most evolved compositions for the samples shown. (b) Tafelberg (KLS 38, 48, 100, 152) and regional (KLS44) dolerites. KLS152 is an evolved dolerite and contains neither orthopyroxene nor olivine.

below. Plagioclase compositions range from An_{78} to An_{48} in the poikilophitic dolerites. Zoning is normal except in some plagioclase grains in KLS100. Collectively, the olivines in the poikilophitic dolerites exhibit a wide range in composition but the variation within any one rock is limited and distinct as follows: KLS48 (FO_{84} - FO_{67}); KLS44 (FO_{58} - FO_{56}); and KLS38 (FO_{53} - FO_{48}). The range for KLS100 overlaps with that of KLS38 and KLS44. As a group the augites also show a range in composition but, as with olivine, the composition variation in individual rocks is limited. Overall there is no distinct Fe-enrichment trend as displayed by augites in the Tafelberg basic lavas.

It is noteworthy that, except for KLS48, the olivines from the other dolerites have higher Fe/Mg ratios than their coexisting augites (Fig. 12b), contrary to what is generally observed in basic rocks. The olivines are also much more Fe-rich than is predicted by the Roeder and Emslie (1970) Fe-Mg partitioning relationship between olivine and liquid assuming their host rock compositions were those of liquids and a Fe_2O_3/FeO ratio of 0.2. For example, the calculated composition for the most Mg-rich olivine in KLS44 is FO_{79} versus a measured value of FO_{58} ; for sample KLS100 the corresponding calculated and measured values are FO_{72} and FO_{56} respectively. Similar features have also been noted in other Karoo dolerites. In a comprehensive study of the Tandjiesberg sill Richardson (1979) has noted that the olivines in the holocrystalline interior of the sill are much more Fe-rich than in the chilled margin. He ascribes this to equilibration of early magnesian olivine with residual liquid during the late stages of crystallization. However, this explanation is not entirely satisfactory as it does not explain the coexistence of Fe-rich olivine with more Mg-rich pyroxenes, unless the kinetics of Fe-Mg partitioning are very different between olivine-liquid and pyroxene-liquid. Alternatively, slight density differences between olivine and pyroxene, coupled with compensated crystal settling (Cox and Bell, 1972), could lead to equilibration of the olivines and not the pyroxenes in dyke-like magma chambers. This situation is envisaged for the picritic lavas of the northern Lebombo (Cox *et al.*, 1984) where the olivines are also more Fe-rich than the coexisting clinopyroxenes.

Alternatively, the question can be asked as to whether the disequilibrium relationships noted above are indicative of open system conditions. This is particularly the case for sample KLS100. We have noted that the olivines (and orthopyroxenes) are more Fe-rich than coexisting clinopyroxenes (Fig. 12b). More particularly, plagioclase laths in large clinopyroxene plates or oikocrysts are more calcic (An_{73-65}) than plagioclase laths in the surrounding groundmass. One large euhedral plagioclase in the groundmass (Fig. 11d) has a core of An_{56-53} , similar to smaller plagioclase laths in the groundmass, but is mantled by a thin rim with a composition (An_{73-66}) analogous to that of the plagioclase laths in the oikocrysts. While magma mixing is implied, these observations indicate simple mixing between less evolved and more evolved basaltic magmas. Thus the less calcic plagioclase laths in the groundmass have similar compositions to typical Tafelberg-type basalts (Fig. 12a). In particular, there is no suggestion of different or enhanced K concentrations in any of the plagioclase cores or rims analysed (Microfiche Card 3), as might be expected if a crustal component or melt was assimilated by a basaltic magma. Thus we conclude that while limited magma mixing may have occurred between different basaltic magmas, as might be expected, that large scale mixing is not suggested by the petrographic evidence, since the disequilibrium relationships present in the dolerites have not been observed in the Tafelberg basaltic lavas. Furthermore, the petrographic evidence does not indicate any mixing between the basaltic rocks and the more acidic latites and quartz latites.

(c) Thin sills and dykes constituting a third group of

intrusives are known only from the vicinity of Horingbaai where they intrude Albin-type basalts. Chemical compositions identify the Horingbaai dolerites as a distinctive type. They are aphanitic fine-grained rocks with sparsely developed microporphyrific textures and most specimens in our collection are very fresh. Plagioclase, together with olivine and/or augite are the phenocryst phases. The groundmass textures are intergranular to subophitic (Fig. 11e). Preliminary mineral composition data (Fig. 13a) indicate that plagioclase is calcic and zoned from An_{87} to An_{74} , augite compositions are in the range $Ca_{43}Mg_{41}Fe_{16}$ to $Ca_{36}Mg_{49}Fe_{15}$ and olivine ranges in composition from FO_{87} to FO_{85} . These olivines are the most forsteritic olivines we have encountered in the Etendeka volcanics.

(d) For completeness we should mention those regional dolerites which occur in pre-Karoo rocks (Fig. 7) and whose true ages (Table II) or possible relationships to the Etendeka lavas are unknown. Some of these have intersertal or intergranular textures and mineralogy similar to the Tafelberg dolerites described in (a); others are olivine bearing with ophitic textures similar to the Tafelberg and regional dolerites described in (b). We have not yet studied these numerous dolerites in any detail and they will not be discussed in this study.

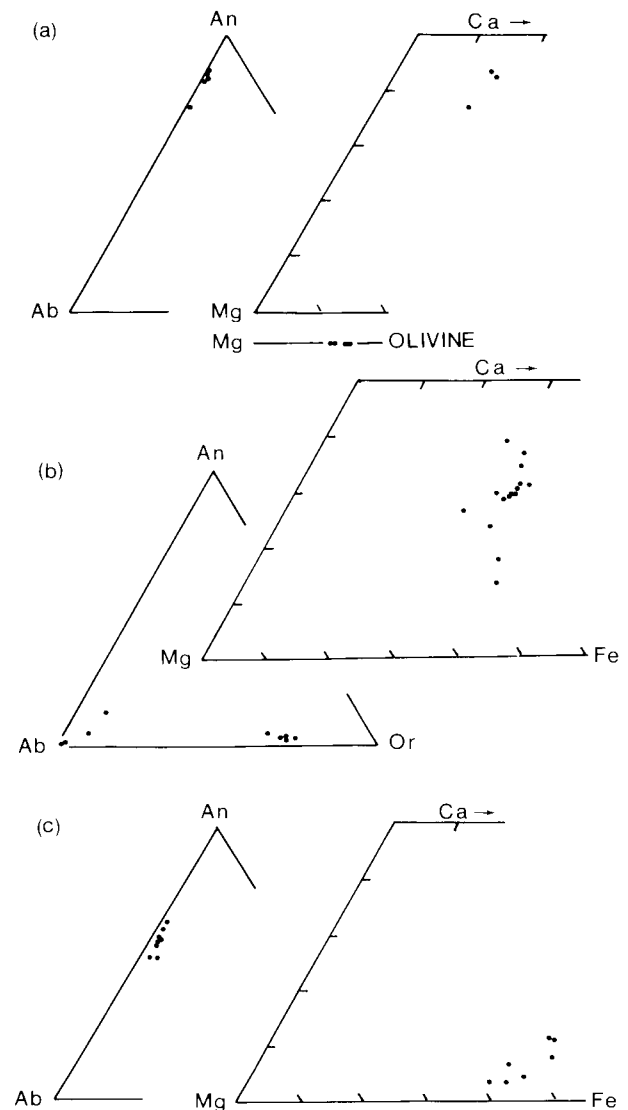


Figure 13

Plagioclase, pyroxene and olivine compositions in Etendeka volcanic rocks. (a) Horingbaai dolerites KLS122 and 145. (b) Tafelberg latites KLS67, 69, 71. (c) Tafelberg quartz latite (KLS36) and high-K dacite (KLS51).

D. Tafelberg Latites

The latites occur as a series of flows in a thin unit which, to date, has only been identified in the Tafelberg region. Compared with the basalts and quartz latites they exhibit relatively constant chemical compositions (e.g. SiO₂ varies from 59.0–59.5%), although only four samples have been quantitatively analysed. The latites are holocrystalline inequigranular rocks with porphyritic or seriate textures. They are characterized by pronounced elongation of clinopyroxene prisms, many of which attain lengths of up to 3–4 mm, and abundant Ti-magnetite which also shows a tendency towards elongation and the development of comb structures (Fig. 11f).

Sparse "phenocrysts" in the porphyritic varieties are almost pure albite up to 3 mm long with cores Ab₉₉An_{0.6}Or_{0.4} and thin rims of a ternary feldspar (Ab₇₉An₁₂Or₉). These large albite grains are presumably either xenocrysts and/or the products of alteration. The groundmass is pilotaxitic with acicular pyroxene and alkali feldspar (up to 0.33 mm in length) and anhedral magnetite accompanied by small amounts of interstitial quartz. In the seriate textured latites the elongated clinopyroxenes are thicker and anhedral, being partially penetrated by and occasionally enclosing small (<0.3 mm) euhedral alkali feldspar laths (compositions ranging from An₅Ab₃₃Or₆₂ to An₃Ab₂₅Or₇₂). The clinopyroxenes are augites, subcalcic augites and pigeonites showing limited variation in Fe/Mg ratio but wide variation in Ca content, ranging across the two-pyroxene field (Fig. 13b). Note that these pyroxenes are not as evolved as the most Fe-rich pyroxenes in the Tafelberg basic lavas (Fig. 12a). Some of these pyroxenes display patchy development of very fine exsolution lamellae (?) parallel to 001 which have not been resolved during microprobe analysis. Minor quartz and devitrified glass occur interstitially.

The latites show varying degrees of oxidation/alteration. Highly oxidised rocks are brick red, the colour being imparted by dark red alteration stains on the rims and along fractures in the pyroxenes which themselves are frequently pseudomorphed by serpentine (?). Similarly, in the vicinity of magnetite, grain boundaries are permeated by a red stain.

E. Tafelberg Quartz Latites

Quartz latites are widespread throughout the Etendeka and although they occur in two distinct units at Tafelberg it has not yet been possible to correlate the coastal outcrops of quartz latite with either of these two units. Compared to the basic lavas the quartz latites exhibit a narrow range in SiO₂ content (67–70%). However, some elements, notably K and Rb, show a much larger range in concentration (Fig. 8), hence our previous distinction between quartz latites and high-K dacites.

At Tafelberg the lower quartz latite unit comprises sparsely porphyritic lavas with an aphanitic hypocrySTALLINE groundmass (Fig. 11g). The phenocryst population consists of plagioclase, pigeonite, Ti-magnetite and, in some specimens, orthopyroxene. The latter mineral is present in the high-K dacite sub-group. Phenocrysts have a maximum size of 1 mm but in some specimens corroded and embayed plagioclase phenocrysts of up to 3 mm are sparsely scattered through the rock. Plagioclase and clinopyroxene occur as microphenocrysts. The groundmass varies from vitrophyric in very fresh specimens to microfelsitic in more altered rocks.

Limited mineral composition data are available for these quartz latites (Fig. 13c). Euhedral plagioclase phenocrysts are normally zoned and range in composition from An₆₆ to An₅₂. Subhedral pigeonite phenocrysts are also zoned and have compositions in the range Ca₇Mg₄Fe₃₉ to Ca₁₁Mg₄₆Fe₄₃. Orthopyroxenes from KLS51 are slightly zoned from Ca₁Mg₅₈Fe₃₈ to Ca₄Mg₅₃Fe₄₃ and are often

rims by pigeonite overgrowths of ca. Ca₈Mg₄₇Fe₄₅ (Fig. 11g). Equant magnetite phenocrysts have compositions in the range Usp₇₃ to Usp₅₅.

Porphyritic quartz latites with similar features are widespread in the Etendeka. Some porphyritic specimens appear to have alkali feldspar phenocrysts. It is not known whether these samples are highly potassic or not as our single analysed K-rich sample (AG38-4 which has 7.9% K₂O) is non-porphyritic.

The upper quartz latite unit at Tafelberg is non-porphyritic. The textures of these rocks are microhypocrySTALLINE when fresh to microfelsitic in devitrified specimens (Fig. 11h). Microlites of plagioclase, clinopyroxene and opaque Ti-magnetite are present but no compositional data for these phases are available.

The Etendeka quartz latites are broadly similar to those of the Jozini and Mbuluzi Formations which crop out on the eastern side of the continent (Cleverly *et al.*, 1984). However, the latter rhyolites are commonly more phyric and the clinopyroxene is generally augite, pigeonite being rare.

VI. CORRESPONDENCE BETWEEN ROCK AND MAGMA COMPOSITIONS

If the chemical and isotopic compositions of the Etendeka volcanics are to be used in any meaningful way to interpret the petrogenesis of these rocks, then it is obviously important to assess whether the analysed rocks are representative of the magmas arriving in the upper continental crust. Processes modifying magma compositions prior, during or subsequent to emplacement are crystal-liquid fractionation, crustal contamination, hydrothermal alteration and weathering. The first two processes are considered in detail in later sections; here we confine our discussion to *in situ* alteration processes that could modify the compositional characteristics of the volcanics. This is appropriate because in the previous section we have indicated that many of the rocks show varying degrees of oxidation and alteration which imparts a reddish colour to the rocks in hand specimen and which often makes it difficult to distinguish between the Tafelberg evolved basalts and the quartz latites in the field. Petrographic observations denote the common presence of alteration minerals pseudomorphing the primary minerals. Calcite is a common replacement mineral in some lavas, especially those from the Albin type-section, while highly amygdaloidal lavas occur in both the mafic and felsic volcanics.

A. Zeolite and Calcite Formation

Although amygdaloidal flows were avoided in our sampling, the presence of highly amygdaloidal flows throughout the lava succession, coupled with the presence of large amounts of secondary calcite in the Albin lavas of the type-section, raises doubts about the modifying effects of hydrothermal solutions circulating through the volcanic pile, either during cooling or subsequently. Amygdales were separated from three (Tafelberg non-porphyritic) samples and analysed together with hand-picked 2–3 mm sized fragments of the host-rock matrix which were as far as possible devoid of amygdales. X-ray diffraction analysis revealed that the amygdales consist mainly of the zeolite heulandite, with minor amounts of calcite. Major and trace element analyses of the basalt and two quartz latite host-rock matrices (not shown here or reported in our data-base in Microfiche Card 1) show concentrations which are within the range reported for other basalts and quartz latites and are thus not particularly instructive.

The amygdales were specifically separated to test their possible influence on ⁸⁷Sr/⁸⁶Sr ratios, and the data obtained are reported in Table V. For the Tafelberg basalt sample the zeolite has an initial ⁸⁷Sr/⁸⁶Sr ratio which, although

TABLE V
Rb, Sr and $^{87}\text{Sr}/^{86}\text{Sr}$ Ratios in Amygdale Minerals and Host Rock Matrices

	Rb ppm	Sr ppm	Rb/Sr	$^{87}\text{Sr}/^{86}\text{Sr}$	$^{87}\text{Sr}/^{86}\text{Sr}$ (121 m.y.)
Tafelberg basalt					
KLS66 host matrix	18.3	189	0.097	0.71208 (6)	0.71160
zeolite	1.9	75.3	0.025	0.71126 (6)	0.71113
Tafelberg quartz latites					
KLS18 host matrix	198	80.2	2.47	0.73182 (5)	0.71951
zeolite	19.2	3154	0.006	0.71678 (4)	0.71675
KLS103 host matrix	165	119	1.39	0.72547 (4)	0.71856
zeolite	17.1	6268	0.003	0.71652 (4)	0.71651
calcite	1.15	43.4	0.026	0.71675 (6)	0.71662
Typical range,	139–	88–	0.85–	0.7209–	0.7187–
quartz latites	225	163	2.56	0.7342	0.7215

Data from Bristow *et al.* (1984). Rb and Sr are measured concentrations, not corrected for volatile content. Figures in parentheses after the $^{87}\text{Sr}/^{86}\text{Sr}$ ratios are in-run uncertainties expressed as two standard errors. KLS18 and KLS103 are from the lower and upper quartz latite units at the Tafelberg type-section, while KLS66 is from the basalt unit just below the latite unit (Fig. 6).

statistically slightly lower than in the host basalt, does not give rise to concern in view of the very much lower Rb and Sr concentrations in the zeolite compared to the basalt. In contrast the zeolites from the two quartz latite samples have much higher Sr contents than in the host quartz latites and which, coupled with their substantially lower initial $^{87}\text{Sr}/^{86}\text{Sr}$ ratios, indicate that the quartz latites may well have had their $^{87}\text{Sr}/^{86}\text{Sr}$ ratios lowered by the solutions that deposited the zeolites. This has already been discussed in Section IV–B and by Allsopp *et al.* (1984a) who point out that this may in part be the reason for the “errorchron” of 154 m.y. obtained in the quartz latites. Nevertheless, we note that the two quartz latite host matrices in Table V have amongst the lowest initial $^{87}\text{Sr}/^{86}\text{Sr}$ ratios in the quartz latites analysed (Allsopp *et al.*, 1984; Bristow *et al.*, 1984) and since we have been careful to avoid amygdaloidal flows it is considered that slight lowering of the $^{87}\text{Sr}/^{86}\text{Sr}$ ratios will not materially affect the discussions in later sections. In passing we also note that the surprisingly low Sr content of the single calcite analysed will presumably not affect the quartz latites as much as the coexisting zeolite (Table V).

Unresolved problems concern the source of the high Sr concentrations in the zeolites from the quartz latites, why the zeolites in the basalt and the quartz latites have such different Sr contents, and whether the solutions are pervasive in their alteration or confined to structural channelways. If the source of the Sr is from the volcanics (e.g. leaching of plagioclase and fixing in zeolite), or from another source, then the possibility of mixing arises. These considerations are important because of the previously mentioned large amounts of replacement calcite in the Albin basic lavas. Some of these have been analysed for their CO_2 contents and yield 2.4–7.7% CO_2 . Even the fresh Horingbaai dolerites intruding the Albin lavas have from 0.1–2.5% CO_2 . If the calcite analysed in the quartz latite (Table V) can be used as a guide to the Sr content of the calcite in the Albin lavas (Bristow *et al.*, 1984 report a similarly low Sr concentration in a calcite from a Sabie River basalt from the southern Lebombo) then perhaps the process leading to replacement by calcite does not cause significant chemical or isotopic changes, other than the introduction of carbonate itself. Nevertheless, the whole question of hydrothermal alteration and amygdale formation in volcanic piles, and consequent changes in chemical and isotopic composition, deserves closer investigation in view of the ubiquitous presence of amygdales in flood basalt lavas.

B. Other Alteration Effects

In contrast to the previous section where specific alteration processes could be documented, chemical

changes relating to variation within and between flows could be caused by a variety of processes. These could be caused by magmatic processes (flow differentiation, migration and concentration of late-stage residual liquids) on the one hand and secondary lower temperature processes (including amygdale formation and hydrothermal alteration discussed above and surface weathering) on the other, or a combination of these processes.

The oxidation of opaque minerals and alteration of the lavas to a reddish colour, and the presence of olivine pseudomorphs, sericitization of feldspars and devitrification of glass *inter alia*, suggests that low temperature processes may have influenced lava compositional characteristics. This is supported by the loss on ignition values for many of the lavas, using the loss on ignition as an approximation of volatile loss. Ignoring the Albin lavas with their high CO_2 contents, discussed in the previous section, the Tafelberg basic lavas, latites and quartz latites typically have loss on ignition values in the range 1.0–1.5%, with some of the Tafelberg basic lavas having high figures of 5–7% (Microfiche Card 1). In contrast the dolerites studied are generally much fresher than the lavas and typically have loss on ignition values of <1%, with the exception of some of the Horingbaai dolerites, where up to 3% H_2O^+ and CO_2 have been determined.

We have only one example where within flow variability can be tested. Two samples from the bottom and top of a typically oxidized and reddish-coloured non-amygdaloidal basalt flow from the Tafelberg locality, KL15 and KL16, have been analysed and the compositional variability for major and trace elements (defined as range in measured concentration $\times 100/X$) calculated. The agreement in the two sets of data is remarkably close. Surprisingly, the variability index for elements normally considered mobile (Ca, K, Rb, Ba and Sr) is low (<4%) as compared to immobile elements such as Ti, P and Zr (3–5%). The largest variations are for H_2O (21%), Nb (14%), Cr (11%), Co (18%) and La (23%), all other variations being <7%. These are somewhat surprising since Nb and Co, for example, are typically considered to be immobile in alteration processes and must therefore be attributed largely to poor analytical precision at low levels of concentration. Within-flow magmatic differentiation can be ruled out because of low variability for Mg, Fe and Ni.

Between-flow variability can be assessed within a typical quartz latite since five samples have been taken from successive flows in a single section of a lower quartz latite unit south of Tafelberg. All are somewhat altered with sericitization of feldspars, devitrification of glass and

TABLE VI
Selected Major and Trace Element Data for Five Quartz Latites
from Successive Lava Flows

%	KLS31	KLS32	KLS33	KLS34	KLS35
SiO ₂	67.19	66.87	67.79	66.40	67.06
TiO ₂	0.96	0.96	0.98	0.94	0.99
Fe ₂ O ₃	7.04	7.32	7.00	7.41	7.30
CaO	2.86	2.69	2.80	2.05	3.29
Na ₂ O	2.23	2.29	2.32	2.91	2.24
K ₂ O	4.34	4.26	4.49	4.18	3.83
P ₂ O ₅	0.29	0.28	0.29	0.29	0.29
L.O.I.	1.14	1.08	1.06	1.63	1.11
ppm					
Rb	158	163	164	163	160
Ba	656	686	681	646	664
Sr	142	152	152	136	144
Zr	279	288	288	287	284
Cu	16	17	35	17	35
Sc	20	21	20	19	20
Nd	49	51	47	49	47
K/Na	2.18	2.08	2.17	1.61	1.91
Ca/Al	0.30	0.29	0.29	0.22	0.35
K/Zr	129	123	129	121	112
Zr/Y	7.6	7.8	7.4	7.4	7.4
Rb/Sr	1.11	1.07	1.08	1.20	1.11
⁸⁷ Sr/ ⁸⁶ Sr			0.7199	0.7197	

All data from Microfiche Card 1, uncorrected for volatile content. Total Fe as Fe₂O₃. L.O.I. is loss on ignition at 950 °C. ⁸⁷Sr/⁸⁶Sr is initial ratio at 121 m.y.

oxidation of opaques being apparent. Rather than calculate statistical variation, we have chosen to present data for selected elements in Table VI, together with some inter-element and two initial Sr-isotope ratios. Inspection of the data shows that in general there is a remarkable degree of compositional uniformity which should be considered in any model for the mode of eruption and petrogenesis of the quartz latites. This is evidenced by the relative constancy of SiO₂, TiO₂, Fe₂O₃*, P₂O₅, Ba, Zr, Sc, Nd concentrations and the Zr/Y ratio, together with other elements and ratios not shown (e.g. Al, Nb and Si/Al, Zr/Nb). In detail, however, it is clear that slight variations are present for other elements and ratios, which are not due to analytical error or magmatic fractionation, and which must therefore be due to alteration processes. This is particularly evident for samples KLS34 and KLS35, as shown by the variations in CaO, Na₂O, K₂O and Cu concentrations and the K/Na, Ca/Al and K/Zr ratios. Surprisingly the variation in Rb concentration is just outside analytical error, while the variation in Sr and Rb/Sr ratio appears to be real, particularly for KLS34. The slight variation in Sr and the ⁸⁷Sr/⁸⁶Sr ratio may be expected in view of the discussion in the previous section. The point of this detailed treatment is to demonstrate that while the quartz latites in general may be expected to be free from gross alteration effects, particular elements and ratios (e.g. Ca, Na, K, Sr, Rb/Sr and ⁸⁷Sr/⁸⁶Sr) in individual samples may well show slight variations due to alteration.

The data presented in this section dealing with alteration, albeit limited, suggest that for the purposes of this study the overall data obtained for the Tafelberg mafic and felsic volcanics, and the various dolerite types, may be used with confidence. Further work is required to evaluate properly the effects of alteration in the carbonated Albin lavas. Reference should however be made to the more detailed work of Marsh and Eales (1984) for the Central area basic rocks. These authors show that Na, K, Rb, Sr and Ba in particular and, to a lesser extent, Cr, Ni, Cu, Fe and Ca, may be expected to be mobile during alteration processes. The results of the present study are in essential agreement with that of Marsh and Eales (1984) regarding the elements mentioned above, with the exception of Fe, Cr and Ni, but the scale of alteration (mobility) or compositional variation

is less than that encountered in the Central area. It should also be obvious that we have not in general been able to distinguish between the effects of hydrothermal alteration and surface weathering, and it is not clear how the effects of these processes can be evaluated separately.

VII. DESCRIPTIVE GEOCHEMISTRY OF ETENDEKA FORMATION MAGMA TYPES

The main purpose of this section is to describe the salient features of the elemental and isotopic geochemistry of the various Etendeka magma types. Attention will also be directed to the compositional variations within and between the various magma types, although the latter aspect will specifically be discussed in the following section. Brief comparisons will be made, where appropriate, to compositionally similar magma types in other areas of the Karoo Igneous Province; however, see Duncan *et al.* (1984) for a detailed treatment of this topic.

The major element and most of the trace element data presented and discussed in this paper have been obtained by X-ray fluorescence spectrometry (XRF). Eighty-four samples have been analysed in this way, commonly for 24–27 elements. A sub-set of 13 samples have been analysed for the REE, Cs, Th, U, Hf and Pb by spark source mass spectrometry. These methods are described in Appendix 1, and the data reported in Microfiche Cards 1 and 2 attached to this volume. Microfiche Card 1 reports measured data while Microfiche Card 2 contains the elemental data recalculated to 100% on a volatile-free basis. It is important to note that in the diagrams that follow all elemental data are plotted on a volatile-free basis (i.e. from Microfiche Card 2). Sub-sets of the Etendeka samples have also been analysed for their Sr-, Nd- and Pb-isotopic

TABLE VII
Pb and Pb-isotope Compositions for Namibian
Karoo Volcanic Rocks

Sample	²⁰⁶ Pb*	²⁰⁷ Pb*	²⁰⁸ Pb*	Pb‡
	²⁰⁴ Pb	²⁰⁴ Pb	²⁰⁴ Pb	
Etendeka Formation (northern Namibia)				
Regional dolerite				
KLS44	18.59	15.63	38.56	2.6
Horingbaai dolerites				
KLS122	17.63	15.53	37.44	
KLS145	17.62	15.52	37.40	2.7
Tafelberg dolerites				
KLS38	18.55	15.64	38.63	
KLS48	17.30	15.55	37.92	
KLS100	17.62	15.53	37.47	29.5
Tafelberg basalt suite				
KLS22	18.86	15.69	38.89	12.2
KLS24	18.65	15.66	38.88	4.9
KLS40	18.78	15.68	38.87	11.7
KLS42	18.67	15.66	38.81	15.2
KLS46	18.81	15.68	38.84	5.3
KLS53	18.95	15.69	38.88	
KLS98	18.62	15.66	38.97	16.4
Tafelberg latites				
KLS69	18.50	15.66	38.96	33.0
KLS71	18.43	15.67	38.90	
Tafelberg quartz latites				
KL20	19.22	15.75	39.02	
KLS36	19.00	15.75	39.04	37.7
KLS51	19.18	15.77	39.08	31.8
Lesotho Formation (southern Namibia)				
MT42‡	18.13	15.60	38.22	

* Errors on isotopic ratios = 0.1% (i.e. 0.018 on ²⁰⁶Pb/²⁰⁴Pb, 0.015 on ²⁰⁷Pb/²⁰⁴Pb and 0.04 on ²⁰⁸Pb/²⁰⁴Pb) for Etendeka Formation samples. Analyses by P.J. Betton.

‡ Data produced by isotope dilution (accuracy 1%).

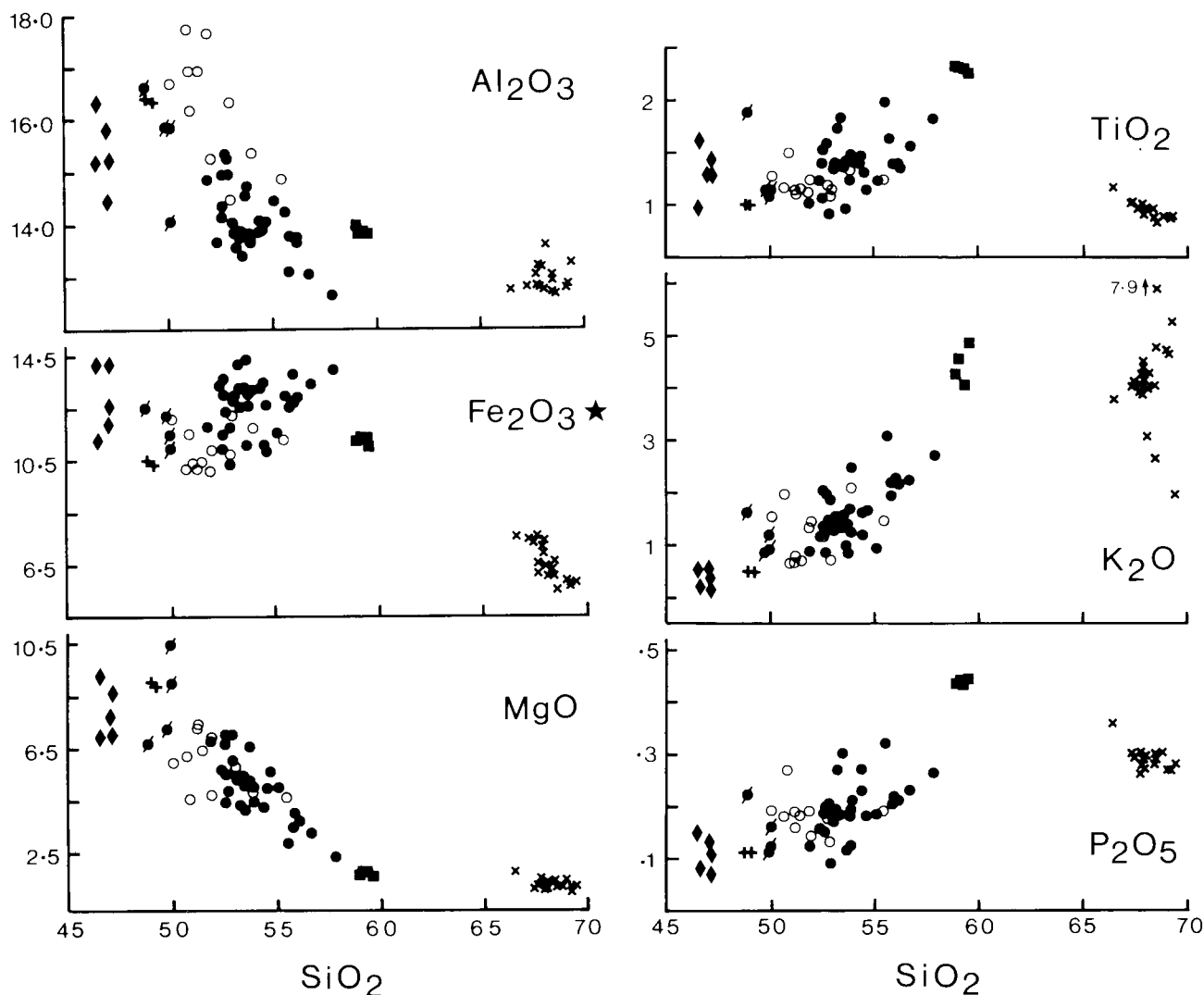
‡ MT42 is sample from centre of Tandjiesberg sill dated at 182 m.y. (Richardson, 1984). Unpublished Pb-isotope data (Richardson, pers. comm.) are given here to facilitate comparison with regional dolerite KLS44 shown above.

compositions. Details of the experimental techniques used and the data obtained for $^{87}\text{Sr}/^{86}\text{Sr}$ and $^{143}\text{Nd}/^{144}\text{Nd}$ may be found in Bristow *et al.* (1984) and Hawkesworth *et al.* (1984) respectively. The Sr-isotope data and some of the Sm and Nd concentration data from these references are also contained in Microfiche Cards 1 and 2. The Pb-isotopic data have not been reported before and are given in Table VII; analytical techniques are described by Betton *et al.* (1984).

At this stage we should mention that we have been greatly aided in our choice of samples for final quantitative analysis, not only by petrographic observations, but by obtaining semi-quantitative XRF data from a technique we have termed "slab analysis" on a larger suite of samples than reported here. This technique involves measurement of selected elements (Si, Fe, K, Rb, Sr) on circular polished discs or slabs of the rocks which are placed directly in the sample holders of the X-ray spectrometer. Details of the technique and its reliability are described in Appendix 1. This technique is particularly effective for fine- or even-grained samples such as those described here and has been most useful for preliminary classification and stratigraphic

purposes (cf. Fig. 6). Furthermore we can be confident that we have encompassed the spectrum of compositions represented in the samples collected for this study. Note, however, that the "slab analysis" data have not been used in the diagrams that follow.

It should also be noted that reference to normative mineralogy is that derived from the volatile-free data in Microfiche Card 2. For most of the samples the difference between these norms and those calculated directly from measured concentrations is slight and insignificant. However, in the case of the Albin lavas, where CO_2 has been determined, large amounts of calcite (5–15%) appear in the norms calculated from measured data. On a volatile-free basis the calcite of course disappears from the norm, and the effective result of this is for olivine to appear in the normative mineralogy for some samples as opposed to quartz in the case of norms calculated directly from measured data. The former observation is in accord with the petrographic evidence of olivine pseudomorphs in the Albin lavas (Section V-B) and is thus considered to be a truer reflection of the normative mineralogy of the



- Tafelberg basaltic rocks ◆ Horingbaai dolerites ■ Tafelberg latites
- ▲ Tafelberg olivine dolerites + Regional dolerites × Tafelberg quartz latites
- Albin basaltic rocks

Figure 14

Plot of major elements vs. SiO_2 (%). All data in this and following diagrams normalized to 100% on a volatile-free basis. Legend shown on diagram also maintained in successive diagrams. Sample numbers shown are prefixed KLS unless otherwise shown.

unaltered lavas. For both sets of norms an oxidation ratio for Fe₂O₃/FeO of 0.15 has been used. This is considered reasonable for the basaltic rocks in general but may be low for the evolved basalts, latites and quartz latites.

In order to facilitate discussion and comparison the same set of diagrams is used throughout this section. These include data for *all* Etendeka magma types. Figs. 14 and 15

are plots of selected major and trace elements vs. SiO₂, the choice of the latter being an obvious one in view of the large overall variation shown by the various rock types (see also Table I). Fig. 16 is a plot of three immobile constituents Ba, Nb and TiO₂ vs. another immobile incompatible element Zr, and has been chosen to portray the varying degrees of geochemical coherence amongst the incompatible

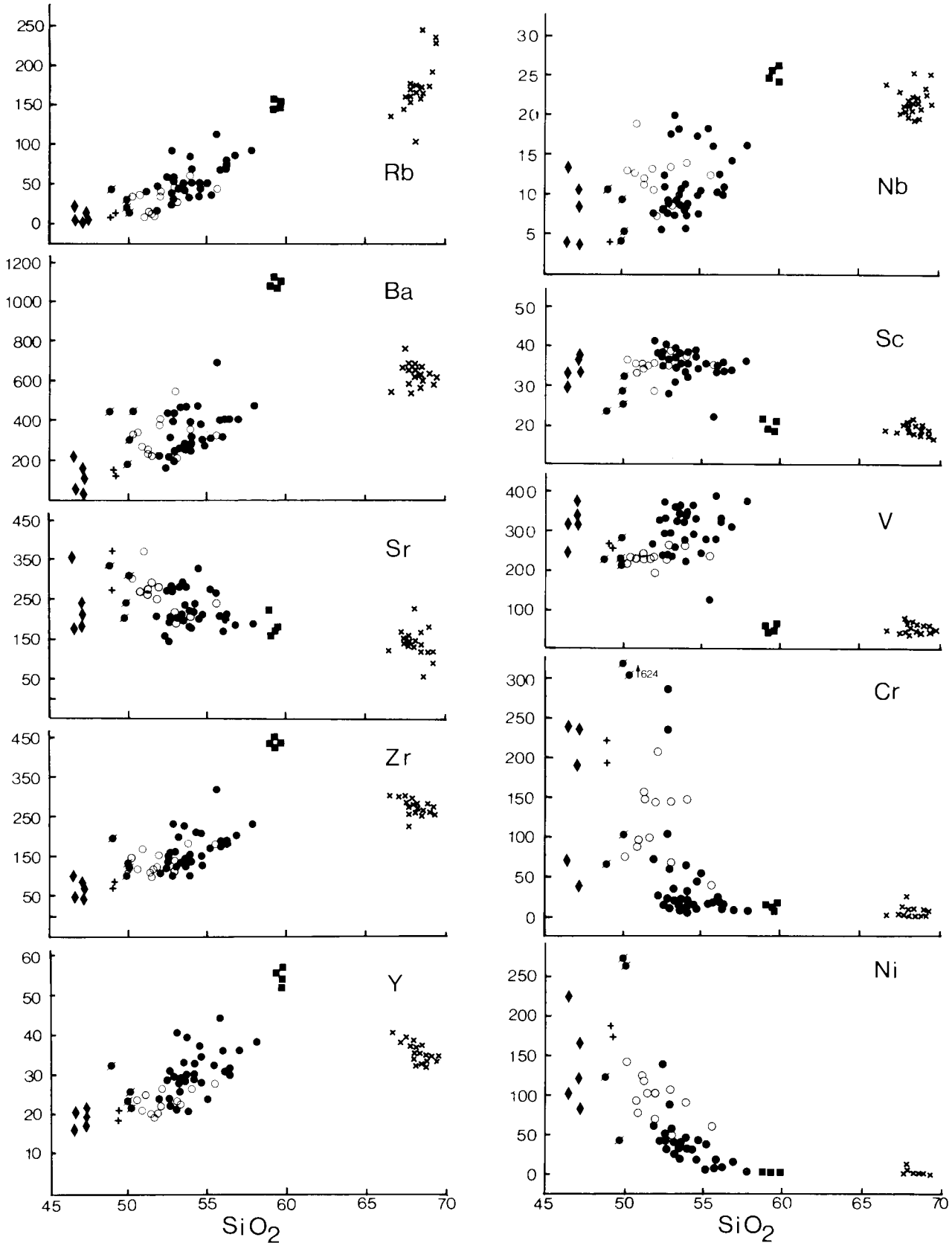


Figure 15
Plot of trace elements (ppm) vs. SiO₂ (%). See Fig. 14 for legend and other details.

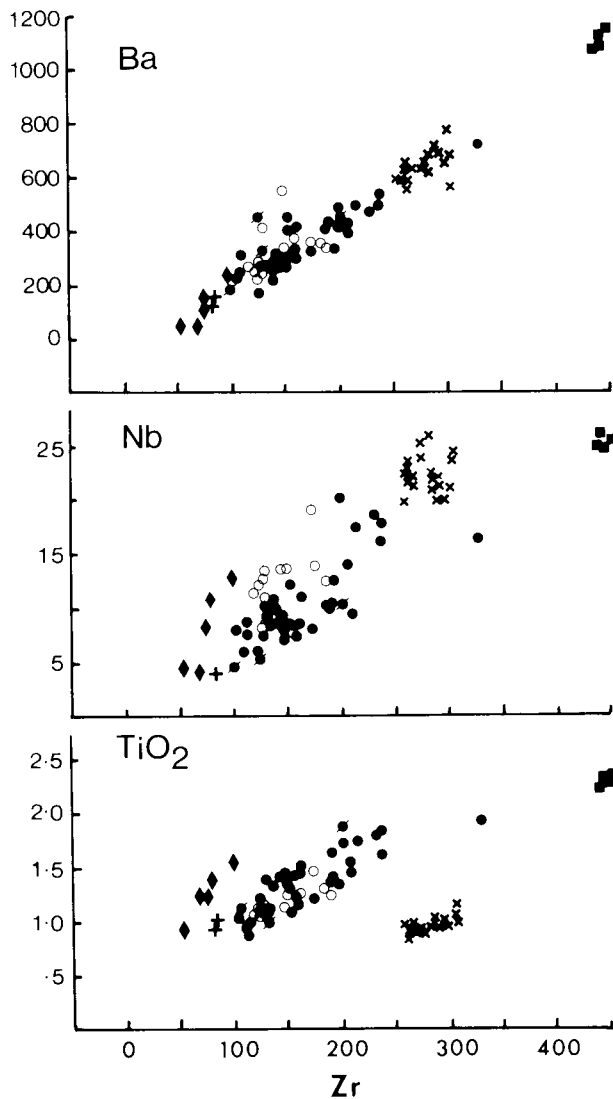


Figure 16

Plot of Ba, Nb and TiO_2 vs. Zr. See Fig. 14 for legend and other details. TiO_2 in %; Ba, Nb and Zr in ppm.

elements. Fig. 17 is a standard rare-earth element (REE) chondrite normalized diagram while Figs. 18 and 19 are standard Rb-Sr and Sm-Nd isochron plots respectively. Fig. 20 illustrates the Pb-isotope systematics observed. The isotopic relationships are an integral and essential feature of the geochemistry and of our interpretation of the petrogenesis of the Etendeka rocks and hence it is necessary to discuss them at the onset together with bulk and trace chemistry. Finally, it should be noted that the symbols characterizing the various rock types are the same in all diagrams that follow and which use analytical data, with the exception of Fig. 17 (REE plot). The terminology employed is given in the caption to Fig. 14 and memorization thereof will facilitate discussion and interpretation.

A. Basic Magma Types

1. Tafelberg basalts and dolerites

Since the geochemistry of the Tafelberg basic lavas and the dolerites that intrude them is similar, we have chosen to discuss them as a group (see also Section III-C). The notable exceptions are the four ophitic olivine-bearing dolerites (KLS38, 48, 100, 186) which are easily recognized in Figs. 14 and 15 by virtue of their lower SiO_2 contents. Nevertheless, their overall geochemistry (see, for example, inter-element relationships in Fig. 16) does not suggest any reason why they should be treated separately.

Apart from the four dolerites mentioned above, which have 49–50% SiO_2 , the remaining Tafelberg basic rocks show a large range in SiO_2 content (51.8–57.8% as indicated for samples KLS24 and 42 in Table I). We have previously referred to these rocks as basalts and evolved basalts, and specifically do not wish to delineate a compositional boundary between these two “end members”, since it is the continuous range in lava compositions that we wish to draw attention to and which we believe is important for the petrogenesis of these rocks (Figs. 14, 15 and 16). Apart from the four olivine-bearing dolerites, only one of the lavas is olivine normative, with the remaining lavas and dolerites being quartz normative (although a few samples are only just quartz normative). Two dolerites and one lava sample have Mg-numbers between 68–61, with all other samples having Mg-numbers within the range 60–28. As a group, therefore, the Tafelberg lavas and dolerites are evolved rocks, and none of them can be considered as primitive or primary in the sense that they can be regarded as being in equilibrium with upper mantle olivines (Cox, 1980; Cox *et al.*, 1984). This is supported by the generally lower Ni and Cr, and higher incompatible element concentrations (Figs. 15, 16 and 17) when compared to other “typical” flood basalts such as the Lesotho Formation of the Central area (Marsh and Eales, 1984; Duncan *et al.*, 1984).

To a first approximation the Tafelberg rocks exhibit many of the features of gabbroic crystal fractionation. Thus amongst the major elements the decrease of MgO , Al_2O_3 and CaO (not shown) and the increase of Fe_2O_3^* , TiO_2 , K_2O and P_2O_5 with increasing SiO_2 content (Fig. 14) is as expected. Likewise the trace element variations (increase of incompatibles and REE, decrease of Ni and Cr, and constancy of inter-element ratios involving TiO_2 , Ba, and Nb with Zr) are entirely rational as shown in Figs. 15, 16 and 17. However, the ranges of concentration involved, especially for major elements (Table I), are large, specifically the marked increase of SiO_2 with decreasing MgO , or vice versa (Fig. 14). Cox (1980) has shown that for many tholeiitic suites protracted fractionation of olivine, clinopyroxene and plagioclase often leads to a buffering effect such that SiO_2 , for example, only shows a slight increase in concentration for up to 60% crystal fractionation. Thus the marked increase of SiO_2 in the Tafelberg lavas requires special attention.

The rational behaviour of the major and trace element variations discussed above must be coupled with the isotopic variations encountered in the Tafelberg basic rocks. In Fig. 18 the $^{87}\text{Sr}/^{86}\text{Sr}$ ratio apparently increases in a regular manner with the Rb/Sr ratio and, by inference, with SiO_2 content as shown by the location of samples KLS24 and 42 on the diagram (see Table I). Fig. 19 shows variation also of the $^{143}\text{Nd}/^{144}\text{Nd}$ ratio, although correlation with

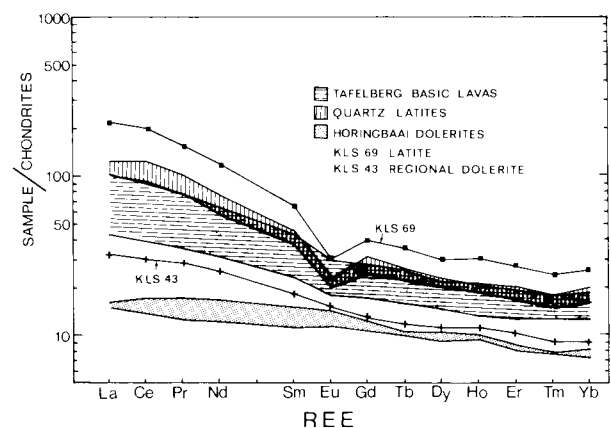


Figure 17

Chondrite-normalized REE diagram for Etendeka volcanics.

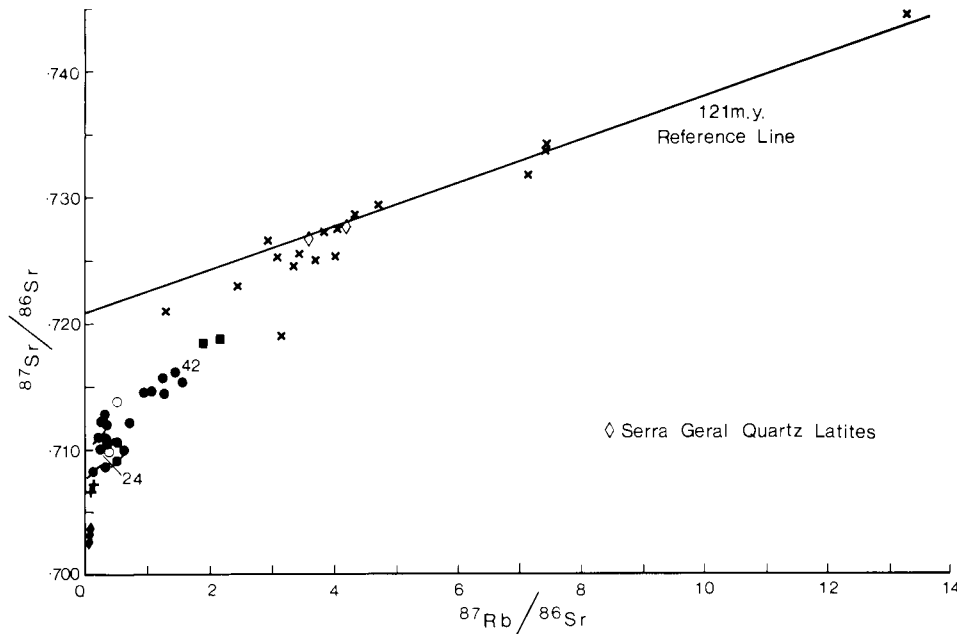


Figure 18

Rb-Sr isochron diagram for Etendeka and Brazilian volcanics. See Fig. 14 for legend and other details.

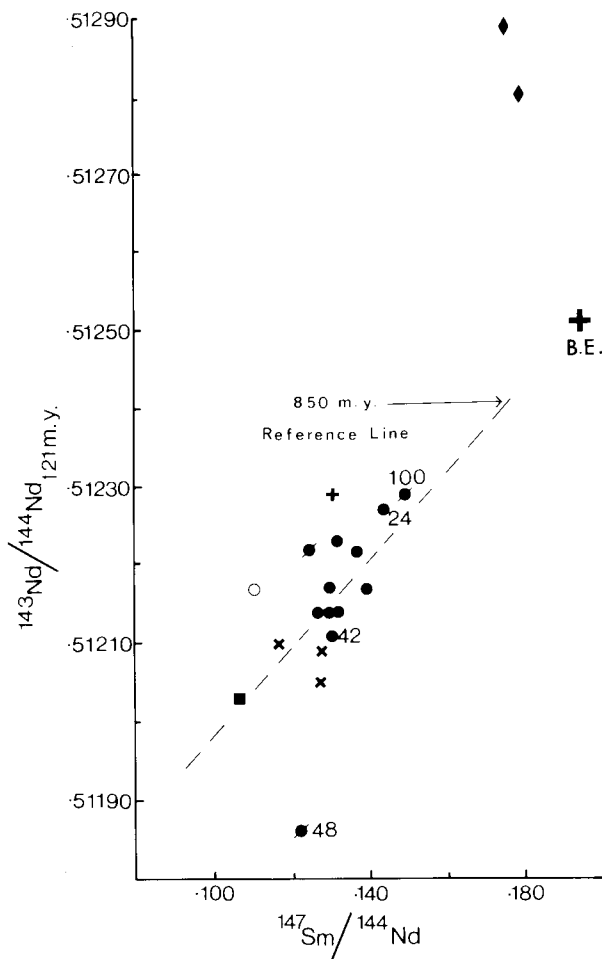


Figure 19

Sm-Nd isochron diagram at 121 m.y. Bulk earth (BE) calculated according to data in Fig. 23. See Fig. 14 for legend and other details.

Sm/Nd is not as marked as in the Rb-Sr diagram. Nevertheless, the relative positions of samples KLS24 and 42 in Fig. 19 may be noted and compared with their positions in Fig. 18. At first sight inspection of Fig. 20 would also suggest regular variation in Pb-isotopic compositions for the Tafelberg lavas. However, in this case samples KLS24 and 42 have virtually identical Pb-isotopic compositions (Table VII) with sample KLS100 having the least radiogenic Pb-isotopic composition amongst the Tafelberg basic rocks, similar to those of two primitive Horingbaai dolerites. These observations imply that no simple relationship exists between the Pb-, Sr- and Nd-isotopic systems. Additionally the "aberrant" behaviour of sample KLS48 in Figs. 19 and 20 can also be noted, as compared with its behaviour in Fig. 18 where it is the least radiogenic of the Tafelberg rocks. This section has deliberately not speculated on possible Rb/Sr, Sm/Nd and U/Pb fractionation since any implied non-coherency of these ratios and the reasons therefor would involve assumptions that are model dependent. Mention has so far not been made of the actual magnitude of the isotopic ratios involved. To take but one isotopic system, initial $^{87}\text{Sr}/^{86}\text{Sr}$ ratios for the Tafelberg rocks range from 0.7080 (KLS48) to 0.7135 (KLS42). These ratios are high for continental flood basalts in general, and are also on average higher than for any other basic magma type in the Karoo Province, although some basic rocks from the southern Lebombo reach values of 0.711 (Bristow *et al.*, 1984). Without wishing to prejudice the significance of these high ratios many isotope cognoscenti would attribute such ratios to continental crustal contamination (e.g. Faure *et al.*, 1974; Moorbath and Thompson, 1980; Carlson *et al.*, 1981; Mahoney *et al.*, 1982) or a crustal imprint of some sort (Hofmann and White, 1982). Thus the high Sr- (and low Nd-) isotope ratios deserve special attention in any mechanism proposed to account for the petrogenesis of the Tafelberg basic magmas.

Another point of relevance concerns the variation of composition with height in the lava sequence, since some authors (e.g. Faure *et al.*, 1974; Mahoney *et al.*, 1982) have observed regular elemental and isotopic variations with stratigraphic position in a lava pile. At the Tafelberg type-locality the three basic lava units are interbedded with a latite and two quartz latite units. A profile of SiO_2 content has previously been presented in Fig. 6. Inspection of the

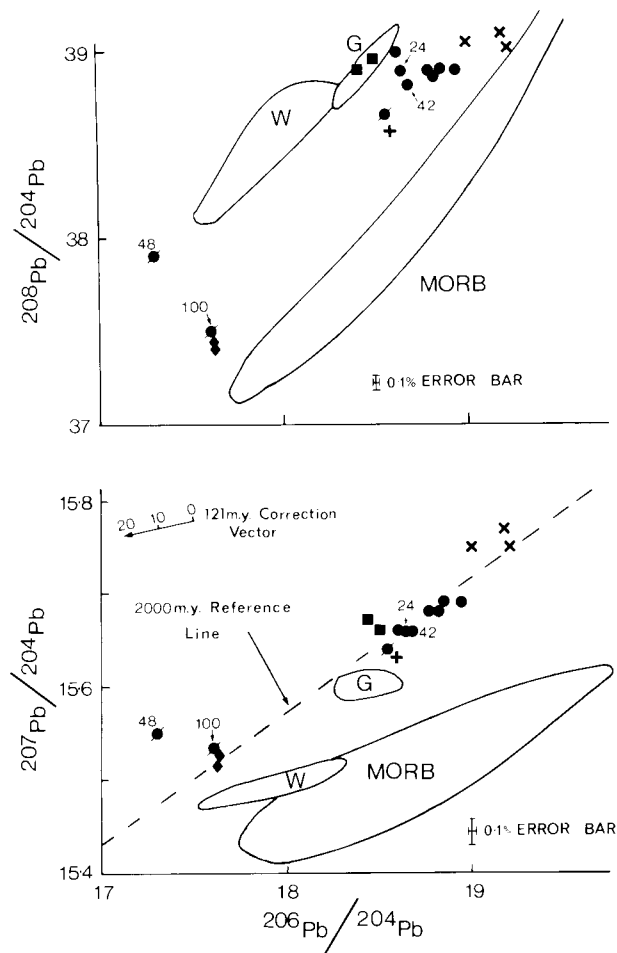


Figure 20

$^{208}\text{Pb}/^{204}\text{Pb}$ vs. $^{206}\text{Pb}/^{204}\text{Pb}$ and $^{207}\text{Pb}/^{204}\text{Pb}$ vs. $^{206}\text{Pb}/^{204}\text{Pb}$ ratio diagrams for the Etendeka volcanics. Legend as in Fig. 14. The fields of data for the Walvis Ridge (W), Gough (G) and mid-ocean ridge basalts excluding the Walvis ridge (MORB) are plotted for comparison, using data from Tatsumoto (1978), Church and Tatsumoto (1975), Sun (1980), Cohen *et al.* (1980), Dupré and Allègre (1980) and Richardson *et al.* (1982). On the $^{207}\text{Pb}/^{204}\text{Pb}$ vs. $^{206}\text{Pb}/^{204}\text{Pb}$ diagram a 2000 m.y. reference line, and a correction vector for 121 m.y. graduated in μ values, are included.

other major element and the trace element data, together with our unpublished "slab analysis" data, shows no regular or systematic variation of concentration or composition with height in the basaltic sequence as a whole, nor are there any compositional trends within the individual basaltic units as the latite and quartz latite units are approached. We have insufficient data to evaluate whether any systematic or regular isotopic variations are present in the Tafelberg sequence. There is, however, a hint that the ratio of evolved basalt to basalt may be higher in the top basaltic unit, although we have fewer samples in the two lower units. In this regard, we note that the majority of our more evolved basalts, including the most evolved sample KLS42, are from the coastal region near the Huab River mouth. This could again be due simply to sampling bias, but recent mapping by S. C. Milner (pers. comm.) north of this area suggests that the evolved basalts may well be more common in the coastal region. If this is confirmed by further work, then it will clearly have implications for the stratigraphy and petrogenesis of the Tafelberg basaltic rocks.

The foregoing has already indicated that the Tafelberg basic magmas are more evolved than the widespread Lesotho Formation magma type, representatives of which are present in the Kalkrand Formation near Mariental in southern Namibia (Fig. 1). The regional study by Duncan *et*

al. (1984) indicates that the Tafelberg basic magmas have higher K_2O , TiO_2 , Rb, Ba, Zr, and LREE contents than any of the other Central area types except the Pronksberg high-K basalts. They also have higher concentrations of these elements when compared to the Sabie River Formation basalts of the southern Lebombo, but are not as enriched in these constituents as the Sabie River basalts of the northern Lebombo. Taken as a whole the Tafelberg basic suite is different from all other Karoo basic lavas by virtue of its age, mineralogy, major and trace element composition and variation, and especially the elevated initial $^{87}\text{Sr}/^{86}\text{Sr}$ ratios shown by this suite. Having characterized this important magma type, discussion of and comparison with the other Etendeka magma types is now facilitated.

2. Albin basalts

It will be recalled that the Albin lavas underlie and are in part interbedded with the Tafelberg lavas. We have not done much work on the Albin lavas for various reasons and have carried out no analyses on Albin dolerites since the presence of the latter was only discovered late in this study. Of the 12 analyses of Albin lavas shown on Microfiche Card 1, nine are from a stratigraphic section at the Albin type-locality (samples KLS106–147). However, the remainder of the samples in the latter numbered sequence have all been analysed by our "slab analysis" technique so that we are confident that we have covered the compositional range present at the type-locality. As mentioned previously in this section and in Section VI, the samples from this locality are heavily calcitized. Although we have indicated that recalculation of the analytical data on a volatile-free basis leads to data which can be used with some confidence (except perhaps for Ca and Sr) the use of analyses such as these with such high CO_2 contents must remain somewhat suspect. As will be shown we believe that the Albin basalts merely represent a variant of the Tafelberg basic magma type, and this is another reason why we have not studied these rocks more thoroughly. Recent field work has shown the presence of thin and poorly exposed Albin lavas amongst the sand dunes north of the Huab River mouth and as far as Terrace Bay (Fig. 1) and these, together with Albin dolerites, are currently being investigated in a follow-up study. Two samples that have already been analysed (KLS190 and 198), while somewhat altered, do not contain replacement calcite that is so diagnostic of the rocks at the Albin locality.

Most of the Albin lavas have SiO_2 contents within the range 50–53%, with two samples having somewhat higher values of 53.9 and 55.4%. Three samples are olivine normative, and of the remaining samples all but one have from 1–4% quartz in the norm, the exception being the sample with highest SiO_2 (KLS144) which has 9% quartz in its norm. Mg-numbers range from 62–48. These features show that as a group the Albin lavas are also not primitive or primary in any sense, but they are not as evolved as the Tafelberg basic rocks, as may be noted in Figs. 14 and 15.

The most striking feature of the major element data shown in Fig. 15 is the generally higher Al_2O_3 contents of the Albin lavas, consistent with the high proportion of phenocrystal plagioclase in these rocks. The trend of the Albin lavas in the Al_2O_3 vs. SiO_2 plot suggests major plagioclase control, together with minor clinopyroxene addition, and hence we currently view these lavas as partial cumulates and thus not entirely representative of liquid compositions. Consequently there is a dilution effect for oxides such as MgO and Fe_2O_3^* although the effect has perhaps produced more striking reduction in these oxides than might be anticipated. CaO (not shown) is consistently and on average (10.1%) higher than in the Tafelberg basic rocks (ave. = 8.6%) but to what extent this is due to plagioclase control or to calcitization cannot be stated.

Amongst the trace elements Sr is on average, as expected, somewhat higher in the Albin lavas (ave. = 268 ppm) as compared with the Tafelberg basic rocks (ave. = 229 ppm). However, the most obvious difference between the Tafelberg basic rocks and the Albin lavas is indicated by the higher Ni and Cr contents of the latter (Fig. 15), reflecting again the less evolved nature of the Albin lavas and consistent with the presence of olivine pseudomorphs in these rocks. Apart from these differences there is no real evidence to suggest that we are dealing with entirely separate magmas derived from separate sources or produced by different processes. Inter-element ratios of the less mobile incompatible trace elements (Fig. 16), together with others such as Zr/Y (not shown), support the above contention, and indicate that the same rational relationships observed in the Tafelberg rocks apply also in the Albin lavas. We have only one REE analysis (for the most evolved sample KLS144) which, although not shown in Fig. 17, plots within the field of the Tafelberg samples with a similar slope to the more evolved varieties of the latter. Likewise the two $^{87}\text{Sr}/^{86}\text{Sr}$ and single $^{143}\text{Nd}/^{144}\text{Nd}$ analyses (Figs. 18 and 19) do not suggest any marked isotopic differences in the two magma types (no Pb-isotopic data are available for the Albin lavas).

Taken as a whole the evidence suggests that the Albin lavas are plagioclase-enriched variants of the less evolved varieties of the Tafelberg magma type which had not undergone marked olivine fractionation (cf. Ni in Fig. 15). The expected lower density of the plagioclase-rich Albin lavas would be consistent with their being emplaced first from a fractionating sub-crustal magma source. However, neither the density difference nor the major and trace element differences resulting from plagioclase fractionation have been quantitatively evaluated, and the implied correlation of chemical and isotopic properties in the Tafelberg basic rocks indicates that such evaluation would not be simple. Further work on the Albin lavas (and dolerites) is clearly required but their altered nature has inhibited us from carrying out detailed calculations at this stage. If our supposition about the petrogenesis of the Albin lavas is correct then they are not central to the arguments we shall make in later sections, where the more abundant Tafelberg basic rocks, being more closely related to liquid compositions and being less altered, are extensively used in petrogenetic modelling. For these reasons we have presented our tentative conclusions in this descriptive section, since no further detailed discussion of the Albin lavas will be given in subsequent sections of this paper.

3. Horingbaai dolerites

These dolerites, typically thin dykes and sills, are mainly found in the Albin type-section where they intrude the Albin lavas, although one sample (KLS157) occurs in basement granites. Surprisingly they are considerably less altered than the Albin lavas as shown by the presence of relatively unaltered olivine. As a group they can easily be distinguished from all other Etendeka basic rock types.

Fig. 14 indicates that on the basis of SiO_2 contents alone they can be distinguished from the other Etendeka basic rocks; their SiO_2 contents are low and relatively uniform (46.5–47.2%). Consequently oxides such as MgO are generally higher in concentration except for the other olivine-bearing rocks, while other oxides such as K_2O are lower in concentration when compared to the other Etendeka basic rocks. Mg-numbers range from 65–53. They are all olivine normative and their olivine and plagioclase compositions are respectively the most Mg-rich and Ca-rich we have encountered (Section V–C). The trace element concentrations (Fig. 15) mirror the major element compositions, i.e. generally lower incompatible element concentrations (Rb, Ba, Zr etc.), extending also to the

REE (Fig. 16), and high but variable Ni and Cr concentrations when compared to other Etendeka basic rocks, excepting again the other olivine-bearing dolerite types.

There are three critical features of the Horingbaai dolerites that require highlighting. Firstly, despite their constant SiO_2 concentrations, there is a fair range in concentration for the other major elements (Fig. 14) and an even larger variation for trace elements (Fig. 15). The enrichment in trace elements from least evolved to most evolved varieties is also not constant (e.g. $\text{Rb} \times 10.4$; $\text{Ba} \times 4.6$; $\text{Nb} \times 3.5$; $\text{Zr} \times 1.9$; $\text{V} \times 1.5$). Secondly, the trends indicated by the Horingbaai dolerites in Figs. 14 and 15, and for Nb and TiO_2 vs. Zr in Fig. 16 are distinctly displaced from the trends shown by the Tafelberg and Albin basic rocks implying of course that the Horingbaai samples have different Ti/Zr and Zr/Nb ratios. In the third place, although only the two least evolved samples (KLS122 and 145) have been analysed for REE and for their Sr-, Nd-, and Pb-isotopic compositions, these data indicate that these samples are geochemically the most primitive we have encountered in the Etendeka. This may easily be seen in Figs. 17, 18, 19 and 20. In fact these two samples have distinctive depleted MORB-type characteristics, contradicting the assertion that no continental tholeiitic basic rocks have such characteristics (Thompson *et al.*, 1983).

Thus the Horingbaai dolerites are easily distinguished from all other Etendeka magmas as a separate and discrete magma type with a distinctive composition, depleted in incompatible elements. The only known counterparts in the Karoo Province are the Rooi Rand dolerites from the Lebombo which have similar REE patterns and Sr- and Nd-isotopic compositions, but which do have markedly different major element compositions (Armstrong *et al.*, 1984; Duncan *et al.*, 1984; Hawkesworth *et al.*, 1984). We consider it no coincidence that the latter are also emplaced as late dykes in the Lebombo basalts, and this will be discussed in subsequent sections.

4. Regional dolerites

These dolerites have been designated as those which cut Karoo sediments but which have not been observed to intrude the Etendeka lavas. Only two (KLS43 and 44) have been analysed and although they were sampled from different dykes their compositions are so similar that they can be treated as a single sample.

Both these olivine-bearing ophitic dolerites predictably are olivine normative. Their SiO_2 and MgO contents of around 49% and 8.9% respectively, and their Mg-numbers of around 66, together with relatively high Ni (~180 ppm) and low incompatible element concentrations indicate that they represent relatively unevolved basaltic magmas. In fact their geochemistry can be summarized by pointing out that in most of the diagrams used in this section (Figs. 14–20) they occupy a position intermediate between the primitive Horingbaai dolerites and the less evolved Tafelberg and Albin basaltic rocks. This is particularly well demonstrated in the REE and Rb-Sr isochron plots (Figs. 17 and 18).

The question of whether or not these regional dolerites are a separate magma type or whether they are related to the Horingbaai dolerites or the Tafelberg and Albin basaltic rocks is explored in subsequent sections. They are, however, important since their mineralogy and elemental and isotopic compositions indicate that they are similar in composition to the Lesotho Formation basalts of the Central area, although the two rocks concerned are slightly more primitive than the average Lesotho Formation basalt (Marsh and Eales, 1984). Positive identification as Lesotho Formation magmas would extend the presently known geographical coverage of the latter and furthermore raises

the question of whether these rocks are the first manifestation of Karoo igneous activity in this area, bearing in mind the older ages obtained for other regional dolerites which intrude basement rocks (Siedner and Mitchell, 1976 and Table II). In this connection cognizance should be taken of the Kalkrand formation basalts in southern Namibia which are indistinguishable in composition from the Lesotho Formation basalts (Duncan *et al.*, 1984) and which have a similar age (184 m.y) to the latter (Siedner and Mitchell, 1976; Fitch and Miller, 1984).

B. Tafelberg Latites

As mentioned previously these enigmatic rocks are known only from one unit at and around the Tafelberg locality, where they overlie the lower basaltic unit (Fig. 6). Their SiO₂ contents of around 59% and their bulk chemistry (Table I) reveals them to be truly intermediate rocks, with substantial quartz in their normative mineralogies, but they have some unusual and distinctive geochemical features.

Their SiO₂ contents dictate that they occupy an intermediate position in the major and trace element diagrams (Figs. 14 and 15) between the evolved Tafelberg basalts on the one hand and the quartz latites on the other. Many of the trends on these diagrams are suggestive of a fractionation sequence between these magma types but closer scrutiny reveals obvious difficulties with such an approach. This aspect is dealt with in the next section but several important features need to be noted here. First, the concentrations of K and incompatible elements are extremely high for rocks of this bulk composition, consistent with the presence of alkali feldspar, and not plagioclase, in these rocks (Section V-D). In fact, apart from K and Rb, the concentrations of all other incompatibles are higher than in the quartz latites (Figs. 14, 15, 16, 17 and Table I). This feature sets the latites apart from all other Etendeka volcanics, and must be explained by any proposed hypothesis for their petrogenesis. In the second place the isotopic characteristics of the latites present further difficulties. In the Rb-Sr diagram (Fig. 18) the latites again occupy an intermediate position between the evolved Tafelberg basic rocks and the quartz latites, but in the Sm-Nd diagram (Fig. 19) the single latite analysed has the lowest ¹⁴³Nd/¹⁴⁴Nd ratio of all samples, consistent with its REE plot (Fig. 17). In contrast the Pb-isotopic data (Fig. 20) show the latites to have closest affinities with the Tafelberg basic rocks but displaced to lower ²⁰⁶Pb/²⁰⁴Pb values relative to equivalent ²⁰⁸Pb/²⁰⁴Pb and ²⁰⁷Pb/²⁰⁴Pb ratios. All in all, the combination of high incompatible element abundances and the isotopic data discussed above imply a complex pre-history for these rocks.

The only comparable rocks to the latites in the Karoo Province are the small amounts of intermediate rocks (Belmore andesites and Pronksberg and Roodehoek dacites) found as basal lava flows in the Central area (Marsh and Eales, 1984). However, these rocks have lower TiO₂, K₂O, P₂O₅ and incompatible trace element contents, and higher SiO₂, MgO, Cr and Ni contents than the Tafelberg latites (Duncan *et al.*, 1984).

C. Tafelberg Quartz Latites

These acidic rocks are extremely important because of their interbedded nature with the Tafelberg basaltic rocks (Fig. 6). We have collectively termed them quartz latites, although we have further recognized that they can be subdivided into quartz latites and high-K dacites (Section III-D), and will make this distinction where appropriate. The location of the quartz latites and high-K dacites in the two units at the Tafelberg location has been dealt with previously (Section III-B) and will not concern us here.

As a group these rocks show very little compositional variation, apart from a few elements which are discussed

below. Thus SiO₂ contents for 22 samples vary from 66.5–69.2%. Their major and trace element concentrations (Table I) are also not unusual for rocks with SiO₂ contents of this magnitude. Although K has previously been used to discriminate between the quartz latites and the high-K dacites (Fig. 8) it is the variation of K, Rb and K/Rb within both groups, but particularly in the dacites, that is noteworthy. The overall variation in K and Rb is apparent in Figs. 14 and 15. However, while the K/Rb ratio varies from 191–267 in the quartz latites, it shows a variation from 69–254 in the dacites (only three samples). The erratic behaviour of Rb in the dacites is hard to explain, even though some crystal fractionation is suggested by the overall behaviour of K, Rb, Ba, Sr and associated inter-element ratios in the suite as a whole. To take but one example the relative constancy of Ba in both groups (Fig. 15) is at variance with the K/Rb variations and would limit the amount of alkali feldspar fractionation in any simple melting and/or crystallization scheme. Apart from K and Rb, there are also differences in CaO and Na₂O between the two types, with the average dacite having higher concentrations of these oxides as compared to the average quartz latite (Duncan *et al.*, 1984). We have insufficient data to evaluate whether any isotopic differences are apparent between these two felsic rock types.

With reference to the diagrams we have in this section (Figs. 14–20) there are only two points to make. First, it is worth re-emphasizing that apart from K and Rb, the latites have higher incompatible element and REE contents, and lower ¹⁴³Nd/¹⁴⁴Nd ratios than the quartz latites as a group. Secondly, if the latites are ignored and only the elemental data are considered then the variations shown (Figs. 14–17) are qualitatively consistent with an igneous fractionation scheme linking the Tafelberg evolved basalts with the quartz latites, although a large silica gap would now be present. However, the isotopic variations (Figs. 18, 19 and 20) again show the complexity of the processes producing the Etendeka volcanics, or deriving one type from another in any petrogenetic scheme.

The Etendeka quartz latites may finally briefly be compared with the Lebombo rhyolites from the eastern edge of the Karoo Province since these are the only two areas where felsic volcanics occur in any abundance. Duncan *et al.* (1984) have shown that the Etendeka quartz latites generally have similar SiO₂ and K₂O contents to the Lebombo rhyolites but differ from the bulk of the Lebombo rhyolites in having higher TiO₂, MgO and CaO and markedly lower Ba, Zr, Nb and Y contents. The Etendeka samples also have distinctly higher initial ⁸⁷Sr/⁸⁶Sr ratios (~0.720) as compared to the Lebombo rhyolites (~0.704) indicating derivation from very different source areas. Interestingly the criteria used above to distinguish the Etendeka quartz latites from the main Lebombo rhyolites are almost the same as those that can be used to distinguish the latter from the Mkutshane beds. The latter are thin rhyolite flows interbedded within the Lebombo Sabie River Formation basalts and are considered by Betton (1979) to represent extreme examples of contamination of Sabie River Basalt by continental crust.

VIII. PETROGENESIS—I. INTER-RELATIONSHIPS BETWEEN BASALTIC ROCKS, LATITES AND QUARTZ LATITES

A. Introduction

Evaluation of the derivation and petrogenesis of the various Etendeka magmas and rocks described in preceding sections had proved to be a complicated exercise, and we have considered a wide variety of processes by which they could be related or derived. In doing so we have found it convenient to document our treatment of this topic in two separate sections. It seems appropriate at this stage to provide an indication of our

modus operandi and a brief outline of the problems and processes we have investigated, and the conclusions we have reached, in an attempt to provide clarity in the ensuing detailed discussions. We emphasize here that a prime feature that has to be accounted for in all these discussions is the range in composition of the basaltic rocks, specifically for the Tafelberg basaltic suite.

In this section attention is directed first to possible processes by which the three major rock types (i.e. the basaltic rocks, latites and quartz latites) could be related in view of their close association in the field. It can be readily shown that all three major rock types cannot be related by simple melting, crystallization or magma mixing processes. A combined magma mixing-fractional crystallization process specifically involving the abundant Tafelberg basalts and the Tafelberg quartz latites, while more attractive, is rejected on the basis of certain critical inter-element and isotopic relationships. Use of other end-members in a similar process, such as the regional and Horingbaai dolerites, or the latites, is rejected on the same grounds. We will conclude that no simple genetic relationship exists between the three major rock types or, for that matter, between any two of them, in spite of their close association in time and space.

In the next section (Section IX) the major rock types are treated separately. Detailed modelling suggests that the more evolved Tafelberg basaltic rocks can be derived from parental magmas (i.e. the less evolved Tafelberg basaltic rocks), which have a range in isotopic compositions, by simple fractional crystallization. While some crustal contamination cannot be ruled out, there is no convincing

evidence that the range in elemental and isotopic compositions in either the less evolved or more evolved Tafelberg basaltic rocks is due to simple bulk crustal contamination or to combined assimilation-fractional crystallization (AFC). Instead, the available evidence suggests that the parental Tafelberg basaltic magmas, together with the Horingbaai and regional dolerites, are derived from heterogeneous and partly enriched upper mantle source areas.

Following this the compositionally intermediate latites are evaluated in the light of whether they represent mantle derived basaltic magmas which have undergone severe crustal contamination, or whether they are direct crustal melts. Finally, consideration of the quartz latites leaves little doubt that they are of crustal derivation. In this regard brief comparison is made with quartz latites, and also the basaltic rocks, of the Serra Geral Formation in Brazil, since the implied volume relationships of all these rock types bears directly on their ultimate derivation.

B. Simple Mixing and Fractional Crystallization

Because of the close association between the various Etendeka Formation volcanics in the field, and the geochemical relationships described in the previous section, consideration must be given to processes whereby the various rock types could be genetically related. It is important to note that such possible processes must also take into account the compositional variations within the basaltic rocks, particularly those of the Tafelberg type. The distinct isotopic differences between the basalts, latites and quartz latites shown in Figs. 18, 19 and 20 demonstrate that

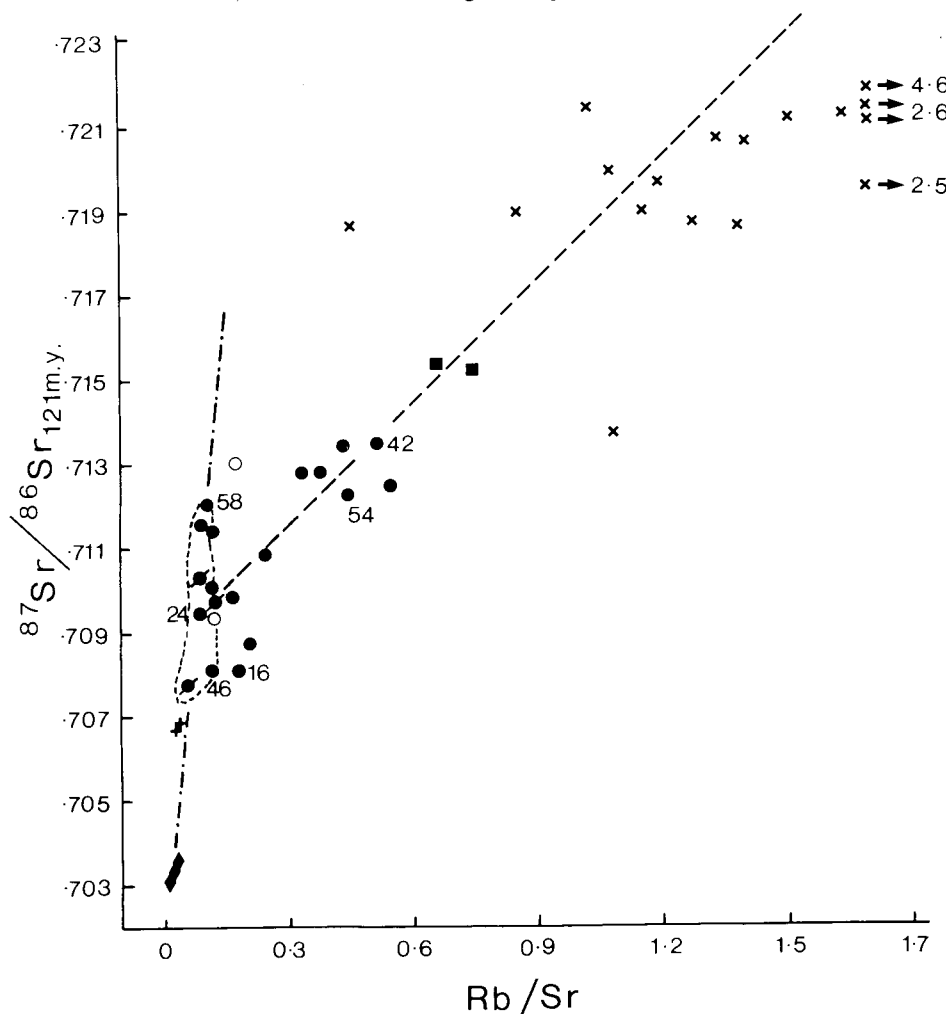


Figure 21

Plot of initial $^{87}\text{Sr}/^{86}\text{Sr}$ ratio vs. Rb/Sr . Circled area (small dashes) encloses less evolved Tafelberg basaltic rocks (Mg-number >55). See Fig. 14 for legend and other details.

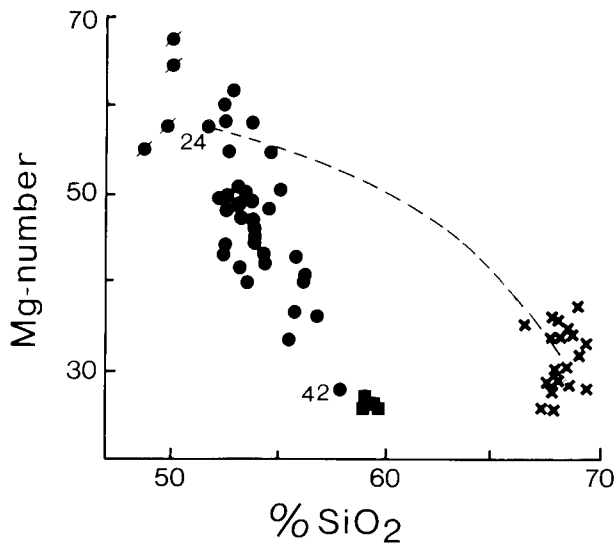


Figure 22

Mg-number vs. SiO_2 plot for Tafelberg-type volcanic rocks. Mixing line between less evolved KLS24 and quartz latites calculated according to Langmuir *et al.* (1978). See Fig. 14 for legend and other details.

they cannot be related by any simple igneous fractionation process or processes. For example, closed system partial melting of a homogeneous mantle source to yield the more primitive basaltic rocks, followed by closed system fractional crystallization to produce the evolved basaltic rocks, latites and quartz latites should result in all these rock types having the same isotopic ratios at the time of emplacement. This is clearly not the case (Fig. 21). On the other hand the isotopic relationships allow the various rock types to be related by some form of mixing process. The possibility of this process being important is also suggested by the interbedding of these rock types within the Etendeka Formation. Thus the dashed line in Fig. 21 could imply a

mixing relationship between typical quartz latite on the one hand and a typical less-radiogenic (and less-evolved) basaltic magma on the other. The more evolved basaltic rocks and the latites could then be interpreted as the result of such a mixing process. However, when considering the elemental compositional data, it is also apparent that the three rock types cannot all be related by any simple mixing relationship. Thus a linear relationship between the different rock types is not observed in many of the plots shown in Figs. 14 and 15. The Ti vs. Zr relationship in Fig. 16 and the magnitude of the Eu anomaly in Fig. 17 likewise argue against a simple mixing relationship. This conclusion is re-inforced by the Mg-number vs. SiO_2 plot in Fig. 22 where the dashed line indicates a calculated mixing line (Langmuir *et al.*, 1978) between less-evolved basalt KLS24 and the average quartz latite. The trend in the basaltic rocks and the latites is clearly displaced from this line. Consequently, it is necessary to consider more complicated processes, specifically those involving combined mixing and fractional crystallization, to test whether the three rock types under discussion are genetically related.

C. Combined Magma Mixing and Fractional Crystallization Processes

In this section we examine in the first instance a mixing-fractional crystallization relationship between the Tafelberg basalts and quartz latites because (a) they are both areally widespread and the most voluminous types in the Etendeka Formation and (b) the significant compositional variation in the basalts is an important feature which requires explanation. In the discussions which follow our principal aim is to answer the following question: "Can the range in the Tafelberg basalt compositions be explained by a mixing-fractional crystallization process involving typical less-evolved Tafelberg basalts (such as KLS24) and average or typical quartz latite?" In doing so it should be borne in mind that the less evolved Tafelberg basalts and the quartz latites exhibit compositional variations within quite narrow limits

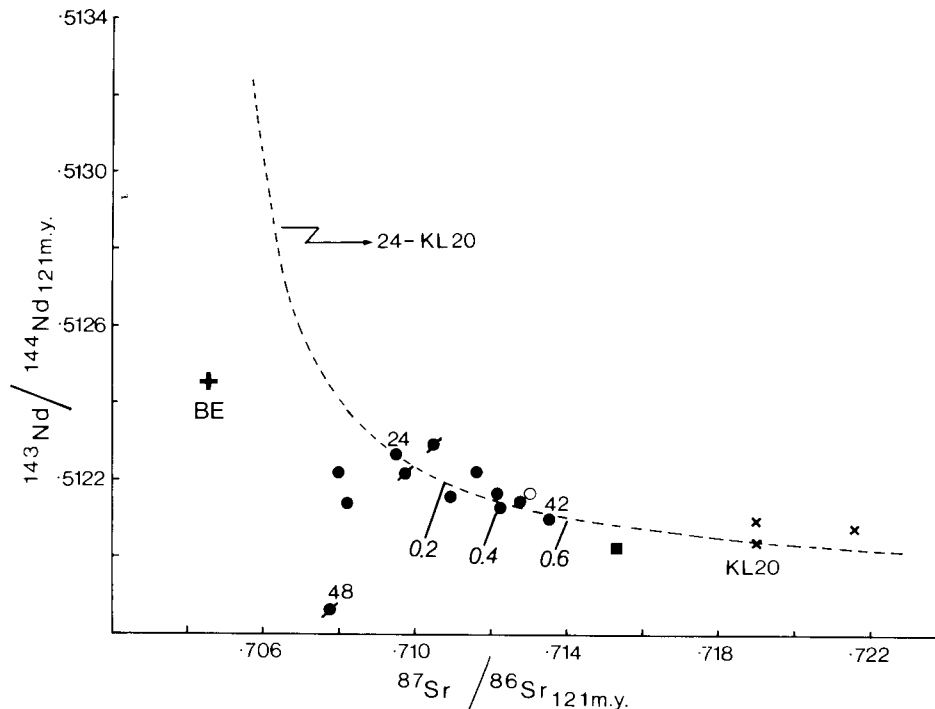


Figure 23

Initial $^{143}\text{Nd}/^{144}\text{Nd}$ vs. $^{87}\text{Sr}/^{86}\text{Sr}$ ratio plot for Tafelberg volcanic rocks. See Fig. 14 for legend. Mixing line between less evolved basalt KLS24 and quartz latite KL20 calculated according to Langmuir *et al.* (1978). Ticks and fractions (0.2, 0.4 etc) along mixing line indicate fraction of admixed KL20. Bulk earth (BE) calculated from present-day reference reservoir $^{143}\text{Nd}/^{144}\text{Nd} = 0.51264$ and $^{147}\text{Sm}/^{144}\text{Nd} = 0.194$, and $^{87}\text{Sr}/^{86}\text{Sr} = 0.7047$ and $^{87}\text{Rb}/^{86}\text{Sr} = 0.086$.

and the use of the average or typical compositions in modelling will yield results applicable to the whole suite of rocks. This evaluation is then extended to consider the role of the latites and the regional and Horingbaai dolerites in other possible mixing relationships.

1. Isotopic constraints

Before evaluating the possible effects of combined magma mixing and fractional crystallization it is appropriate to consider an isotope-isotope initial ratio diagram. On such a diagram it is possible to examine the mixing process alone (if the data are to be interpreted in this manner) and to calculate mixing proportions since fractional crystallization does not affect the position of data points on this diagram provided that mixing precedes crystallization. Fig. 23 is a plot of initial $^{143}\text{Nd}/^{144}\text{Nd}$ vs. initial $^{87}\text{Sr}/^{86}\text{Sr}$ for Tafelberg type rocks only, with a calculated mixing curve between sample KLS24 and quartz latite KL20. The mixing curve fits the data points fairly well and it is apparent from the diagram that in order to generate sample KLS42 (the most evolved Tafelberg basaltic rock) that some 55% admixture of KL20 with 45% KLS24 is required. This figure is high but is not impossible in view of the very evolved nature of KLS42, and with the appreciation that we are discussing a process of magma mixing which does not suffer the same thermal constraints as wall rock assimilation.

2. Inter-element constraints

A large number of computer generated inter-element diagrams have been examined. Some of these suggest that a combined magma mixing and fractional crystallization process is perfectly feasible for deriving the evolved Tafelberg basaltic rocks (and the latites) by fractional crystallization following mixing between a typical less-evolved basaltic magma and a quartz latite magma (e.g. Ba vs. Zr in Fig. 16). However, while many of the diagrams are equivocal in this regard, there are several diagrams that provide strong constraints on the way such a process would have to operate, and we have chosen three to illustrate specifically some of the difficulties involved. Note that only Tafelberg-type rocks are plotted, and that the field containing data points for the less-evolved Tafelberg basalts (Mg-number >55) can easily be distinguished on these diagrams.

Mg-number vs. SiO_2 (Fig. 22): As noted previously, the trend defined by the evolved basalts and the latites diverges markedly from the calculated mixing line between the less-evolved basalt KLS24 and the average quartz latite, with the more evolved basaltic rocks being systematically

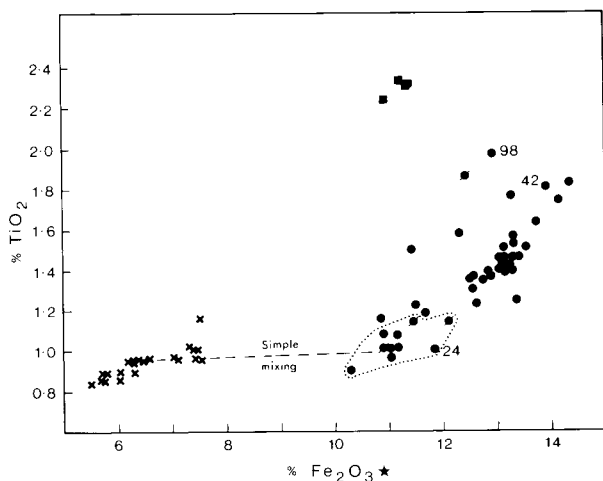


Figure 24

TiO_2 vs. Fe_2O_3^* diagram for Tafelberg volcanic rocks. Circled area encloses less evolved basaltic rocks (Mg-number >55). See Fig. 14 for legend and other details.

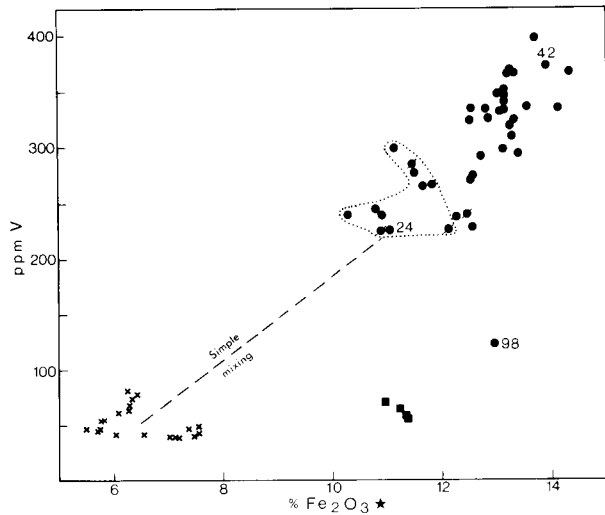


Figure 25

V vs. Fe_2O_3^* diagram for Tafelberg volcanic rocks. Circled area encloses less evolved basaltic rocks (Mg-number >55). See Fig. 14 for legend and other details.

displaced from the mixing line. Any mixing-crystallization process would have to operate in such a way that no products of extensive mixing remain on or near the mixing line, and the subsequent crystallization process requires that the SiO_2 content be held approximately constant (or even reduced) in the production of the evolved basaltic rocks.

TiO_2 vs. Fe_2O_3^* (Fig. 24): In this example the trend of the evolved basaltic rocks is completely displaced from a mixing line joining the quartz latites and the less-evolved basaltic rocks, and no evolved varieties plot near the mixing line. The mixing-crystallization process would have to operate as in the previous example, and the crystallization process could only involve minor Ti-magnetite fractionation, if any. A further example of this type of diagram has previously been presented (TiO_2 vs. Zr in Fig. 16).

V vs. Fe_2O_3^* (Fig. 25): This diagram is particularly important for a number of reasons. In the first place the magma mixing stage of the process must be followed by extensive fractional crystallization, since there are no evolved basaltic rocks which have compositions between KLS24 and the quartz latites. Because the well defined trend between samples KLS24 and KLS42 is also one of increasing SiO_2 (Fig. 22), K_2O and other incompatible elements, it is also necessary that mixing be followed by a proportional degree of fractional crystallization, such that the basaltic rocks with the highest amount of admixed quartz latite would have to have undergone the greatest amount of fractional crystallization. Such a process would also require a systematic increase of initial Sr-isotope ratios within the sequence KLS24 to KLS42 and while this may superficially appear to be true (Fig. 21), it is not strictly correct (see next section). The implied reversal of the crystallization trend, suggested by the disposition of KLS42, KLS98 (repeat crushing and analysis for V) and the latites, would require either Ti-magnetite control (at variance with Fig. 24) or, less likely, protracted clinopyroxene crystallization, if all these samples are related.

In summary, the relationships described above demand that any proposed magma mixing process must be followed by a proportional degree of fractional crystallization because of the systematic displacement of the actual compositions of the evolved basaltic rocks away from the mixing lines. Although the process evaluated is the simplest one of magma mixing followed by crystallization, consideration of more complex and multi-stage scenarios (e.g. limited crystallization of less evolved basalt, followed

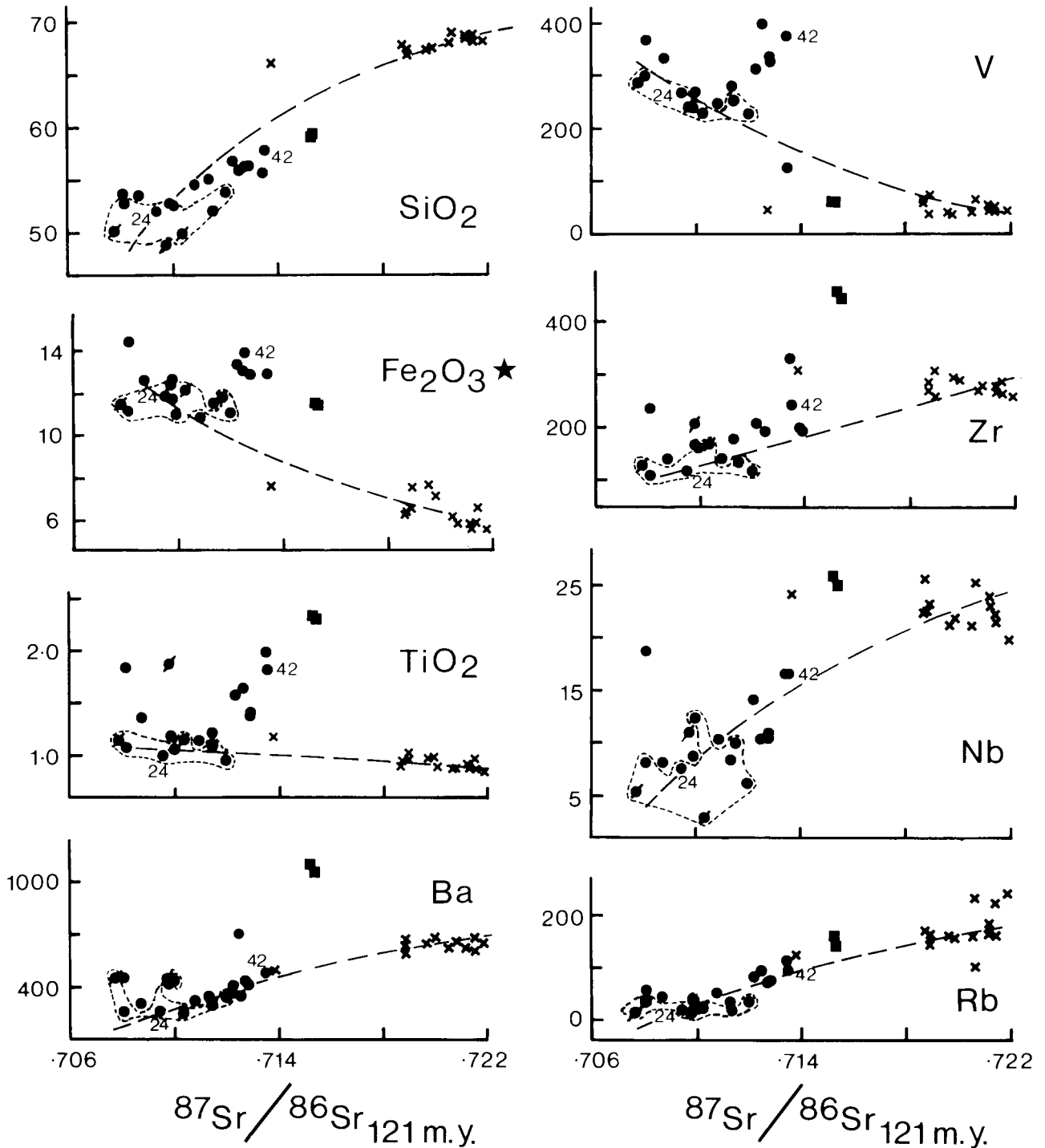


Figure 26

Plots of SiO_2 , Fe_2O_3^* , TiO_2 (%) and Ba, V, Zr, Nb, Rb (ppm) vs. initial $^{87}\text{Sr}/^{86}\text{Sr}$ ratio for Tafelberg volcanic rocks. Circled areas enclose less evolved basaltic rocks (Mg-number >55). Mixing lines between less evolved basalt KLS24 and average quartz latite calculated according to Langmuir *et al.* (1978). Note relative displacement of evolved basalt KLS42 from the mixing lines. See Fig. 14 for legend and other details.

by mixing and further crystallization and variants thereof) would not alter the general sense of our arguments in view of the rational relationships shown in the basaltic rocks. We consider it highly implausible that a mixing-crystallization process could operate as described above, as we do not know of any physical mechanism that would produce extensive fractional crystallization in proportion to the amount of mixing that had occurred. The experimental work of Kouchi and Sunagawa (1983), involving mixing between basaltic and dacitic magmas by forced convection, supports our contention since the mixing observed produced homogeneous andesite, with no crystals, from the basaltic starting material.

3. Constraints imposed by combined use of initial Sr-isotope ratios and elemental data

Figure 26 presents plots of the initial $^{87}\text{Sr}/^{86}\text{Sr}$ ratio vs. a number of oxides and elements for the Tafelberg basaltic rocks, latites and quartz latites, with the less-evolved basaltic rocks being indicated as before. The use of an isotope ratio vs. element plot is helpful in that while a mixing vector is not constrained in any direction, a fractional crystallization vector can only be orientated in a direction perpendicular to the isotope ratio axis, i.e. initial isotope ratios do not change with fractional crystallization. Thus in Fig. 26 all concentration changes in the vertical plane (parallel to the element or oxide axes) away from the

mixing line may be attributed to fractional crystallization only, and allow easy evaluation of the nature of any such process consequent upon a mixing process. Although more comprehensive mixing–crystallization calculations can and have been performed (see subsequent sections) the use of Fig. 26 suffices for present purposes, since the detailed calculations merely confirm what is shown in simpler form in this diagram.

The mixing lines in Fig. 26 have been calculated between the less-evolved basalt KLS24 and the average quartz latite. The prime purpose of this diagram is to evaluate the consistency of elemental changes accompanying fractional crystallization subsequent to magma mixing in order to model the composition of the evolved basaltic rocks, as typified by KLS42. This has been done by using the measured initial $^{87}\text{Sr}/^{86}\text{Sr}$ ratio of KLS42 to first calculate the amounts of KLS24 and average quartz latite required to generate such an $^{87}\text{Sr}/^{86}\text{Sr}$ ratio, and then using these proportions to calculate for each element a hypothetical KLS42 concentration that reflects the mixing process only and thus lies on the mixing line. The difference between the actual concentrations of the elements depicted in Fig. 26, and the calculated hypothetical concentrations, are thus considered to be due to fractional crystallization. These concentrations, and the ratio of observed/calculated concentrations, are given in Table VIII. This ratio serves as a measure of the amount of fractional crystallization required and indicates whether enrichment or depletion is involved. The particular value of these ratios becomes obvious when the ratios for the elements that have been shown to behave as incompatible trace elements in basaltic rocks are compared. Thus the postulated crystallization process would have to operate in such a manner as to hold Rb constant, increase Nb, Ba and Zr only slightly, but greatly increase the concentrations of TiO_2 and especially V. These trends are completely at variance with known basaltic or gabbroic fractionation trends and with known partition coefficients in likely liquidus phases (see Table XI in subsequent section).

TABLE VIII
Enrichment/Depletion Factors for Evolved Basalt KLS42

Oxide, Element	KLS42 ^a Obs.	KLS42 ^b Calc.	Ratio ^c Obs./Calc.
%			
SiO_2	57.81	59.82	0.97
Fe_2O_3	13.94	9.15	1.52
TiO_2	1.81	0.96	1.89
ppm			
Zr	238	192	1.24
Nb	16.4	14.7	1.12
Rb	96	96	1.00
Ba	496	420	1.18
V	372	161	2.31
Ni	5.1	32	0.16

a — Data normalized to 100 % on a volatile-free basis; total Fe as Fe_2O_3 .

b — Calculated concentrations derived from mixing lines in Fig. 26 and which represent hypothetical concentrations of KLS42, due to mixing between KLS24 and average quartz latite, prior to inferred crystal fractionation.

c — Amount of enrichment or depletion for oxides and elements due to inferred crystal fractionation.

It is also theoretically possible to calculate an “extract” resulting from the crystallization of KLS42 if we return to the measured concentrations and data in Table VIII. However, we note merely that such an “extract” would have to have ~60 % SiO_2 and bulk $D_{\text{Rb}} \sim 1$. These features imply the presence of substantial amounts of liquidus phases such as K-feldspar and mica in the “extract” in order to reduce SiO_2 (K-feldspar has >60 % SiO_2) and hold Rb

constant (only mica has $D \gg 1$ for Rb; Arth, 1976) in the derivative liquid. These minerals are not present either as phenocryst phases in the rocks concerned or in similar tholeiitic rocks.

The discussion above has dealt specifically with the modelling of the evolved Tafelberg basaltic rocks, but similar comments can also be made regarding the possible origin of the latites by magma mixing and fractional crystallization between basalt and quartz latite. Thus in Fig. 26 the latites would represent a greater proportion of admixed quartz latite than that inferred for KLS42. Although some of the elements in Fig. 26 behave differently in the latites when compared with their behaviour in the evolved basalts (e.g. Fe_2O_3^* and V) the same general observations can be made. Thus the enrichment factors (observed/calculated concentrations as in Table VIII) for TiO_2 , Ba, Zr and Rb are 2.4, 2.2, 2.1 and 1.3 respectively, which would again imply that Ti is more “incompatible” than Rb!

4. Other possibilities involving magma mixing

We now extend the above treatment to consider the possibility that the least evolved components in the mixing process may be represented by other groups of basic rocks, namely the Horingbaai or regional dolerites. We also consider the latites as the evolved component in a magma mixing process.

Fig. 27 presents a diagram of initial $^{143}\text{Nd}/^{144}\text{Nd}$ vs. initial $^{87}\text{Sr}/^{86}\text{Sr}$ similar to Fig. 23 which was discussed in the previous section, but illustrating mixing between the Horingbaai dolerite KLS145 or the regional dolerite KLS43 and quartz latite KL20. To produce the evolved basalt KLS42 from either of these dolerites requires a mixture containing some 70 % of quartz latite. This is a very high proportion of the acid component and is not supported by major and trace element calculations. In addition, the initial $^{87}\text{Sr}/^{86}\text{Sr}$ vs. $^{206}\text{Pb}/^{207}\text{Pb}$ diagram shown in Fig. 28 clearly shows that although there is a spread of isotopic compositions for the basaltic rocks, the mixing curves between Horingbaai dolerite KLS145 or regional dolerite KLS44 and the quartz latite KLS36 do not pass through the majority of the data points for the Tafelberg basaltic rocks. We have therefore eliminated the possibility that the Horingbaai dolerites or regional dolerites participate in a large-scale magma mixing and fractional crystallization process with quartz latite to produce the Tafelberg basaltic suite, and they will not be discussed further in this regard.

With regard to the latites, they cannot be considered as a possible end-member component in any magma mixing and fractional crystallization process which is intended to model both the range of basaltic compositions and the composition of the quartz latites. The lower $^{87}\text{Sr}/^{86}\text{Sr}$ and $^{206}\text{Pb}/^{207}\text{Pb}$ ratios of the latites compared to the quartz latites (Figs. 18 and 19) precludes this possibility. Although it appears impossible to accept a genetic relationship between all three rock types represented in the Tafelberg section (basalts, latites, quartz latites) there is still the question as to whether the evolved basaltic rocks can be derived by magma mixing and fractional crystallization processes involving less-evolved basalts and the *latites*.

In several of the diagrams we have discussed above the latites appear to be more suitable end-members for explaining the range in basaltic compositions than do the quartz latites (e.g. Fig. 22: Mg-number vs. SiO_2 ; Fig. 16: TiO_2 vs. Zr). However, this possibility cannot be sustained for several reasons. A general problem is that the most evolved basalts, such as KLS42, are close to the latite in bulk composition which would imply incorporation of approximately 80–90 % latite in the magma mixing stage of the process. This seems unlikely as the evolved basalts are geographically widespread whereas the latite unit is known only from the Tafelberg locality.

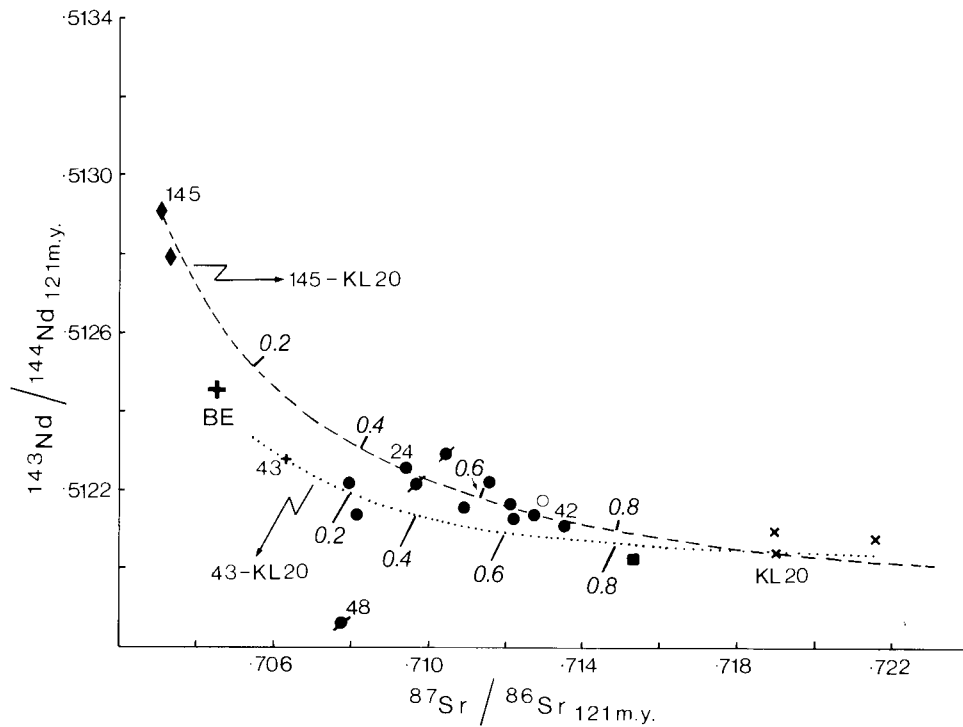


Figure 27

Initial $^{143}\text{Nd}/^{144}\text{Nd}$ vs. $^{87}\text{Sr}/^{86}\text{Sr}$ ratio diagram for all Etendeka volcanics. Mixing lines between Horingbaai dolerite KLS145 and quartz latite KL20, and between regional dolerite KLS43 and KL20, calculated according to Langmuir *et al.* (1978). Ticks and fractions (0.2, 0.4 etc) along mixing lines indicate fraction of admixed KL20. Bulk earth (BE) parameters as in Fig. 23 and legend as in Fig. 14.

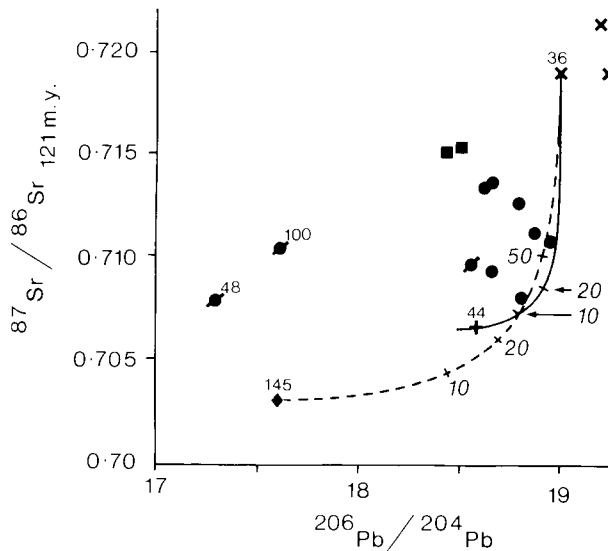


Figure 28

Initial $^{87}\text{Sr}/^{86}\text{Sr}$ vs. $^{206}\text{Pb}/^{204}\text{Pb}$ ratio diagram for all Etendeka volcanics. Mixing lines between Horingbaai dolerite KLS145 and quartz latite KLS36, and between regional dolerite KLS44 and KLS36, calculated according to Langmuir *et al.* (1978). Ticks and numbers (10, 20 etc) along mixing lines indicate percentage admixed KLS36. Legend as in Fig. 14.

More specifically, the latites occupy positions on $^{208}\text{Pb}/^{204}\text{Pb}$ vs. $^{206}\text{Pb}/^{204}\text{Pb}$ and $^{207}\text{Pb}/^{204}\text{Pb}$ vs. $^{206}\text{Pb}/^{204}\text{Pb}$ diagrams (Fig. 20) and on an initial $^{87}\text{Sr}/^{86}\text{Sr}$ vs. $^{206}\text{Pb}/^{204}\text{Pb}$ diagram (Fig. 28) which mitigate against any genetic relationships between the basalts and the latites. Furthermore, the same general arguments that were made against quartz latite as a suitable end-member component (see above for discussion of Figs. 24, 25 and 26) can also be made against the latite.

The overall conclusion must be that in spite of the close association between the three Tafelberg rock types in time

and space there is no evidence for a simple genetic or closed-system type relationship between them. Specifically, the combination of elemental and isotopic data does not support a common source region for any pair of these rock types, nor does it support any link between them by magma mixing, fractional crystallization or any combination of these processes. Other and more complex scenarios relating these rocks are possible, but it is now more appropriate to consider them and the petrogenesis of the various Etendeka magma types by discussing the major rock types on an individual basis.

IX. PETROGENESIS—II. DERIVATION OF MAJOR ROCK TYPES

A. Tafelberg Basaltic Rocks

The crux of the problem in interpreting the petrogenesis of the Tafelberg basaltic suite as a whole lies in reconciling the elemental and isotopic abundance variations. The rational compositional variations shown by individual minerals (e.g. pyroxene trends in Fig. 12a) and by the rocks themselves (e.g. the Fe_2O_3^* -V correlation in Fig. 25) clearly indicates the influence of fractional crystallization processes in the derivation of the Tafelberg basaltic suite. Any suggestion that the rational trends in these rocks are due to simple mixing with crustal material can be dispelled by reference to Fig. 25. It is clear that the putative crustal material would have to contain in excess of 14% Fe_2O_3^* and 400 ppm V which is implausible for any known major material in the continental crust. Faure *et al.* (1974) encountered similar difficulties when attempting to ascribe the compositional variations of the Kirkpatrick basalts in Antarctica to the effects of crustal contamination, and postulated the existence of a biotite-rich layer in the crust to overcome this problem. However, the high concentrations of Fe_2O_3^* , V and other elements required, coupled with low concentrations of MgO and Ni (see analysis of sample KLS42 in Table I as a guide to the minimum concentrations required) negates this possibility on chemical grounds, let alone in terms of volume proportions of the hypothetical

biotite-rich layer and the Tafelberg basaltic rocks themselves.

Besides the influence of fractional crystallization processes, it should now also be clear from diagrams we have presented that isotopic variations do not correlate systematically with increasing fractionation within the Tafelberg basic suite. Thus the less-evolved rocks with highest Mg-numbers (>55) have variable initial $^{87}\text{Sr}/^{86}\text{Sr}$ ratios (0.7078–0.7120) which almost encompass the range shown by the more-evolved rocks (0.7081–0.7135). This may be readily seen in Fig. 21. Nd-isotopic data, though fewer in number, show the same tendency. In the case of the Pb-isotopic data, the two samples that have been used as typical of least- and most-evolved basaltic rocks (KLS24 and KLS42 respectively) have virtually the same isotopic compositions (Table VII). Consequently, the possibility that we wish to consider is, quite simply, that the evolved rocks have been derived by fractional crystallization from parental lavas which had a range in isotopic compositions. This is most readily evaluated by first considering the nature and viability of such a process and then discussing reasons for the isotopic variations in the less-evolved rocks.

1. Derivation of evolved rocks

(a) *Fractional crystallization.* The proposition that the evolved Tafelberg basic rocks are derived by fractional crystallization from parental lavas with variable isotopic compositions can be conceptually understood by reference to Fig. 29. Ti and Zr are generally regarded as immobile incompatible elements in basaltic rocks, and the increase in concentration of these two elements can thus be attributed to fractional crystallization. We envisage that the more primitive basalts KLS46 and KLS58 can potentially be regarded as parental magmas to the more evolved basaltic rocks KLS16 and KLS54 respectively, as shown by the solid lines in Fig. 29, since in the case of KLS46 and KLS16 there is no change in the initial $^{87}\text{Sr}/^{86}\text{Sr}$ ratios shown, while for the pair KLS58 and KLS54 there is only a slight change in initial

$^{87}\text{Sr}/^{86}\text{Sr}$. Similar constructions could be made for other pairs of elements such as in Figs. 24 and 25. Fig. 30 portrays a three-dimensional representation in an attempt to further illustrate the variation of initial $^{87}\text{Sr}/^{86}\text{Sr}$ ratios with increasing fractionation. It can be seen that there is no systematic increase of initial $^{87}\text{Sr}/^{86}\text{Sr}$ ratios with increasing TiO_2 and Zr concentrations, and the postulated fractionation paths for KLS46 to KLS16 and from KLS58 to KLS54 are again apparent. Furthermore, while there is a suggestion that initial $^{87}\text{Sr}/^{86}\text{Sr}$ ratios increase towards the quartz latites in Fig. 29 (i.e. from KLS46 to KLS58), this is

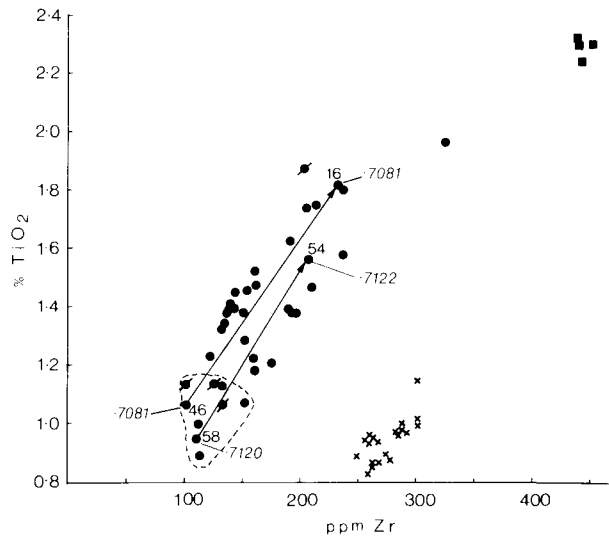


Figure 29

TiO_2 vs. Zr diagram for Tafelberg volcanic rocks. Circled area encloses less evolved volcanic rocks (Mg-number >55). Numbers with decimals (.7081 etc) are initial Sr-isotope ratios, other numbers (46 etc) are KLS sample numbers. See Fig. 14 for legend and other details.

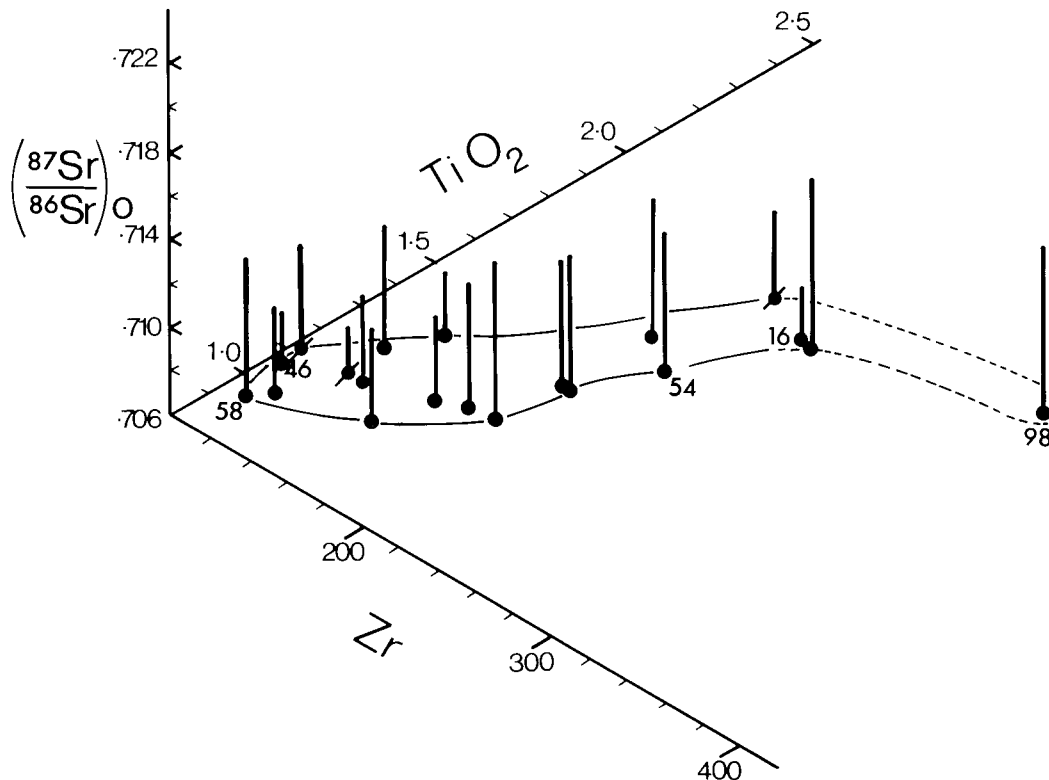


Figure 30

TiO_2 -Zr-initial $^{87}\text{Sr}/^{86}\text{Sr}$ ratio pin diagram for Tafelberg volcanic rocks. See Fig. 14 for legend and other details.

merely a question of sample selection, since in Fig. 30 there is no clear evidence for any increase in $^{87}\text{Sr}/^{86}\text{Sr}$ across the main TiO_2 vs. Zr trend, i.e. in the direction of the Zr axis where the quartz latites (and other crustal rocks) would plot.

On the basis of the above interpretation, we have attempted to quantitatively evaluate the derivation of the evolved basaltic rocks by simple closed system low pressure fractional crystallization. We have first used the unconstrained least squares approximation technique of Bryan *et al.* (1969) with the observed rock and mineral composition, in order to obtain a solution for major elements. Thereafter we have, following the approach employed by many workers (e.g. Le Roex *et al.*, 1981), used the amount of fractionation obtained from the major element calculations (F, the fraction of liquid remaining) to predict trace element concentrations in presumed derivative liquids using the well-known Rayleigh fractionation law (e.g. Arth, 1976).

Dealing first with the major elements, we have adopted a variety of approaches and computed a number of least squares approximations in order to best depict the fractionation path(s) of the Tafelberg basaltic suite. A general problem with all of these has been the choice of parent and daughter magmas, because although it has been argued earlier that such pairs could be chosen on the basis of isotopic data, this would only be potentially valid if initial isotopic ratios from all three isotopic systems are similar, and such examples are not available (it is noted that such a choice is more important for the more variable trace elements than for the major elements). A further problem is that the rocks in question are essentially aphyric, with plagioclase being the only convincing phenocryst phase. Sparse microphenocrysts of pseudomorphed olivine and augite do occur, but the question of whether pigeonite and Ti-magnetite are also possible liquidus phases cannot be resolved by the petrographic evidence (Section V-A).

Despite these problems, we have used a variety of mineral combinations and compositions, and different parent-daughter pairs representing both small and large degrees of fractionation, in our model calculations. The following points can be noted. First, because of the relatively sharp increase of SiO_2 content with decreasing MgO concentration (Fig. 14) the use of Fe-rich olivine as analysed in the Tafelberg dolerites (Section V-C) is more efficient in causing such an increase in SiO_2 . The use of either Mg-rich olivine or pigeonite, with their higher SiO_2 contents as compared with the Fe-rich olivines, yields poorly constrained solutions with large standard deviations (particularly for the less-evolved rocks) unless used in combination with Ti-magnetite. However, in the latter case, the models require large amounts of Ti-magnetite fractionation, typically 3–4%, which is too high for trace elements such as V and Ni (see later), and in any case still yield solutions with high standard deviations. However, even if Fe-rich olivine is used, better solutions are obtained

for TiO_2 if small amounts of Ti-magnetite are also used in the mixing calculations, unless Ti-rich clinopyroxene (found in some of the Tafelberg dolerites) is utilized. Finally, all reasonable mixing calculations require the use of augite even though it is not a major phenocryst phase, together with the fractionation of Ca-rich plagioclase.

For present purposes, we present data only for the parent-daughter pair KLS24–KLS42 since these are the examples of less-evolved and evolved basalt we have consistently used in our discussions. This covers nearly the entire fractionation sequence, apart from some dolerites which have higher Mg-numbers, and thus the solutions obtained cannot be generally applicable to any particular interval of fractionation. Nevertheless, this approach can be justified bearing in mind the general problems raised above and by the results we have obtained. Input data for the model calculations are given in Table IX. Since KLS24 is aphyric and does not contain olivine we have mostly used mineral data from the dolerite KLS100 which is olivine-bearing and which occurs in the lava pile at Tafelberg itself. Additionally we have utilized a Ti-rich augite from another Tafelberg-type dolerite KLS48 in an attempt to obtain a reasonable solution without the use of Ti-magnetite.

The results of two mixing calculations are given in Table X. Both have been back-calculated to the parent KLS24 in order to provide direct estimation of F (i.e. KLS42). For mixing calculation A, which utilized Ti-magnetite, a good solution is obtained as indicated by the data shown in Table X, except for K_2O . The relevance of this and the small amount of Ti-magnetite (1.2%) fractionation involved will be discussed in the trace element evaluation that follows. For mixing calculation B, the approximation is not as well constrained, particularly for TiO_2 and K_2O , but is nevertheless reasonable. Recalculation of A without Ti-magnetite (i.e. with low Ti-augite) results, as expected, in a poor solution for TiO_2 (1.01% observed vs. 0.77% calculated) and an overall approximation that is poorer than for B. The relevant point to make at this stage is that both A and B yield solutions that involve similar mineral proportions that are not petrologically unrealistic, and similar degrees of fractionation.

Trace element calculations have been made using the parameters mentioned above and as shown in Table X. Distribution coefficients used are given in Table XI. The results obtained, corresponding to major element models A and B, are given in Table XII. For both A and B the general agreement between predicted and observed concentrations is satisfactory, bearing in mind the range of distribution coefficients and the compatible and incompatible elements tested. The obvious disparity in both models is for Rb. In greater detail it should be noted that in order to obtain satisfactory agreement for model A, very low distribution coefficients have had to be used for Ni and V, particularly for the latter. This suggests that model B, where the trace element agreement is in any case slightly better, may be the model that is more applicable. For model B itself, the

TABLE IX
Input Data for Least Squares Approximation Calculations

	KLS24	Plag.	Cpx 1.	Cpx 2.	Oliv.	Ti-Mt.	KLS42
SiO_2	52.44	51.95	52.92	50.61	35.45	0.02	58.63
TiO_2	1.01	0.06	0.44	0.87	0.02	20.91	1.84
Al_2O_3	15.01	29.94	1.43	3.87	0.02	2.45	12.84
FeO	10.76	0.49	8.17	7.50	37.04	75.02	12.72
MgO	6.86	0.11	17.18	16.23	26.64	1.11	2.33
CaO	10.63	13.35	19.47	20.15	0.28	0.02	6.16
Na_2O	2.14	3.91	0.16	0.32	0.02	0.02	2.29
K_2O	0.84	0.18	0.04	0.02	0.02	0.02	2.73

All data normalized to 100% on volatile-free basis with total iron calculated as FeO. P_2O_5 and MnO have been excluded from the calculation. KLS24 and 42 from Table I; mineral data from Microfiche Card 3. Plag., Cpx. 1, Oliv. and Ti-Mt. are from KLS100; Cpx. 2 is from KLS48.

TABLE X
Least Squares Approximations Relating KLS42 (Daughter) to KLS24 (Parent) Obtained by Adding the Listed Quantities of the Minerals Shown in the Mix to KLS42 to Produce the Calculated Concentrations in KLS24

	Mixing Calculation A				Comp.	Mix Wt. %	S.D.
	Obs.	Calc.	Diff.	Comp.			
SiO ₂	52.44	52.42	-0.02	KLS42	35.41	0.86	
TiO ₂	1.01	1.01	0.00	Oliv.	9.58	0.60	
Al ₂ O ₃	15.01	15.02	0.01	Plag.	33.93	0.64	
FeO	10.76	10.76	0.00	Cpx. 1	20.11	0.67	
MgO	6.86	6.88	0.02	Ti-Mt.	1.19	0.27	
CaO	10.63	10.65	0.02				
Na ₂ O	2.14	2.17	0.03	Total	100.22	1.42	
K ₂ O	0.84	1.04	0.20				
Sum of squares of differences = 0.04							
	Mixing Calculation B				Comp.	Mix Wt. %	S.D.
	Obs.	Calc.	Diff.	Comp.			
SiO ₂	52.44	52.47	0.03	KLS42	38.36	1.44	
TiO ₂	1.01	0.90	-0.11	Plag.	31.23	1.14	
Al ₂ O ₃	15.01	15.03	0.02	Oliv.	11.12	0.70	
FeO	10.76	10.60	-0.16	Cpx. 2	19.39	0.99	
MgO	6.86	7.04	0.18				
CaO	10.63	10.47	-0.16	Total	100.10	2.20	
Na ₂ O	2.14	2.16	0.02				
K ₂ O	0.84	1.11	0.27				
Sum of squares of differences = 0.17.							

crucial distribution coefficient is for V in clinopyroxene, but the value we had earlier chosen (Table XI) is in excellent agreement with the recently obtained ion-probe value given by Shimizu (1983).

Bearing in mind our postulate of fractionation from parental magmas which had variable isotopic compositions, it can be expected that such magmas would also have variable incompatible element concentrations. We have noted serious discrepancies in our model calculations for K and Rb, which denote that the parent used (KLS24) has measured concentrations of these elements that are too low. Since this is one of our freshest samples, this would not seem to be due to alteration. An alternative is to consider another sample which has a similar Mg-number and bulk composition. Sample KLS46 is in many respects similar to KLS24 but has 1.15 % K₂O and 33 ppm Rb. The K₂O value of KLS46 is closer to the predicted values of 1.04 % K₂O in model A and 1.11 % K₂O in B (Table X) than the K₂O value of KLS24. In a similar vein, if the value of 33 ppm Rb had been used in Table XII, the predicted concentrations of Rb in models A and B would be 92 ppm and 85 ppm Rb respectively, in much better agreement with the observed

concentration of 96 ppm Rb in KLS42. Likewise, another less-evolved basalt, KLS58, has 0.95 % TiO₂ and here again this would improve the situation for model B (Table X) where the predicted concentration is 0.90 % TiO₂. Such manipulations are somewhat subjective, but do illustrate the difficulty of obtaining reasonable agreement between observed and predicted concentrations, given the premise we have adopted in this section. Also, noting the discrepancies encountered with Rb above and in Section VIII-C, it is pertinent to point out that if KLS46 (33 ppm Rb) had been used in the calculations derived from Fig. 26 and shown in Table VIII this would only worsen the situation, as the enrichment factor for Rb in Table VIII would be <1.

In summary, we consider that the major and trace element calculations performed provide strong support for the derivation of the evolved basaltic rocks from the less-evolved basaltic rocks by fractional crystallization processes. The fractionation models we have presented have little to choose between them, and the question of whether or not small amounts of Ti-magnetite have fractionated is not important in the wider context. Indeed,

TABLE XI
Distribution Coefficients Used in This Study

	Plag.	Oliv.	Cpx.	Ti-Mt.
Zr	0.01	0.01	0.30	0.24
Nb	0.01	0.01	0.15	2.30
Y	0.20	0.10	0.70	0.20
Rb	0.01	0.01	0.01	0.01
Ba	0.20	0.01	0.10	0.01
Sr	2.2	0.01	0.10	0.01
V	0.01	0.01	2	5 ^a
Ni	0.01	15	3	10 ^b
La	0.12	0.01	0.10	0.01
Ce	0.11	0.01	0.12	0.01
Eu	0.60	0.01	0.39	0.01
Yb	0.10	0.01	0.60	0.01

Data from compilation by Le Roex (1980), Le Roex *et al.* (1981) and Le Roex *et al.* (1982).

a — literature values range from 5–100 (Le Roex, 1980).

b — literature values range from 5–77 (Le Roex, 1980).

TABLE XII
Calculated and Observed Trace Element Abundances in KLS42 (Daughter) using KLS24 (Parent), F Values Derived from Table X and Distribution Coefficients Listed in Table XI

	KLS24		KLS42		
	Obs.		Obs.	Calc. A	Calc. B
Zr	114		238	289	269
Nb	7.5		16	19	19
Y	24		39	48	46
Rb	19		96	53	49
Ba	217		496	532	497
Sr	216		188	178	188
V	264		372	353	375
Ni	63		5.2	5.5	5.0
La	14		33	35	32
Ce	32		73	82	76
Eu	1.28		2.15	2.29	2.21
Yb	2.63		4.12	5.78	5.44

Calc. A — based on mixing calculation A in Table X.

Calc. B — based on mixing calculation B in Table X.

these models are only approximations considering that we have covered the entire spectrum of lava compositions to show that fractional crystallization can explain observed compositional variations over this range. In reality, as indicated by our calculations (not shown) involving step-wise crystallization over smaller fractionation intervals there are likely to be changes in the mineralogy and mineral proportions of the fractionate as crystallization proceeds. Were such step-wise mixing calculations to be carried out with more clearly defined parent and daughter compositions, then it can be confidently predicted that the solutions obtained would be even more satisfactory than those presented above.

In this context a final point needs emphasizing. The fractional crystallization processes documented above are of a simple closed-system type. In reality, since there is some evidence for magma mixing between basaltic magmas (Section V-C) and in view of our postulate that the Tafelberg parental magmas had a range in isotopic compositions, it is likely that some open system behaviour prevailed during crystallization. This does not seriously detract from our contention that the rational chemical variations exhibited by the Tafelberg basaltic suite as a whole are essentially caused by fractional crystallization processes.

(b) *Crustal Contamination.* From the above discussion it appears that the evolved basalts can be accounted for by invoking a fractional crystallization process operating on isotopically variable parent magmas. Thus, contamination is not required to explain the major and trace element compositions of the evolved basalts. Nevertheless, the possibility of crustal contamination is discussed here because it is considered by many (e.g. Faure *et al.*, 1974; Moor bath and Thompson, 1980; Carlson *et al.*, 1981; Mahoney *et al.*, 1982; Thompson *et al.*, 1982, 1983) to play a

prominent role in the petrogenesis of continental flood basalts. The contamination process we discuss is one where the evolved basalts are generated from the less-evolved basalts by bulk assimilation of crust or mixing with partial melts of the crust. The process will also most likely be one of assimilation (or mixing) accompanied by fractional crystallization (AFC) and, because of heat budget constraints, the amount of crystallization probably exceeds the amount of assimilation (Nicholls and Stout, 1982).

An important question to pose at the outset is: "Do the quartz latites represent the most likely crustal contaminants for the Etendeka basic lavas?" In view of their undoubted crustal character, their voluminous and widespread nature and their intimate temporal and spatial association with the basalts, we feel the answer is, almost certainly, yes. If this is accepted then the arguments concerning basalt-quartz latite relationships in Section VIII should apply equally here. This discussion assumed the ready availability of the contrasting magma compositions, but it may be argued that the generation of quartz latite magma requires heat released by crystallizing basic magmas and that the relationship between the two is one of progressive crystallization, melting and mixing, i.e. an AFC relationship. This possibility has been investigated using the equations of DePaolo (1981) and the results are discussed below.

Consistency between AFC compositional trends and those observed in the basalt suite is only obtained when the ratio mass of contaminant/mass of crystallization is very low, as might be expected from the success of the simple fractional crystallization models discussed above. This also applies when hypothetical contaminants, e.g. average crust, are considered. However, AFC models with low amounts of contamination fail to account for the necessary increase in Sr-isotope ratios within the observed range of

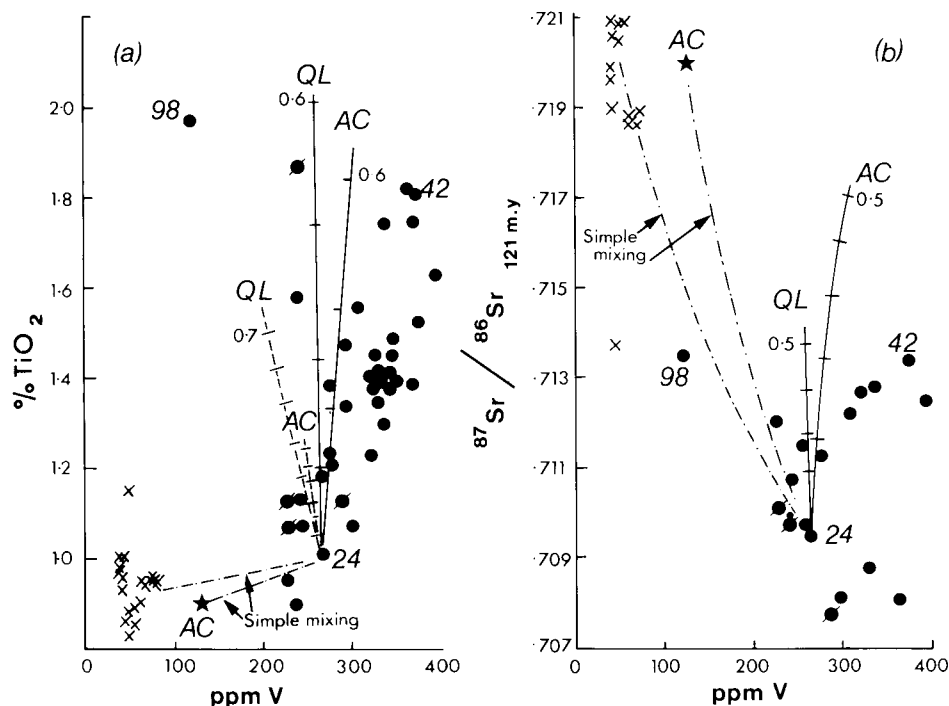


Figure 31

Results of AFC modelling of (a) TiO₂ vs. V, and (b) initial ⁸⁷Sr/⁸⁶Sr ratio vs. V, in the Tafelberg basaltic suite. Contaminants are average quartz latite (QL) and average crust (AC) whose compositions are listed in Table XIII. Continuous curves are for trends where R (mass of contaminant/mass of crystallization) = 0.5 and ticks on these curves represent changes in the ratio mass of magma/mass of original magma of 0.1. Dashed curves are for R = 1.0 and ticks represent increments of 0.1 in the ratio mass of assimilated material/mass of magma. Simple mixing curves (dot-dashed) between less evolved basalt KLS24, and quartz latite and average crust, are also shown. For higher values of R and AFC curves approach the simple mixing trends. In (a) the less evolved basalts (Mg-number >55) are those with TiO₂ <1.3%. See Fig. 14 for legend.

TABLE XIII
Data for End-member Components used in Assimilation–Fractional Crystallization (AFC) Calculations

	TiO ₂ %	V ppm	Sr ppm	Rb ppm	⁸⁷ Sr/ ⁸⁶ Sr (121 m.y.)
KLS24	1.00	264	216	19	0.7095
Average Quartz Latite	0.95	53	131	175	0.7200
Average Crust	0.50	130	498	50	0.7200
B2			159	329	0.8111
Typical Damara Crust 1			50	75	0.7400
Typical Damara Crust 2			200	300	0.7400
DG13			194	69	0.7417
KLS145			196	2.3	0.7030
Bulk D	0.10	0.62	1.15	0.01	

Bulk D calculated from data in Table XI assuming fractional crystallization extract of 51 % Plag., 31 % Cpx., 18 % Oliv. (Table X–B). Composition B2 is a 2 b.y. Abbabis gneiss (Hawkesworth, unpubl.). DG13 is a gneiss from the Khan Formation (Kröner *et al.* 1978). Typical Damara crust has Rb/Sr = 1.5 and (⁸⁷Sr/⁸⁶Sr) 121 m.y. = 0.740 and was estimated from data plotted in Fig. 10 of Bristow *et al.* (1984). The limits of 50 and 200 ppm Sr cover the range of most Damara rocks which have been analysed for ⁸⁷Sr/⁸⁶Sr. The average crustal composition is after Weaver and Tarney (1984) except for V which is from Taylor (1964), and ⁸⁷Sr/⁸⁶Sr, which is estimated to be similar to that of the quartz latites.

trace element concentrations of the basalt suite unless their Sr-contents or ⁸⁷Sr/⁸⁶Sr ratios are unusually high.

To illustrate the failure of AFC to account for the evolution of the basalt suite we present plots of TiO₂ and ⁸⁷Sr/⁸⁶Sr vs. V in Fig. 31 as these parameters have been particularly useful in elucidating relationships within the Etendeka suite. The parent basalt composition is KLS24 and details of contaminants and fractional crystallization parameters are presented in Table XIII. Fig. 31 indicates that it is not possible to produce the V enrichment observed in the basalts by AFC using reasonable contaminants. Similar observations can be made from a Zr–V plot (not shown). In this regard it is important to note that the bulk distribution coefficient for V which we have adopted was obtained using a value for clinopyroxene (Table XI) at the lowest end of the range reported in the literature, i.e. using the value most favourable for V enrichment. Note that it is not just for V that the AFC modelling is inadequate; calculation of AFC trends on a TiO₂ vs. Zr diagram (not shown, but see Fig. 29) reveals that the AFC trends for R = 1.0 and 0.5 pass below and to the right of the observed data trend, i.e. there is insufficient enrichment of TiO₂ (cf. Table VIII). In essence Fig. 31(a) indicates that any contaminant in an AFC model has to be of rather unusual composition. Especially critical in this regard is the necessity for rather high V and Fe₂O₃* contents (cf. Fig. 25), unless resort is made to massive amounts of crystallization, i.e. F << 0.5. It may be that rocks of such composition exist in the crust but partial melts of the crust are highly unlikely to be of such character (e.g. note the positions of average crust and the quartz latites in Fig. 31).

Another important aspect of the AFC calculations is the extent of assimilation and fractional crystallization required to produce the observed trace element concentrations in the evolved basalts. For example, Fig. 31(a) indicates that for R = 0.5 the TiO₂ content of the most evolved basalts is achieved through AFC involving quartz latite as a contaminant, when the mass of evolved magma is about 65 % of the original magma (KLS24). Calculations show that for this ratio the evolved magma would have about 64 % SiO₂ because it would have been generated from the original magma by nett addition of 35 % quartz latite and nett removal of 70 % crystals. This is much greater than that observed in the evolved basalts (in KLS42 SiO₂ = 58.63 %). This underscores the failure of AFC—it cannot consistently account for the major, trace element and isotopic variations in the Tafelberg basaltic suite. We thus prefer a model of fractional crystallization from isotopically variable parent magmas for the generation of the evolved basalts. The development of the isotopic heterogeneity in the parent magmas is now discussed below.

2. Derivation of less-evolved rocks

Given that the arguments presented in the preceding section for the derivation of the evolved basaltic rocks by simple fractional crystallization processes are accepted, then we are still left with the problem of explaining the range in isotopic ratios in the parental or less evolved Tafelberg basaltic rocks (i.e. those that have Mg-numbers >55). This problem can be quite simply stated in terms of whether the steep trend shown by these rocks in Fig. 21 (dot-dashed line) is due to crustal contamination or whether it is a reflection of a heterogeneously enriched mantle source, or both. These alternatives, discussed separately below, are not easily resolved, but whatever the correct interpretation this will not materially affect the crystal fractionation scheme outlined in the previous section for the derivation of the more-evolved Tafelberg basaltic rocks.

(a) *Crustal Contamination.* The high ⁸⁷Sr/⁸⁶Sr and low ¹⁴³Nd/¹⁴⁴Nd ratios repeatedly highlighted in this study (Fig. 23) can be interpreted as strong evidence for direct crustal contamination of the less-evolved Tafelberg basaltic rocks. Even though we have termed these rocks less-evolved, the majority have Mg-numbers within the range 55–60 (Fig. 22) and thus cannot be classed as “primary” in any sense. This would be consistent with a derivation through either bulk assimilation or combined assimilation–fractional crystallization (AFC).

Further suggestions of crustal contamination are indicated in Fig. 20 where two Tafelberg dolerites, KLS48 and KLS100, have much lower Pb-isotope ratios than all other Tafelberg rocks analysed. One of them, KLS100, in fact has Pb-isotopic compositions that are indistinguishable from the primitive Horingbaai dolerites (Fig. 20) and the 2 b.y. reference line in this diagram could well be a mixing line with an unknown crustal contaminant, possibly of the same age. However, the less radiogenic Pb-isotopic characteristics of KLS100 (and KLS48) contrast with the Sr- and Nd-isotopic characteristics of these samples (e.g. Fig. 19); furthermore the two samples we have consistently used as representative examples of less-evolved and evolved Tafelberg lavas, i.e. KLS24 and KLS42, have virtually identical Pb-isotopic compositions (Fig. 20). The implied coherency between Rb/Sr and Sm/Nd ratios (Fig. 23) clearly does not extend to the U/Pb system where the situation is apparently more complex (Fig. 28). This is supported by the variable Pb contents of the Tafelberg basaltic rocks, and in particular the high Pb content (29.5 ppm) of sample KLS100 (Table VII).

The non-radiogenic Pb-isotope character of KLS100 coupled with its high Pb content suggests that it may well be a sample that escaped crustal contamination with respect to

Pb, but not with respect to Sr and Nd. The mineral disequilibrium noted in KLS100 (Section V-C) could be taken to support this possibility, even though arguments were presented to show that the observed disequilibrium was best explained by mixing of two basaltic magmas. Nonetheless, the similarity of the Pb-isotopic composition of KLS100 to the Horingbaai dolerites (Fig. 20) invites inclusion of the latter together with the regional dolerites, in any possible crustal contamination scheme involving the less evolved Tafelberg basaltic rocks. This is considered further by reference to Rb-Sr isotopic data in view of the larger sample database that exists for this isotopic system. The relationship between these basaltic rocks is shown by the steeper (dot-dash) trend line in Fig. 21, and in more detail in the isochron plot displayed by Fig. 32, where only the less evolved Tafelberg basaltic rocks are portrayed.

The steeper trend line in Fig. 21, shown as a 1.8 b.y. reference line in Fig. 32, can be interpreted in terms of crustal contamination, either through simple mixing (i.e. involving no fractional crystallization) or as a trend of AFC. In the first instance the two compositions involved would be a basaltic component, like the regional dolerites, and a crustal component lying on the extension of the trend line. Under these rather special conditions the "age" of 1.8 b.y. could represent the approximate age of the crustal contaminant (similar arguments can be made for the Horingbaai dolerites and the 2.1 b.y. reference line). However, Bristow *et al.* (1984, Fig. 10) have shown that from a large number of analyses of upper crustal rocks from northern Namibia only *three* plot on or near the inferred 1.8 b.y. mixing line. The latter are Damaran rocks of Pan-African age. The remaining Damaran metasedimentary and granitic rocks, together with a few samples of ~2 b.y. Abbabis granite-gneiss, have compositions that plot well to the right (higher Rb/Sr) of the inferred 1.8 b.y. mixing line and are unsuitable as mixing components. Partial melts of these rocks will have even higher Rb/Sr ratios and will be even less suitable as contaminants in a simple mixing process.

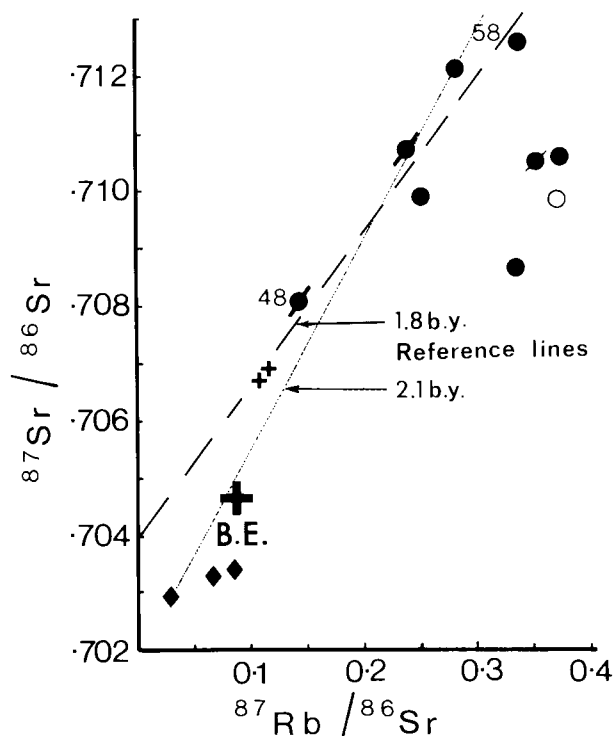


Figure 32

Rb-Sr isochron plot for less evolved Etendeka basic rocks with Mg-number >55. Bulk earth (BE) parameters from Fig. 23. Legend as in Fig. 14.

Whether a suitable contaminant exists in the lower crust is not known, but this contaminant would have to have high $^{87}\text{Sr}/^{86}\text{Sr}$ and low Rb/Sr, contrary to what has been observed in the only available analyses of lower crustal rocks from southern Africa, namely xenoliths from Lesotho kimberlites (Rogers and Hawkesworth, 1982). To further emphasize these difficulties we note that the average crust composition of Weaver and Tarney (1984) has Rb/Sr = 0.10 and, assuming an age of 2 b.y., would have evolved to $^{87}\text{Sr}/^{86}\text{Sr} = 0.711$ by single stage growth from bulk earth by the early Cretaceous. This composition plots on the trends defined by the least-evolved basalts in Fig. 32 but at lower $^{87}\text{Sr}/^{86}\text{Sr}$ than some of the basalts, clearly showing that any putative contaminant requires a much higher $^{87}\text{Sr}/^{86}\text{Sr}$ ratio.

A more realistic contamination process is AFC and we have attempted to model the observed $^{87}\text{Sr}/^{86}\text{Sr}$, Rb/Sr and Sr variations in the least-evolved basalts by this process, utilizing a variety of likely crustal components and a Horingbaai dolerite as end-members (Table XIII). In general the results (Fig. 33) are similar to those obtained from consideration of simple mixing. The typical Damara crustal compositions and the Abbabis sample B2 produce trends which lie at lower Sr and higher Rb/Sr than the observed data. Varying the R-ratio does not improve the fit between modelled trends and the basalt compositions. For example, DG13, which was identified as a suitable contaminant by simple mixing on Fig. 10 of Bristow *et al.* (1984), the AFC trends are to lower Sr and Rb/Sr, and again these cannot be reconciled with the basalt data by varying R to higher or lower values. It is clear from Fig. 33(a) that the high and variable Sr contents of most of the basalts and dolerites require a range of contaminants with high and variable Sr (and $^{87}\text{Sr}/^{86}\text{Sr}$). The average crust composition could represent one such contaminant. However, Fig. 33b suggests that such contaminants will have Rb/Sr ratios that are too low to produce AFC trends that fit the basalt data. The available analyses of silicate rocks in the Damara orogen and its basement (Haack *et al.*, 1982; Hawkesworth *et al.*, 1983) suggests that high-Sr rocks are not common and, moreover, tend to have low $^{87}\text{Sr}/^{86}\text{Sr}$ ratios either overlapping with, or slightly greater than those exhibited by the least-evolved basalts.

Another important feature of Fig. 33 is that, apart from composition B2, the mass of contaminant required to generate the basalts with the highest $^{87}\text{Sr}/^{86}\text{Sr}$ is substantial, ranging from about 25% (DG13 and DC2) to nearly 40% (average crust). Furthermore, in the AFC process the amount of crystallization will be the same or greater. This is inconsistent with the overall basaltic nature of all the rocks plotted in Fig. 33. For example, the Mg-number of KLS145 (the parental magma in our AFC models) is 61.2 and that of KLS58 (the basalt with the highest $^{87}\text{Sr}/^{86}\text{Sr}$ ratio) is slightly lower at 57.6.

The above has dealt with the Horingbaai dolerites as least contaminated end-members, and no mention has been made of the regional dolerites in this regard. We have not been encouraged to carry out detailed AFC calculations with these rocks because of their position in Fig. 33a, a viewpoint which is supported by their Nd- and Pb-isotopic relationships (Figs. 19 and 20), and they are not considered further here.

The AFC modelling for the less-evolved Tafelberg basaltic rocks is perhaps less constrained than for the evolved varieties, and more trace element and isotopic data are required for further evaluation. However, at this stage we find no compelling evidence that the less-evolved Tafelberg basaltic rocks have acquired their isotopic compositions by crustal contamination since we have not been able to identify potential crustal contaminants. Such contaminants would necessarily require a range in elemental and isotopic compositions (Fig. 33). It is possible that further work could identify such contaminants in the

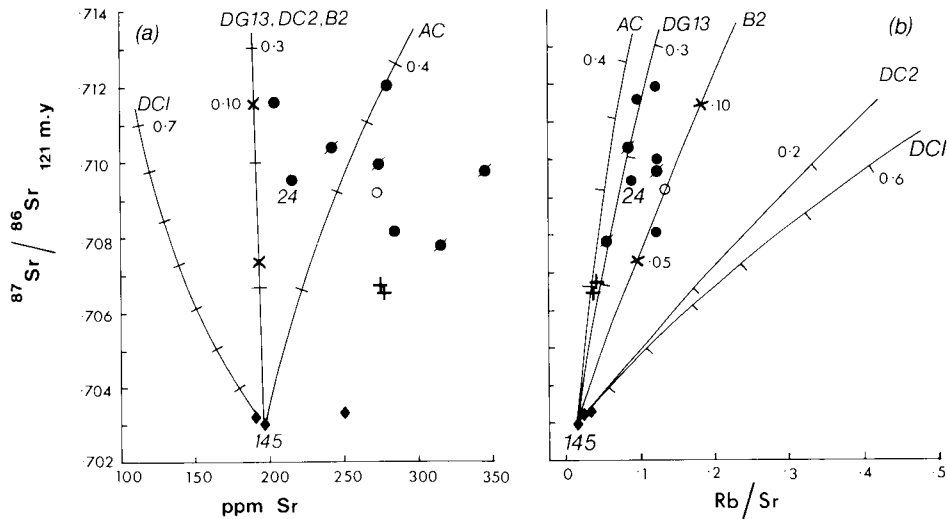


Figure 33

Results of AFC calculations in relation to initial $^{87}\text{Sr}/^{86}\text{Sr}$ ratio, Sr and Rb/Sr variations within the less-evolved (Mg-number >55) Etendeka basaltic rocks. Horingbaai dolerite KLS145 is the uncontaminated parent magma. All AFC trends are for $R = 1.0$ (i.e. mass of assimilation = mass of crystallization) and ticks on the curves are for increments of 0.1 in the ratio mass of contaminant/mass of magma, except for contamination by B2 where crosses on the trend are for increments of 0.05 in this ratio. In (a) the trends of contamination of DG13, DC2 and B2 are coincident. Contamination parameters are summarized in Table XIII. DC1 and DC2 are typical Damara crust compositions 1 and 2. AC is average crust. DG13 and B2 are specific rock compositions identified on Fig. 10 of Bristow *et al.* (1984); see Table XIII for further details and Fig. 14 for legend.

underlying and surrounding Pan African and basement rocks, or as xenoliths in Namibian kimberlites. Planned $^{18}\text{O}/^{16}\text{O}$ isotope ratio determinations may also assist in characterizing a crustal imprint in these rocks (e.g. Hoefs *et al.*, 1980). However, in view of the large volume of Tafelberg-type basaltic rocks in the Etendeka, and apparently also in the southern Paraná basin of Brazil (Ruegg, 1976) we concur with Nelson (1983) that crustal contamination will be found in isolated members of formations (see sample KLS48 in Fig. 19), rather than in formations as a whole. This situation might be more appropriate for selective contamination, which we have not considered here since it has been discussed in detail by Bristow *et al.* (1984) for other Karoo lavas, and is in any case a process which is not easy to evaluate. Furthermore, crustal contamination in any form is likely to give rise to scatter of data on many of the diagrams we have used, rather than the systematic or rational trends observed.

(b) *Mantle enrichment.* Consideration of the proposition that the isotopic signature of the less-evolved Tafelberg basaltic rocks are mantle-derived does not follow simply as an alternative to crustal contamination because of a lack of compelling evidence for the latter. On the contrary, although some of it is circumstantial, there is independent evidence that the more primitive Tafelberg lavas could be derived from old, heterogeneously enriched, lithospheric mantle sources.

The crux of the problem relates to the high initial $^{87}\text{Sr}/^{86}\text{Sr}$ ratios (0.7081–0.7120) in these less-evolved rocks (Figs. 21 and 23) such that their isotopic compositions plot in the enriched quadrant well to the right of the “mantle array” (and all other Karoo volcanics) on a $\epsilon_{\text{Sr}}-\epsilon_{\text{Nd}}$ diagram (Hawkesworth *et al.*, 1984, Fig. 4). Thus the Tafelberg basaltic rocks do not have exceptionally low initial $^{143}\text{Nd}/^{144}\text{Nd}$ ratios when compared to other Karoo volcanics. Their Pb-isotopic compositions are close to those obtained from Gough Island (Fig. 20) and, although enriched, it could be argued that they are of mantle derivation.

Derivation of the Tafelberg basaltic rocks from heterogeneously enriched mantle implies high time-integrated Rb/Sr ratios for a considerable length of time. The less-evolved Tafelberg rocks shown in Fig. 32 have an

average Rb/Sr ratio of 0.10 (average Rb/Sr for all Tafelberg basaltic rocks is 0.24) as compared with an average Rb/Sr ratio of 0.068 for the most voluminous Karoo volcanics, i.e. the Lesotho Formation of the Central area (Marsh and Eales, 1984). If the dashed reference line in Fig. 32 has any age significance then the mantle source must in part have been enriched to a Rb/Sr ratio of 0.12 some 1.8 b.y. ago in order to generate the observed $^{87}\text{Sr}/^{86}\text{Sr}$ ratio shown for sample KLS58 in this diagram. This is in close agreement with model $T_{\text{Bulk Earth}}^{\text{Sr}}$ ages of around 2 b.y. for the low Rb/Sr ratio Tafelberg basaltic rocks, as can be inferred from Fig. 32.

The question arises as to whether upper mantle source regions exist with the Rb-Sr characteristics inferred above. Enrichment of the sub-continental lithosphere beneath southern Africa can now be inferred from several different approaches. Rb-Sr and Sm-Nd isotopic systematics in sub-calcic garnets contained as inclusions in diamond and from kimberlite concentrates indicate that diamonds formed some 3.2–3.3 b.y. ago following enrichment ($\text{Rb/Sr} = 0.22\text{--}0.38$) of residual sub-cratonic mantle (Richardson *et al.*, 1984), leading to present day $^{87}\text{Sr}/^{86}\text{Sr}$ ratios as high as 0.732 and 0.755 for concentrate sub-calcic garnets from the Finsch and Bultfontein kimberlites respectively. Ancient enrichment (>1 b.y.) is also indicated by high $^{87}\text{Sr}/^{86}\text{Sr}$ and low $^{143}\text{Nd}/^{144}\text{Nd}$ ratios of garnet peridotite xenoliths and constituent minerals (one diopside has a $^{87}\text{Sr}/^{86}\text{Sr}$ ratio of 0.7134) from the Bultfontein kimberlite, South Africa, and by low $^{143}\text{Nd}/^{144}\text{Nd}$ ratios in the incompatible element enriched and high MgO picritic rocks from the northern Lebombo and Nuanetsi regions (Kramers, 1977; Menzies and Murthy, 1980; Erlank *et al.*, 1982; Hawkesworth *et al.*, 1984). In contrast garnet-free modally metasomatized phlogopite \pm K-richrichterite bearing xenoliths from the Bultfontein kimberlite have Rb-Sr isotopic relationships which suggest that this metasomatism is the result of a younger enrichment event which occurred prior to and is not related to kimberlite emplacement at 90 m.y. (Erlank and Shimizu, 1977; Erlank *et al.*, 1980, 1982). These xenoliths have relatively high Rb/Sr ratios of 0.12–0.87 and thus could have generated the observed range in $^{87}\text{Sr}/^{86}\text{Sr}$ ratio (0.7052–0.7104) in just 150 m.y. As Hawkesworth *et al.*

(1984) have noted, different styles of trace element enrichment can thus be recognized in both mantle xenoliths and Karoo basalts, and with time these result in different trends on an $\epsilon_{\text{Sr}}-\epsilon_{\text{Nd}}$ diagram. Thus the Tafelberg basaltic rocks and the phlogopite \pm K-richterite xenoliths both have high Rb/Sr (and Rb/Ba) ratios such that their present-day $^{87}\text{Sr}/^{86}\text{Sr}$ ratios are displaced to the right of the "mantle array" in the enriched quadrant of an $\epsilon_{\text{Sr}}-\epsilon_{\text{Nd}}$ diagram (Hawkesworth *et al.*, 1984, Fig. 9).

The phlogopite \pm K-richterite metasomatism mentioned above is clearly a recent mantle enrichment event, and in view of the inferred age of enrichment shown in Fig. 32 for the Tafelberg lavas, cannot be the cause of enrichment in the source areas of these lavas. No chemical or isotopic information is available for xenoliths from Namibian kimberlites, but if the same style of Rb/Sr and Nd/Sm enrichment as observed in the phlogopite \pm K-richterite metasomatism at Bultfontein (see also Haggerty *et al.*, 1983) had occurred some 2 b.y. ago in the mantle source areas of the Tafelberg basaltic rocks, then it is quite feasible that the latter could have been derived from old, heterogeneously enriched mantle.

The above discussion has documented the possibilities for enrichment in the lithospheric mantle beneath southern Africa because that is where variations in Rb/Sr and Sm/Nd are likely to persist long enough for isotopic variations to occur (Erlank *et al.*, 1982; Hawkesworth *et al.*, 1984). A thick (>150 km) enriched lithospheric mantle "keel" was already in existence beneath the Archaean Kaapvaal craton some 3.2–3.3 b.y. ago (Richardson *et al.*, 1984), but the latter could not have given rise to the Tafelberg basaltic rocks since both the inferred age of mantle enrichment and the ages of oldest basement cover rocks surrounding the Etendeka volcanics (Miller, 1983) suggest derivation from Proterozoic mantle. Future work should thus attempt to identify enriched Proterozoic lithospheric mantle beneath north-west Namibia.

Support for the above ideas comes from isotopic variations observed in other Gondwana basaltic rocks. The Tasmanian dolerites, and Ferrar dolerites and Kirkpatrick basalts from Antarctica, have high $^{87}\text{Sr}/^{86}\text{Sr}$ ratios (generally >0.710) and have long been cited as examples of crustally contaminated basalts (e.g. Faure *et al.*, 1974). However, recent work by Hoefs *et al.* (1980), Kyle *et al.* (1983) and Mensing *et al.* (1984) has shown, on the basis of combined $^{87}\text{Sr}/^{86}\text{Sr}$ and $^{18}\text{O}/^{16}\text{O}$ studies on Antarctic samples, that even though there is evidence for some crustal contamination leading to elevation of $^{87}\text{Sr}/^{86}\text{Sr}$ ratios, that the parental uncontaminated magmas had $^{87}\text{Sr}/^{86}\text{Sr}$ ratios of about 0.710. The geochemical and isotopic characteristics of these magmas are thus essentially those of their mantle source regions; by implication the same situation may apply for the Tafelberg basaltic suite.

Consequently, although some crustal contamination cannot be ruled out, and could well be superimposed upon pre-existing geochemical characteristics, it seems likely that the geochemical and isotopic signatures of the Tafelberg basaltic rocks are essentially those of their lithospheric mantle source regions. These appear to have been variably enriched at least as far back as the Proterozoic and their geochemical nature is discussed further in the following sections.

Three final points need to be made. First it could be argued that the Tafelberg basaltic magmas originate in the asthenosphere, with isotopic and elemental characteristics similar to those of the Horingbaai dolerites (Figs. 17 and 21), and are subsequently modified as they pass through enriched lithospheric mantle, i.e. a form of "mantle contamination". Apart from the fact that some inter-element trends do not support this possibility (e.g. Nb and TiO_2 vs. Zr in Fig. 16), the relationships shown in Fig. 33 provide further constraints on the operation of such a

process. This must involve assimilation of small volume melts or small pockets of enriched lithospheric mantle of variable composition by Horingbaai type basaltic magma in view of the high and variable Rb and Sr contents of the less evolved Tafelberg basaltic rocks. In addition the $^{87}\text{Sr}/^{86}\text{Sr}$ ratio of assimilated lithospheric mantle would have to be at least as high as 0.714 in order for such a process to be feasible. We cannot evaluate this possibility further at this stage and thus prefer the simpler alternative of deriving the Tafelberg basaltic rocks directly from enriched lithospheric mantle, even though there is potentially a heat problem in deriving large volumes of basaltic magma from "cold" lithosphere.

The second point refers to a disparity between calculated $T_{\text{Bulk Earth}}^{\text{Sr}}$ and $T_{\text{CHUR}}^{\text{Nd}}$ model ages. As indicated in Fig. 32, Sr model ages are of the order of 2 b.y. for the less evolved Tafelberg rocks, a figure which is also obtained by consideration of Pb-isotope systematics (Fig. 20). Hawkesworth *et al.* (1984) have shown that the average Nd model age for these rocks is approximately 0.9 b.y. (see Fig. 19). A possible explanation is to assume that the Sr model ages are meaningful with the Rb/Sr, but not the Sm/Nd ratios, of the less evolved rocks approximating those of their source areas. Calculation shows that Sm/Nd ratios of these rocks are on average 16% lower than what would be required to yield Nd model ages of around 1.8 b.y. Numerical modelling indicates that such a shift in Sm/Nd could be affected by small degrees of partial melting (~5%) of a 3 or 4 phase peridotite provided about 5–7% garnet remained in the restite assemblage, and provided also that clinopyroxene is either absent or not a significant constituent in the latter, so that Rb/Sr fractionation is minimal.

In the third place it is now necessary, for several reasons, to explain the relatively low Mg-numbers of the least evolved basaltic rocks. Since this is not considered to be due to crustal contamination we speculate that these magmas have undergone crystal fractionation *en route* to the surface. Such fractionation could have been initially dominated by olivine, later joined by clinopyroxene. However, fractionation of the latter mineral in the least evolved rocks would again have to be minimal (cf. discussion of model ages above) in order not to fractionate Rb/Sr ratios, although some fractionation is evident from those samples with higher Rb/Sr ratios, and lower Sr model ages, in Fig. 32.

B. Other Basaltic Rocks

We have not considered it necessary to deal at length with the petrogenesis of the other Etendeka basic rock types because (a) they are less abundant and more restricted in their occurrence than the Tafelberg basaltic suite, (b) they apparently show less compositional variation than the latter, even though we have analysed fewer samples, and (c) some aspects of their petrogenesis has been covered in the preceding discussions.

As noted previously we have not placed much emphasis on the plagioclase-phyric *Albin basalts* because of their altered nature (Section VII-A). Nevertheless, mineralogical and chemical variations such as Al_2O_3 vs. SiO_2 (Fig. 14) suggested that the Albin basalts could be cumulus enriched, specifically in plagioclase, counterparts of the Tafelberg basaltic rocks. In view of the generally higher concentrations of Ni and Cr in the Albin lavas (Fig. 13) this could suggest that such cumulus enrichment occurred in less fractionated Tafelberg basic magmas. However, since both petrographic evidence and calculations according to the formulation of Nathan and Van Kirk (1978) show that plagioclase is not a liquidus phase in the latter, it is more likely that the Albin parental lavas differed slightly in their evolutionary history from the Tafelberg parental lavas. The limited isotopic evidence

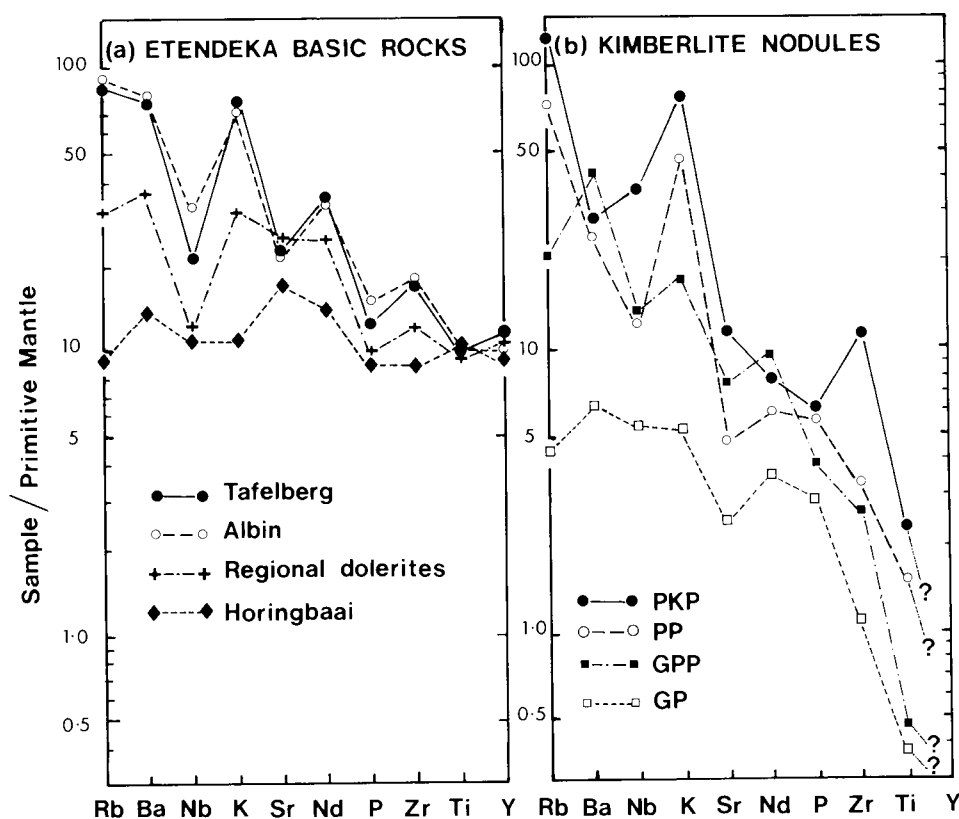


Figure 34

Mantle normalized incompatible element diagrams, using normalizing values given by Rogers (1979). (a) Less evolved Etendeka basaltic rocks (Mg-number >55). Number of samples given in parentheses: Tafelberg (8), Albin (6), Horingbaai (2), regional dolerites (2). (b) Kimberlite nodules from Bultfontein floors (Erlank *et al.* 1982; Erlank and Waters, unpubl. data). GP—garnet peridotite (3), GPP—garnet phlogopite peridotite (5), PP—phlogopite peridotite (3), PKP—phlogopite K-richertite peridotite (9). Numbers in parentheses are numbers of samples used.

available (Figs. 18 and 23) is consistent with the above suggestions. Further evidence for the similarity in magma compositions is shown by the absolute and relative incompatible element abundance variations for Albin and Tafelberg basaltic rocks with Mg-numbers >55 in Fig. 34a. We have not carried out crystallization or density calculations to test the qualitative conclusions reached above and this should be done when additional data become available; in this context we have become aware of and intend to analyse fresh Albin-like dolerites and lavas along the coast north of the Albin type area (Fig. 4) as far as Terrace Bay (Fig. 1).

In the case of the *Regional dolerites* (i.e. those that cut Karoo sediments but not the lavas) only two, KLS43 and 44, have been analysed in this study. Nevertheless they have distinctive compositional characteristics that set them apart from other Etendeka basic rocks, and since they do not appear to be related to the latter by contamination processes, their isotopic characteristics (e.g. Fig. 21) suggest a separate petrogenesis. Their high Mg-numbers (66) and their incompatible element abundance variation trends would support this suggestion (Fig. 34a). We have noted that both north and south of the Messum lava field (Fig. 1) a great many dolerite dykes occur cutting Damaran schists and granites (e.g. Fig. 7). Since their precise ages are unknown they have not been included in the present study. However, many of them are olivine-bearing with ophitic textures similar to the regional dolerites, and since comparison has already been made between the regional dolerites and the voluminous Lesotho Formation basalts and dolerites of the Central area it is obviously important to document further the ages and geochemistry of this magma type in northern Namibia. For the present we assume that the petrogenesis of the regional dolerites is similar to that

proposed by Marsh and Eales (1984) for the Lesotho Formation Volcanics.

The primitive nature of the *Horingbaai dolerites* has repeatedly been emphasized in this study. However, it is important to note that the two samples, KLS122 and 145, for which isotopic and rare earth element data have been obtained, are also those which have highest Mg-numbers and lowest incompatible element contents. Nevertheless, the relatively flat REE (Fig. 17) and incompatible element abundance patterns (Fig. 34a), at approximately 10× chondrite or primitive mantle concentrations, coupled with Nd-, Sr- and Pb-isotopic compositions (Figs. 20 and 27) for these two samples attests to their depleted MORB-like nature. The overall sense of the incompatible element variations in Fig. 34a supports the previous arguments made on isotopic grounds that the other Etendeka basaltic rocks are not related to the Horingbaai dolerites by contamination processes. However, it is also important to note that although the 5 Horingbaai samples analysed show a narrow range of SiO₂ content (46.5–47.2%), K, Ba and Nb concentrations show a fourfold variation. Concomitant Mg-number (65 to 53) and Ni (219 to 79 ppm) variations are suggestive of some fractional crystallization control coupled with variable degrees of partial melting if these features are to be reconciled. In addition, other incompatible elements show varying and erratic enrichment (Table I) and hence we have not attempted to quantitatively model these variations. Further field work is warranted to confirm the apparent confinement of these dolerites to the Albin type locality (Fig. 4), and it will be of considerable interest to see whether there is any correlation between incompatible element and isotopic abundance variations in these important dolerites when further analyses become available.

In summary, it is clear that further field and geochemical work, together with age and palaeomagnetic measurements, on the Albin basic rocks and the Regional and Horingbaai dolerites is necessary before a better understanding of the various Etendeka basic magma types is to hand.

C. Source Area Characteristics of Basic Magma Types

It is not our intention here to model quantitatively the actual compositions of the mantle source areas which gave rise to the various Etendeka magma types, since we cannot adequately constrain the possible mineralogies of potential source areas for major and trace element modelling at this stage. Rather, we wish to consider relative and absolute abundance patterns of trace elements which show varying degrees of "incompatibility" in order to characterize source area identities, and then to discuss the implications of these abundance patterns with respect to source area evolution prior to the melting events which produced the Etendeka basic magmas. The approach used is similar to that of Duncan *et al.* (1984) who have provided an overview of source area characteristics for all the important basic magma types from the Karoo Province as a whole.

From previous discussions, and as shown simply by isotopic variations and in more detail by the comprehensive modelling carried out, it is logical to conclude that three separate mantle sources were involved in producing the Etendeka basic magmas. These can be readily distinguished in Fig. 34a, where the relative nature of the abundance patterns reinforces the basic postulate made above. For example, even if the isotopic variations and the previous arguments and modelling were ignored, it would be highly unlikely that the different Etendeka magma types could be derived from the same mantle source by different degrees of partial melting taking into account, *inter alia*, the Nb–Sr–Nd relationships shown. The assumptions made here involve: (a) more than about 5% partial melting of the respective source areas so that small differences in distribution coefficients do not become important, (b) no restite minerals are present that can retain such trace elements in the melting residue (e.g. Nb in ilmenite), and (c) no major plagioclase fractionation has occurred that could affect Sr concentrations. The magma characteristics shown in Fig. 34a are therefore taken to be those of their sources.

It is convenient to discuss the abundance patterns in Fig. 34a, and also the REE patterns in Fig. 17, in terms of geochemical "primitiveness", rather than order of intrusion or emplacement. Thus the Horingbaai dolerites have relatively flat incompatible element and REE patterns consistent with derivation from a depleted MORB-type source. As noted by Duncan *et al.* (1984) the only other Karoo basic magmas which have similar patterns are the Rooi Rand dolerites which intrude the Sabie River basalts in the Lebombo monocline on the eastern extremity of the Karoo Province. The coincidence of abundance patterns and timing and location of intrusions, together with asthenospheric geochemical characteristics, can hardly be fortuitous, and the geodynamic significance of these features is discussed in the next section.

The second mantle source involved is that which produced magmas with the characteristics of the regional dolerites. As repeatedly noted in this contribution, the regional dolerite abundance patterns in Figs. 17 and 34a are remarkably similar to those of the Lesotho Formation of the Central area, and to the Lesotho-type Kalkrand basalts near Mariental in southern Namibia (Fig. 1). More particularly, the two samples analysed, KLS43 and 44, have enriched Sr-, Nd-, and Pb-isotopic characteristics almost identical to the 182 m.y. Lesotho-type Tandjiesberg dolerite sill (Hawkesworth *et al.*, 1984; Richardson, 1984; Table VII) situated in southern Namibia just north of

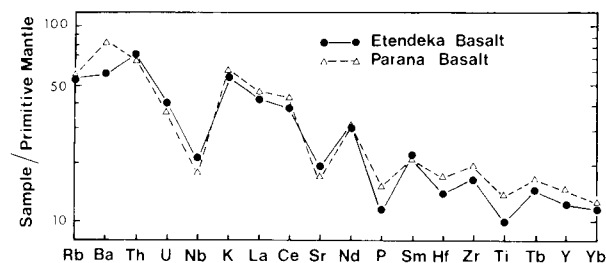


Figure 35

Mantle normalized incompatible element plot for Tafelberg basalt KLS24 and Serra Geral (Paraná) low-TiO₂ basalt BRA17. Normalizing values after Rogers (1979). Data from Microfiche Card 2.

Noordoewer (Eales *et al.*, 1984, Fig. 1). These details are provided in order to document the possible extent of this mantle source, and to reinforce the possibility of Jurassic Karoo activity in northern Namibia, as indicated by individual K-Ar ages of up to 196 m.y. for dolerite intrusives from this area (Siedner and Miller, 1968). The enriched nature of the inferred sub-continental lithospheric source of Lesotho-type magmas has been evaluated by Marsh and Eales (1984).

The third mantle source is that from which the volumetrically dominant Tafelberg and Albin lavas were derived. As indicated in Figs. 17 and 34a this source is geochemically the most enriched of the Etendeka magma sources, though not as enriched as might be expected from consideration of the high ⁸⁷Sr/⁸⁶Sr ratios of these rocks, and certainly less enriched than the picrites and basalts from the northern Lebombo and Nuanetsi areas which in turn have lower ⁸⁷Sr/⁸⁶Sr ratios (Duncan *et al.*, 1984; Hawkesworth *et al.*, 1984). The extent of this source is evident from Fig. 1, but is much greater when the contiguous Serra Geral basaltic lavas from the Paraná basin in Brazil are considered. The geochemistry of these basaltic lavas is similar to those of the Sabie River Basalt Formation in the Lebombo (Cox, 1983; Cox and Bristow, 1984) in that a northern province of high TiO₂ and incompatible element enriched basalts can be distinguished from a southern low TiO₂ and less incompatible element enriched basaltic province (Ruegg, 1976; Ruegg and Amaral, 1976; our data, Microfiche Cards 1 and 2). The similarity of composition of a Tafelberg basalt and a low TiO₂ basalt we have analysed from the southern Paraná basin is self evident (Fig. 35) and attests to the widespread nature of this enriched mantle source, which is also inferred to be sub-continental lithosphere. During the course of the Karoo Geodynamics Project we did not encounter any basaltic lavas in the Etendeka with high TiO₂ and incompatible element contents as mentioned above for the northern Paraná and northern Lebombo. However, recent additional work has revealed the presence of such high TiO₂ basaltic types interbedded with low TiO₂ basalts at Terrace Bay (Fig. 1) and further north in a section inland along the Khumib River. These new data are not discussed here but will be the subject of a future contribution when further analysis and evaluation is completed.

The next point we wish to pursue is the evolution and pre-history of the enriched mantle sources we have identified. In previous discussion, comparisons have been made between enriched and metasomatized peridotite nodules from kimberlites and Tafelberg basaltic rocks, mainly on the basis of Sr- and Nd-isotopic characteristics, in terms of the Rb/Sr (also Rb/Ba) and Sm/Nd *styles* of enrichment observed in these diverse mantle-derived rocks. However, when considering other incompatible element abundances it is apparent that none of the kimberlite nodule groups portrayed represent the exact type of mantle sources that could produce the Tafelberg and regional dolerite magma types in view of the steepness of the nodule abundance

trends (compare Figs. 34a and b). Similar steep REE patterns are also shown by these nodule groups (Erlank *et al.*, 1982). The enriched nodule types could potentially each represent an end-member in a simple two-component mixed mantle source, with the other end-member having relatively flat abundance patterns within the range 1–5× primitive mantle abundances (cf. Fig. 34). Nodules with relatively flat to slightly enriched LREE patterns within the range 1–5× chondrites, and with more fertile major element compositions, have been recognized by Nixon *et al.* (1981).

If the possibility of the existence of enriched mantle lithospheric sources for the Tafelberg, Albin and regional dolerite magmas is accepted, then the question arises as to how such sources could develop. One obvious possibility is through plume or hot spot activity since it is well documented that the Tristan da Cunha hot spot was situated approximately underneath the present location of the Etendeka lavas at the time of eruption (Duncan, 1981; Morgan, 1983). However, isotopic abundances, notably $^{87}\text{Sr}/^{86}\text{Sr}$ ratios of near 0.705 in Tristan da Cunha and from the Walvis Ridge (White and Hofmann, 1982; Richardson *et al.*, 1982) are much lower than those encountered in the Tafelberg, Albin and regional dolerite rocks (Fig. 18; see also Pb-isotope relationships in Fig. 20).

On the other hand the Sr- and Nd- model ages of the Tafelberg, Albin and regional dolerite rocks imply Proterozoic enrichment and the further question arises as to whether early subduction influenced the composition of their source regions (Duncan *et al.*, 1984; Hawkesworth *et al.*, 1984), as opposed to younger subduction postulated as being related to the breakup of Gondwanaland (Cox, 1978). It is emphasized that comparisons made here with abundance patterns of young calc-alkaline volcanics from destructive plate margins are not on the basis of defining tectonic environment, but rather from the point of view of deciphering whether subduction related processes have compositionally modified the Etendeka basic magma sources. Indeed, since the Etendeka magmas have obviously been emplaced in an extensional tectonic environment at a constructive plate margin, the ensuing discussion casts doubt on the use of some discriminant diagrams and trace element abundance patterns for inferring tectonic environment *per se*, since it appears that they can equally be used to infer source related processes and pre-history.

A simple first approach is to use discriminant diagrams such as the ternary Ti–Zr–Y diagram of Pearce and Cann (1973), as shown in Fig. 36. Only one sample, the most evolved Horingbaai dolerite, falls in the within-plate basalt (WPB) field. The other Horingbaai samples have compositions consistent with ocean floor basalt (OFB) or MORB characteristics, but this is not rigorously defined as low-K tholeiites (LKT) and calc-alkali basalts (CAB) can also plot in this field. The two regional dolerites have compositions that also plot just within the same ambiguous

field although Cox (1983) has noted that the average Lesotho Formation basalt plots within the CAB field. The salient point, however, is that all Tafelberg and Albin basaltic rocks have compositions that fall within the CAB field. Following the recommendations of Pearce and Cann (1973) we next plotted the same compositions in a Ti–Zr–Sr diagram (not shown). In this case the Horingbaai dolerites fall in the LKT field (oceanic arcs), the regional dolerites plot in the CAB field, while the Albin and Tafelberg basaltic rocks fall mostly in the CAB field, with some plotting in the OFB field.

With this in mind it is pertinent to re-examine the abundance patterns in Figs. 34a and 35, since this type of normalized diagram provides a convenient means of comparing samples on a more extended trace element database. This has been done by Pearce (1983) who observed characteristic patterns for island arc and other calc-alkaline volcanics, within-plate basalts and MORB. Note that while Pearce (1983) used MORB-normalized patterns the essential features to be discussed and compared are readily discernible from Figs. 34a and 35; however, MORB-normalized patterns for some of the Etendeka basic rocks are presented by Duncan *et al.* (1984, Fig. 18). On this basis the MORB-like (but not LKT) characteristics of the Horingbaai dolerites are obviously confirmed. Tafelberg and Albin basic rocks have negative Nb, Sr, P and Ti anomalies (see also Duncan *et al.*, 1984; Hawkesworth *et al.*, 1984), while the regional dolerites have well-developed negative Nb and P anomalies, but only poorly-developed negative Sr and Ti anomalies. The negative Nb anomalies, in particular, are most similar to those characteristic of subduction-related magmas (Pearce, 1983; Weaver and Tarney, 1984). However, although the overall features of the abundance trends in Figs. 34a and 35 are, in general, similar to those in calc-alkaline magmas, in detail they differ. For example, Sr/Nb ratios are much lower than in the calc-alkaline rocks examined by Pearce (1983). Hawkesworth *et al.* (1984) have noted this and pointed out that subduction-related magmas also have higher Sr/Nd ratios than inferred from Fig. 34a. It is, furthermore, not clear why the Tafelberg, Albin and regional dolerite basic rocks have high Zr/Nb ratios indicative of depletion processes (Erlank and Kable, 1976) in view of our contention that they are derived from enriched lithospheric mantle. In a wider context, it is noted that while negative Nb anomalies are present in most other Karoo rocks they are lacking in some minor types (e.g. Moshesh's Ford Formation of the Central area; Duncan *et al.*, 1984) in other Gondwanaland basic volcanics from Antarctica (Pearce, 1983), and the Deccan traps (Hawkesworth *et al.*, 1984).

Given that there is evidence for early subduction-related processes affecting the sources of the Tafelberg, Albin and regional dolerite magmas, then there are inevitably some explanations that can be advanced to explain why the abundance patterns in Figs. 34a and 35 do not match those of modern calc-alkaline magmas in greater detail. The most obvious explanation is that the sources bear the imprint of two types of enrichment process (Hawkesworth *et al.*, 1984). Alternatively, we do not yet understand the residual mineralogies developed after melting in the mantle wedge situated above subduction zones, nor do we understand the scavenging effects of H₂O-rich fluids derived from the subducting slab and the relative trace element contribution from the slab itself. In any event, in the simplest scenario dewatering of a subducted slab could potentially transport mobile elements such as K, Rb and Ba, either from the slab itself and any associated subducted sediment, or from the immediately overlying mantle wedge, into the higher levels of the latter, causing enrichment in these elements, which are, of course, those most enriched in the Etendeka basic magmas under discussion (Fig. 34a). The process is effectively then one of subduction-related metasomatism.

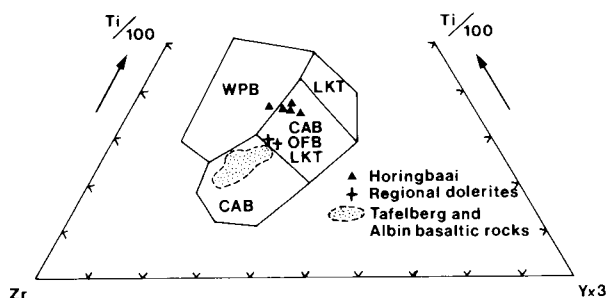


Figure 36

Ti–Zr–Y discriminant diagram after Pearce and Cann (1973). WPB — within plate basalt, LKT — low K tholeiite (island arc), OFB — ocean floor basalt (MORB), CAB — calc-alkaline basalt.

The negative Nb, Sr, P and Ti anomalies noted above are not easily explained. Buffering by restite minerals during melting could provide a partial explanation, but is not easily envisaged for Sr. Alternatively, removal of these elements at an early stage of the evolution of the source rocks is possible, but experimental data are lacking. Note, however, that under certain conditions geochemically dissimilar elements such as K, Ti, Sr, Zr and Ba, together with lesser amounts of LREE and Nb, can be transported in H₂O-rich fluids, as manifested by the occurrence of the minerals lindsleyite and mathiasite, which contain high concentrations of these elements, in metasomatized phlogopite and K-richite bearing peridotite nodules (Haggerty *et al.*, 1983). Note the relative abundance of these diverse incompatible elements in these PKP nodules in Fig. 34b in this regard. What is needed are some experimental studies of the relative solubilities of incompatible elements in H₂O-rich fluids under upper mantle conditions. Taken together, there are probably several processes involved in producing the geochemical characteristics of the sources of the Tafelberg, Albin and regional dolerite magmas. However, most importantly, the development of relatively high Rb/Sr ratios in the mantle wedge above a Proterozoic subduction zone is a feasible proposition and would, with time, allow the generation of the high ⁸⁷Sr/⁸⁶Sr ratios now observed particularly in the Tafelberg and Albin basic lavas.

The basement rocks in the vicinity of the Etendeka lava field are those of the 2 b.y. Abbabis Metamorphic Complex (Miller, 1983). To our knowledge no trace element analyses are available for these rocks which would allow evaluation of their geochemical characteristics and the implied tectonic history discussed above. We note, however, that there is strong geophysical evidence for the existence of a Proterozoic subduction zone to the south in the Namaqualand Metamorphic Complex (De Beer *et al.*, 1982). In this regard there is a major 2 b.y. calc-alkaline volcanic province along the Orange River (situated around Noordoewer in Fig. 1 of Eales *et al.*, 1984) described by Reid (1977) and Reid and Erlank (1979). Furthermore, evidence summarized by Miller (1983) suggests that there was also north-west subduction of the Kalahari craton beneath the Congo craton during Damaran times (some 0.65–0.70 b.y. ago). All these features provide scope for speculation by proponents of subduction-related enrichment.

In the final analysis, however, it is not clear at all that the enriched Etendeka basic magmas have been derived from sources with calc-alkaline affinities or that subduction-related processes have been active in the production of these enriched sources. There is at present no compelling evidence why the Tafelberg, Albin and regional dolerite basic magmas should not simply be accepted as continental flood basalts (CFBs) with their own distinctive characteristics derived from enriched lithospheric mantle. The latter could equally well have undergone sub-cratonic metasomatism by fluids emanating continuously from the deep mantle as envisaged by Bailey (1978, 1982). Alternatively the enrichment could be due to veining by small volume melts (Sun and Hanson, 1975; Le Roex *et al.*, 1983) or even due to a combination of melt and fluid introduction (Richardson *et al.*, 1982). The prime requirement of the enrichment process remains one in which suitably high Rb/Sr ratios, and sufficient time, allows the generation of the relatively high initial ⁸⁷Sr/⁸⁶Sr ratios inferred for the source areas of the Tafelberg and Albin basic magmas.

D. Tafelberg Latites

As indicated in Section VII-B, these enigmatic rocks are characterized by high concentrations of K and incompatible trace elements contents for their SiO₂ contents of around 59

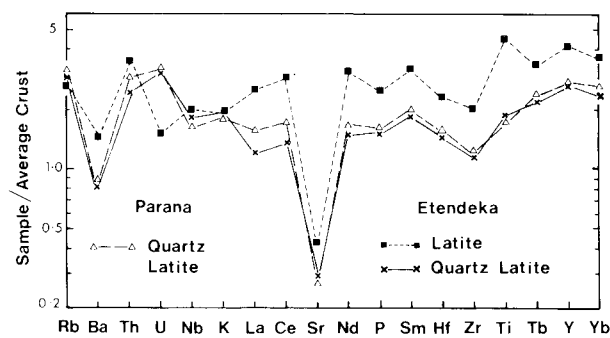


Figure 37

Average crust normalized incompatible element plot for Tafelberg latite (KLS69), Tafelberg quartz latite (KL20) and Serra Geral (Paraná) quartz latite (BRA12). Normalizing values from Weaver and Tarney (1984). Data from Microfiche Card 2.

%, and by the presence of abundant K-feldspar rather than plagioclase. This is demonstrated in Fig. 37 where it can be seen that, except for Sr, the latites have higher concentrations of K and the trace elements shown when compared to average crust. Additionally, apart from U (which may be due to alteration), and K, Rb and Nb, where concentrations are roughly similar, the latites also have higher concentrations of the other trace elements shown as compared to the more SiO₂-rich quartz latites, attesting to their evolved nature.

In Section VIII it was shown that the latites could not be related to the Tafelberg basaltic rocks, with which they are interbedded, or the quartz latites, by simple crystallization, melting or magma mixing processes, or combinations thereof. Their overall characteristics indicate that they could be derived by two processes, discussed separately below.

In the first place the latites could represent extreme examples of crustal contamination of say the least evolved Tafelberg basaltic rocks. Such a process would intuitively be one of combined assimilation–fractional crystallization (DePaolo, 1981) but even so the high levels of K₂O (average = 4.4%) and other trace elements, in excess of crustal levels (Fig. 37), would necessitate extremely large amounts of contamination and/or crystallization depending on the ratio of contaminant to crystallization. Our experience in modelling contamination in the basic rocks does not lead us to accept such an origin as being likely.

A more obvious explanation is that the latites represent crustal melts, albeit not minimum melt compositions in view of their low SiO₂ contents. On the basis of Fig. 37 their trace element contents (ignoring U) indicate that their source rocks are either strongly depleted in Sr, and perhaps (in a relative sense) other elements such as Ba, K, Nb and Zr, or alternatively that these negative anomalies are due to plagioclase, K-feldspar and zircon control, probably during both melting and crystallization, in view of the magnitude of the Sr anomaly. From an isotopic viewpoint, the Sr- and Nd-isotope ratios of the single latite analysed (Fig. 23) are within the range of isotopic ratios reported for Damaran granitic rocks and metasediments at 121 m.y. (for further details see next section) and thus the latites could potentially be derived by partial melting of appropriate Damaran rocks, which of course need not have the same composition as the average crust in Fig. 37.

A final clue to their origin is provided by “phenocrysts” of Ab₉₉ (mantled by rims of Ab₇₉) in one of the latites studied. Such a composition is not of igneous origin and these almost pure albites are presumably xenocrysts, or due to alteration (Section V). It is also worth recalling that these rocks apparently are geographically restricted to the vicinity of the Tafelberg type locality. Furthermore, perusal of the large numbers of analyses presented by Ruegg (1976) for Serra Geral volcanics from Brazil indicates that only 2 or

3 samples have compositions similar to the Etendeka latites.

E. Tafelberg Quartz Latites

The rocks we have collectively termed the quartz latites, which include the sub-group referred to as high-K dacites, do not have unusual compositions for their SiO₂ contents (66.5–69.2%). As noted in Section VII-C they show a relative uniformity of composition, except for K, Rb, Sr, K/Rb, Rb/Sr and initial Sr-, Nd- and Pb-isotope ratios, suggestive of some compositional variation in their source rocks (Figs. 14, 15, 18, 19, 20).

We have previously assumed (Section VIII) that the quartz latites represent crustal melts and have not found it necessary to invoke other explanations, such as partial melting of basaltic material underplated at or near the base of the crust. This has been proposed by Cleverly *et al.* (1984) for the Lebombo rhyolites on the eastern margin of the Karoo Province, partly on the basis of low ⁸⁷Sr/⁸⁶Sr ratios of near 0.704 in the rhyolites, which are similar to those in some of the Lebombo basaltic rocks. The Etendeka quartz latites clearly have isotopic ratios (Figs. 18, 19 and 20) and an overall chemistry consistent with crustal derivation. This is shown in Fig. 37 where a Tafelberg quartz latite is compared with average crust. Except for Ba and Sr, all other trace elements are enriched with respect to average crust, although the LREE are not as enriched as the HREE. The well-developed Ba and Sr, and to a lesser extent Zr, negative anomalies are consistent, as with the latites, with K-feldspar, plagioclase and slight zircon control both during the melting and crystallization processes that produced these rocks.

From the isotopic viewpoint Bristow *et al.* (1984, Fig. 10) have shown, from a compilation of a large number of available Sr-isotopic measurements of Damaran rocks, that many of them would have possessed suitable Rb/Sr and ⁸⁷Sr/⁸⁶Sr ratios 121 m.y. ago for such rocks to have produced melts with Rb/Sr and ⁸⁷Sr/⁸⁶Sr characteristics similar to the quartz latites. The limited available ¹⁴³Nd/¹⁴⁴Nd isotopic data for Damaran rocks also encompass (at 121 m.y.) the range observed in the quartz latites (Hawkesworth *et al.*, 1981; Hawkesworth *et al.*, 1984). Interestingly, there is no suggestion of an older component in the quartz latites, since two 2 b.y. Abbabis granitic basement rocks have, at 121 m.y., much higher ⁸⁷Sr/⁸⁶Sr and much lower ¹⁴³Nd/¹⁴⁴Nd ratios than observed in the quartz latites (Hawkesworth, unpublished data).

We have not extended our studies on the quartz latites since they are currently being investigated in a separate study. Results to date indicate that the quartz latites are very widespread in the Etendeka, and that they can be divided into several stratigraphic units (S.C. Milner, pers. comm.). Their widespread extent is even more evident when the Serra Geral volcanics of the Paraná basin in Brazil are considered. Many of the analyses presented by Ruegg (1976), from rocks sampled near the point of juxtaposition of the Paraná and Etendeka volcanics in Gondwanaland pre-drift reconstructions, are clearly of quartz latite composition. Two Serra Geral quartz latites analysed by us (Microfiche Cards 1 and 2) have compositions virtually indistinguishable from their Etendeka counterparts, as may be noted from the Sr-isotope and trace element data shown in Figs. 18 and 37. Clearly, we are dealing with the same rocks (and sources) and the implications for future thermal and trace element modelling are obvious.

X. GEODYNAMIC IMPLICATIONS

One of the main aims of this project has been to investigate the relationship between the breakup of Gondwanaland and the generation of Karoo magmas. In this paper we are specifically concerned with the question of whether the rifting that led to the separation of South America from Africa imposed any geodynamic control on

Karoo volcanism in Namibia. Various factors related to the above include the relative ages of Karoo volcanism in Namibia and the onset of sea floor spreading in this area; the location and variability of magma compositions with respect to the Namibian continental margin; the mechanism of rifting and crustal thinning and the heat required for crustal melting; and the influence of basement structural trends and mantle source area compositions in determining the actual site of rifting. No attempt will be made to treat these topics in detail as such discussion would be lengthy and would have to be concerned with the Karoo volcanic province as a whole. In this regard frequent reference will be made to a companion paper by Duncan *et al.* (1984) where the overall question of geodynamic control of Karoo volcanism is considered on a regional basis.

As summarized by Duncan *et al.* (1984) there is uncertainty in the older literature regarding both the identification, and the geochronological calibration, of the magnetic anomaly sequence off the west coast of southern Africa. However, the results of seismic reflection profiling by Austin and Uchupi (1982) suggest that rift propagation in the south Atlantic proceeded from south to north, with the ocean-continent boundary becoming progressively younger northward. They suggest that the oldest sea-floor spreading anomaly in the south Atlantic at the latitude of Cape Town is anomaly M9, while the oldest ocean-floor anomaly that can be recognized with any certainty off the Namibian coast is anomaly M4. The latter would correspond either to an age of 127 m.y. (Cox in Harland *et al.*, 1982) or 123 m.y. (Lowrie, 1982). On the adjoining landmass the oldest confirmed Karoo volcanicity is represented by the Lesotho-type 184 m.y. Kalkrand basalts near Mariental (Fig. 1), and by the 182 m.y. Lesotho-type Tandjesberg sill (Richardson, 1984), both in southern Namibia. Numerous dolerite dykes and sills in northern Namibia in the Etendeka region have yielded conventional K-Ar ages of 134–196 m.y. (Siedner and Mitchell, 1976; Table II) and it is for this reason that reliable ages should be obtained for what we have called the regional dolerites in this study. Together with the vast amounts of basalt and rhyolite emplaced during a Middle to late Jurassic volcanic event in southern South America (Dalziel, 1981), and ages between 130–240 m.y. for Paraná volcanics, carbonatites and other alkaline rocks from Brazil (Ulbrich and Gomes, 1981), these older Karoo volcanics heralded the rifting that led to the separation of South America from southern Africa. Although the onset of Karoo volcanicity in Namibia predates the opening of the south Atlantic, the main phase of Karoo volcanism near the present-day Atlantic coast of southern Africa, represented by the Etendeka Formation lavas, is much closer in age to the M4 magnetic anomaly (123–127 m.y.) mentioned above. In Section IV we adopted the Siedner and Mitchell (1976) age of 121 m.y. for the Etendeka lavas but suggested, on the basis of new age determinations, that the minimum age of these lavas is 130 m.y. If so this would mean that the lavas are slightly older than the age of the adjacent sea-floor in the south Atlantic. On the eastern extremity of the Karoo province (Lebombo monocline) the evidence is more clear-cut and here the main phase of volcanicity (together with that in the Central Karoo area) is substantially earlier than the oldest ocean-floor anomaly (Duncan *et al.*, 1984). Taken as a whole it therefore seems clear that Karoo volcanicity predates sea-floor spreading adjacent to any particular locality.

Duncan *et al.* (1984) have observed that the location of Karoo volcanism as a whole is clearly not a direct consequence of Gondwanaland intercontinental rifting since the basaltic products of the Karoo magmatic event are distributed over the entire subcontinent of southern Africa and are not preferentially located near the sites of rifting or plate separation. However, as noted by these authors, the

Karoo acid volcanics are only found adjacent to the continental margin in Namibia, and along the Lebombo monocline and in the Nuanetsi area, i.e. adjacent to the developing Gondwana plate boundaries. Since the evidence favours a crustal origin for the Etendeka quartz latites (Section IX-E) and probably also for the Lebombo and Nuanetsi rhyolites (Bristow *et al.*, 1984; Duncan *et al.*, 1984) this implies that crustal temperatures were significantly elevated in these two rift margin settings. Furthermore, it is significant that late-stage dolerite dykes with MORB-like compositional characteristics (i.e. the Horingbaai dolerites in the Etendeka and the Rooi Rand dolerites in the Lebombo) are found only in these same settings.

These features dictate that we now consider the mechanism of rifting, evidence for crustal thinning, and the problem of heat supply for crustal melting together with the bimodality of volcanicity in the Etendeka region. There is currently considerable controversy as to whether rifting is of the active or passive type (see recent summary by Morgan and Baker, 1983). Partly this is due to problems with semantics and definition and we do not wish to enter this debate. However, we note that the results presented by Austin and Uchupi (1982) provide evidence for crustal thinning or stretching adjacent to the present-day Namibian continental margin. The modelling of Le Pichon *et al.* (1982) indicates the large amount of lithospheric thinning that can occur just prior to asthenospheric breakthrough while Keen and Barrett (1981) estimated a 50% thinning of the continental crust on the rifting margin of eastern Canada as a result of rifting. Regarding the mechanism of thinning Turcotte and Emmerman (1983) prefer a diapiric penetration mechanism for the ascent of hot asthenospheric rock to the base of the crust. We are inclined to agree with these authors that "an important question is whether the diapiric upwelling is triggered by a mantle plume (active rifting) or is triggered by an instability caused by tensional stresses in the lithosphere (passive rifting)". The Tristan da Cunha plume has been located beneath the Etendeka region during the period 140–110 m.y. ago (Morgan, 1983) and therefore could well have triggered the rise of asthenospheric material as envisaged by Turcotte and Emmerman (1983). We note also the work on the west African rift system by Fitton (1983) who concludes that the south Atlantic rift system as a whole may have been initiated by plumes but most probably evolved through stretching of the lithosphere in the areas around and between these hot spots with subsequent passive upwelling of the hot asthenosphere into the lithosphere. In the east African rift system Girdler (1983) envisages that as extension reaches an advanced stage, the asthenosphere replaces the lower lithosphere and starts to replace the lower crust.

The importance of the above discussion with respect to the Etendeka lavas and intrusives is three-fold. First, penetration of the lithosphere by the asthenosphere to or near the base of the crust, by whatever mechanism, would raise isotherms in both the lithospheric mantle and in the crust and lead to melting in both these locales to produce the bimodal and interbedded basalt–quartz latite association observed so well at the Tafelberg type-locality (Fig. 6). Elevated crustal temperature in Karoo times cannot be simply a product of basaltic intrusion (Hildreth, 1981) since no acid volcanics occur in the Central Karoo area (Marsh and Eales, 1984; Duncan *et al.*, 1984; Bristow *et al.*, 1984). Secondly, the lack of magma mixing between the interbedded Etendeka basaltic rocks and acid volcanics (Section VIII) can be explained by a further conclusion reached by Hildreth (1981), namely that extension of the lithosphere reduces the susceptibility of basaltic magmas to hybridization in the crust. In the third place, several of the authors cited above (see also Bailey, 1983) agree that as

soon as lithospheric rupture occurs there will be bulk mantle penetration with ascent of magmas from sub-lithospheric sources. This is clearly consistent with late-stage emplacement of the Horingbaai (and Rooi Rand) dolerites with their depleted MORB-like geochemistry from an asthenospheric source during the final stages of crustal thinning. In this regard electrical sounding studies have detected the presence of a prominent conductive structure in the Damara orogen, one explanation for this being shallow emplacement of asthenospheric material (~20 km depth in the Messum–Brandberg area, Fig. 1) in a weak zone (Van Zyl and De Beer, 1983). Whether this explanation is correct, and whether such asthenospheric emplacement occurred in Karoo or Damaran times, remains to be verified. It should also be noted that although we believe the Horingbaai dolerites are of asthenospheric derivation they cannot represent material sampled from the Tristan plume since the latter has higher initial $^{87}\text{Sr}/^{86}\text{Sr}$ ratios (~0.705) than the former (~0.703).

The final geodynamic question we wish to consider concerns the influence of mantle source compositions and basement structural trends in determining the actual site of rifting. It should now be abundantly clear that we consider that the Etendeka Formation volcanics mark the surface expression of a distinct thermal and geochemical anomaly in the underlying upper mantle. The Tristan plume may have acted as the thermal trigger to initiate the melting which produced the Etendeka basic volcanics, but cannot have contributed materially to the enriched nature of these volcanics, since we have previously shown that the Tristan and Walvis Ridge volcanics have much lower $^{87}\text{Sr}/^{86}\text{Sr}$ ratios than observed in these volcanics, and since their source area enrichment is inferred to be of Proterozoic age (Section IX-C). Duncan *et al.* (1984) envisage that the source of most Karoo basic magmas is a heterogeneously enriched lithospheric mantle "keel", parts of which were already in existence some 3.3 b.y. ago (Richardson *et al.*, 1984). The Proterozoic enrichment implied for the Etendeka and other Karoo basic magma sources has several consequences. First, enhanced levels of K, Th and U can obviously contribute over a period of time to raising the ambient temperature of the sub-continental lithosphere prior to the thermal input of the Tristan plume. Secondly, if the enrichment process introduces hydrous minerals this will lead to a lowering of the solidus. These two factors will help in melting "cold" lithospheric mantle. In the third place such lithosphere may be more readily thinned and penetrated by a rising asthenosphere, because it is hotter and therefore less viscous and weaker than less enriched lithosphere. The association of highly enriched (and probably hydrous) lithospheric mantle with continental rifting, specifically in the Etendeka and Lebombo–Nuanetsi regions (Bristow *et al.*, 1984; Duncan *et al.*, 1984) suggests that the distribution of the most enriched zones in the sub-continental lithosphere influenced the pattern of continental rifting, i.e. the sites of rifting were ultimately controlled by enriched mantle locations, either with or without associated plume activity. If this is accepted then the question arises as to the influence of basement control on rifting. Cox (1978) noted that the alignment of both the south Atlantic and Indian ocean rifts show a broad dependence on basement structure. Of relevance to the Etendeka region is Bailey's (1978) observation that the zones of crustal weakness are typically the most recent orogenic belts. The electrical sounding studies of Van Zyl and De Beer (1983) confirm that the Damara mobile belt is in general a weak portion of the crust. The structural form lines in the coastal arm of the Damara orogen north of the main Etendeka lava field (Fig. 1) trend in a north-north-west direction (Miller, 1983), parallel to the present continental margin and presumed axis of rifting. The same generalized structural trend is also apparent south of this

lava field (Fig. 7). This supports Cox's (1978) contention that rifting and plate separation occurred along the structural grain in basement rocks. In short, we contend that whereas the direction and alignment of Gondwana rifting was crustally controlled, the question of where rifting actually occurred was ultimately controlled by the distribution of highly enriched domains in the sub-continental lithosphere.

XI. CONCLUSIONS

1. The volcanic rocks of the Etendeka Formation have a present-day coverage of 78,000 km² and comprise a series of interbedded basaltic, intermediate and acidic lavas, together with four varieties of intrusive dolerites. The lavas, from the base upwards, consist of the plagioclase-phyric Albin basalts followed by the volumetrically dominant aphyric Tafelberg basalts which are commonly interbedded with the Tafelberg quartz latites over a wide area. At the Tafelberg type-locality (~900 m) the Tafelberg basalts are, in ascending sequence, interbedded with the Tafelberg latites (found only at this locality) and the Tafelberg quartz latites, with the whole sequence being capped by quartz latite (Fig. 6). The relative stratigraphic thicknesses at this locality are: 70% basalt, 25% quartz latite and 5% latite. The regional dolerites cut the underlying Karoo sediments but not the lavas and appear also to be abundant in basement rocks. The Horingbaai dolerites intrude the Albin lavas and appear to be confined to the coastal region. The Albin dolerites appear to be restricted to their associated lavas, while the Tafelberg dolerites cut both the Albin and Tafelberg basaltic lavas.
2. Apart from the regional dolerites, which have mineralogical and geochemical similarities to the Lesotho Formation lavas of the Central area, the Etendeka Formation volcanics differ from all other Karoo volcanics by virtue of their Cretaceous age, stratigraphy, mineralogy, geochemistry, and range in mineralogical, elemental and isotopic compositions for the basaltic rocks. Thus the Albin and Tafelberg basic lavas consist of basalts and evolved basalts, with SiO₂ contents ranging from 51.2–55.4% and 51.8–57.8%, and Mg-numbers ranging from 61.8–48.7 and 56.8–27.5 respectively.
3. The interbedded Tafelberg basic rock–latite–quartz latite sequence exhibits many regular and rational compositional variations, not only for major elements, but also for trace elements and associated incompatible inter-element and Sr- and Nd-isotopic ratios. In contrast Pb-isotope variations do not show the same rationality. These data preclude the derivation of the basic rock–latite–quartz suite by any simple closed system model involving either partial melting on an isotopically homogeneous source or fractional crystallization of a homogeneous parent magma. Consideration of certain critical inter-element and isotopic ratio inter-relationships also precludes any simple two-component magma mixing between less evolved Tafelberg basalt and quartz latite, or latite, and any other simple magma mixing model involving any of the other basic rocks with quartz latite. The most likely magma mixing model, between Tafelberg basalt and quartz latite, is one requiring that mixing be followed by a proportional amount of fractional crystallization, but this is also ruled out on the basis of inconsistent incompatible trace element enrichment following mixing and fractional crystallization. Thus no simple genetic relationship exists between the basaltic rocks and the interbedded latites and quartz latites.
4. Interpretation of the petrogenesis of the voluminous Tafelberg basaltic suite is strongly influenced by the observation that the isotopic variations do not correlate precisely with increasing fractionation within this suite. Less evolved basic rocks (Mg-numbers >55) have variable initial ⁸⁷Sr/⁸⁶Sr ratios which almost encompass the range shown by the evolved basic rocks. We contend that the evolved rocks have been derived by crystal fractionation from less evolved basaltic parental magmas which had a range in isotope compositions, and the results of quantitative major and trace element modelling across the Tafelberg basalt spectrum strongly support this contention. Detailed assimilation–fractional crystallization (AFC) modelling, using a variety of actual and putative rock compositions, either as starting materials or as contaminants, cannot consistently explain inter-element and isotopic variations in either the evolved or less evolved Tafelberg lavas, and we conclude that crustal contamination has played only a minor role, if any, in the petrogenesis of the Tafelberg lavas. Conversely, evidence from metasomatized kimberlite nodules provides evidence for enrichment processes in the sub-continental lithosphere and isotopic considerations show that it is permissible to derive the less evolved Tafelberg basaltic rocks from such enriched lithospheric mantle sources.
5. The Albin basaltic rocks appear to have had a slightly different evolutionary history from the Tafelberg basic suite but their isotopic data permit derivation from the same enriched source. The regional dolerites have compositional characteristics which are intermediate in composition between the Tafelberg and Albin basalts on the one hand and the Horingbaai dolerites on the other, and have been derived from a separate source similar in composition to that which produced the Lesotho Formation basalts of the Central area. The Horingbaai dolerites have depleted trace element and isotopic characteristics and are derived from the MORB-like asthenospheric source.
6. Detailed consideration of incompatible trace element abundances in metasomatized kimberlite nodules shows that if such material is involved in the genesis of the Tafelberg, Albin and regional dolerite magmas then a two component source is required, the other component having lower abundances and flatter mantle normalized trace element abundance patterns than in the kimberlite nodules. Evaluation of the role of subduction-related enrichment processes, which would be of Proterozoic age because of Sr- and Nd- model ages, in the source areas of these basic magmas provides no compelling evidence for the operation of such processes. Instead the “calc-alkaline” affinities inferred for these basic magmas are thought to be spurious and we conclude that the Albin, Tafelberg and regional dolerite magmas should be simply accepted as continental flood basalts (CFBs) with their own distinctive characteristics derived from enriched lithospheric mantle. The precise nature of the enrichment process(es) cannot be defined at this time.
7. The latites and quartz latites have not been modelled in any detail, but their overall compositional characteristics are most consistent with a crustal derivation. Their Sr- and Nd-isotopic characteristics are also consistent with derivation from Damaran granitic rocks and metasediments and they show no signature for an older derivation, such as that represented by the ~2 b.y. Abbabis granite-gneiss. The quartz latites, and also the Tafelberg basalts, show strong compositional similarities with quartz latites and low TiO₂ basalts from the Serra Geral Formation in Brazil.
8. From a geodynamic viewpoint the regional dolerites would appear, together with other confirmed Jurassic Lesotho-type basalts and dolerites, to mark the first manifestations of volcanicity in Namibia. New age determinations suggest that the minimum age of the

Tafelberg basaltic and acidic lavas (i.e. the main volcanic phase) is 130 m.y. which would predate very slightly the oldest confirmed sea-floor spreading anomaly (M4) off the Namibian coast. Both the timing and location of Karoo volcanicity as a whole are not a *direct* consequence of Gondwana intercontinental rifting. The Etendeka Formation basic volcanics are considered to mark the surface expression of a distinct thermal and geochemical anomaly in the sub-continental lithosphere. The interbedded nature of the basaltic and acidic volcanics indicates that asthenospheric material (Tristan da Cunha plume ?) penetrated lithospheric mantle to or near the base of the continental crust in order to raise isotherms sufficiently for both lithospheric mantle and crust to melt simultaneously. Geophysical evidence provides support for crustal extension required to allow such asthenospheric penetration and for the latter itself. This scenario is also consistent with late-stage emplacement of the Horingbaai dolerites from an asthenospheric source. It is suggested that whereas the direction and alignment of Gondwanaland rifting and breakup was crustally controlled, the question of where rifting actually occurred was ultimately controlled by the distribution of highly enriched domains in the sub-continental lithosphere.

9. This account documents the first comprehensive report on the Etendeka volcanics, but their obvious importance is such as to warrant further work, not only on our existing collection (e.g. $^{18}\text{O}/^{16}\text{O}$ variations), but also on additional samples, particularly for the diverse dolerites encountered. Such work, together with further work on the quartz latites, is currently in progress. Detailed geochemical studies on some of the post-Karoo complexes (e.g. Messum) will also be required before a full understanding of this important and fascinating volcanic province is to hand.

ACKNOWLEDGMENTS

Posthumous credit is due to Harro Fesq and to Eric Simpson, who first supplied samples to the senior author from the Etendeka and Paraná regions respectively, and in which interbedded quartz latites were first recognized in both areas (Erlank, 1971), providing much of the stimulus for the present study. We are grateful to the following for analytical or other assistance during the course of this study: Y. Abraham, M. Brauteseth, J. Bristow, A. Gledhill, J. Kibby, J. Lilburn, R. Rickard, J. Roddick, A. Simpson, P. van Calsteren and F. Waters. Most of the radiogenic isotope measurements were carried out at Oxford University (A.J.E.) and at The Open University (J.S.M. and C.J.H.) and we thank these Institutions for their hospitality. H.L. Allsopp kindly supplied additional isotopic measurements. We are indebted to S.R. Taylor for allowing one of us (A.R.D.) access to his spark source mass spectrometric facilities at the Australian National University. Discussions with several colleagues but particularly with Keith Cox, Tony Ewart and Chris Hartnady were most helpful. Financial support and encouragement was supplied by our host universities, the Geological Survey of SWA/Namibia, and the CSIR and NERC. The first author also wishes to thank his co-authors, other colleagues, typists Jackie, Lynn and Susie, and five lovely ladies from Wolmunster Towers for their patience and encouragement during the lengthy preparation of this paper.

REFERENCES

Allsopp, H.L., Bristow, J.W., Logan, C.T., Eales, H.V., and Erlank, A.J. (1984a). Rb-Sr geochronology of three Karoo-related intrusive complexes. *Spec. Publ. geol. Soc. S. Afr.*, **13**, 281–287 (this volume).

- , Manton, W.I., Bristow, J.W., and Erlank, A.J. (1984b). Rb-Sr geochronology of Karoo felsic volcanics. *Spec. Publ. geol. Soc. S. Afr.*, **13**, 273–280 (this volume).
- Amaral, G., Bushce, J., Cordani, U.G., Kawashita, K., and Reynolds, J.H. (1967). Potassium-argon ages of alkaline rocks from southern Brazil. *Geochim. cosmochim. Acta*, **31**, 117–142.
- , Cordani, U.G., Kawashita, K., and Reynolds, J.H. (1966). Potassium-argon dates of basaltic rocks from southern Brazil. *Geochim. cosmochim. Acta*, **30**, 159–189.
- Armstrong, R.A., Bristow, J.W., and Cox, K.G. (1984). The Rooi Rand dyke swarm, southern Lebombo. *Spec. Publ. geol. Soc. S. Afr.*, **13**, 77–86 (this volume).
- Arth, J.G. (1976). Behaviour of trace elements during magmatic processes—a summary of theoretical models and their applications. *J. Res. U.S. geol. Surv.*, **4**, 41–47.
- Austin, J.A., Jr., and Uchupi, E. (1982). Continental-oceanic crustal transition off Southwest Africa. *Amer. Assoc. Petrol. Geol. Bull.*, **66**, 1328–1347.
- Bailey, D.K. (1978). Continental rifting and mantle degassing, 1–14. In: Neumann, E.-R., and Ramberg, I.B., Eds., *Petrology and Geochemistry of Continental Rifts*, Reidel, Holland, 296 pp.
- (1982). Mantle metasomatism—continuing chemical change within the Earth. *Nature*, **296**, 525–530.
- (1983). The chemical and thermal evolution of rifts. *Tectonophysics*, **94**, 585–597.
- Betton, P.J. (1979). Isotopic evidence for crustal contamination in the Karoo rhyolites of Swaziland. *Earth Planet. Sci. Lett.*, **45**, 263–274.
- , Armstrong, R.A., and Manton, W.I. (1984). Variations in the lead isotopic composition of Karoo magmas. *Spec. Publ. geol. Soc. S. Afr.*, **13**, 331–339 (this volume).
- Botha, B.J.V., and Hodgson, F.D.I. (1976). Karoo dolerites in north-western Damaraland. *Trans. geol. Soc. S. Afr.*, **79**, 186–190.
- Bowen, N.L. (1928). *The evolution of igneous rocks*. Princeton Univ. Press, Princeton, 334 pp.
- Briden, J.C., Rex, D.C., Faller, A.M., and Tamblin, J.F. (1979). K-Ar geochronology and palaeomagnetism of volcanic rocks in the Lesser Antilles island arc. *Phil. Trans. R. Soc. Lond.*, **291**, 485–528.
- Bristow, J.W., Allsopp, H.L., Erlank, A.J., Marsh, J.S., and Armstrong, R.A. (1984). Strontium isotope characterization of Karoo volcanic rocks. *Spec. Publ. geol. Soc. S. Afr.*, **13**, 295–329 (this volume).
- , and Cleverly, R.W. (1979). Volcanology of the Lebombo rhyolites. *Geogr. 79, Geol. Soc. S. Afr.*, 60–63.
- , and Cox, K.G. (1984). Volcanic rocks of the Lebombo-Nuanetsi-Sabi zone: classification and nomenclature. *Spec. Publ. geol. Soc. S. Afr.*, **13**, 69–75 (this volume).
- Bryan, W.B., Finger, L.W., and Chayes, F. (1969). Estimating proportions in petrographic mixing equations by least-squares approximation. *Science*, **163**, 926–927.
- Carlson, R.W., Lugmair, G.W., and MacDougall, J.D. (1981). Columbia River volcanism: the question of mantle heterogeneity or crustal contamination. *Geochim. cosmochim. Acta*, **45**, 2483–2499.
- Church, S.E., and Tatsumoto, M. (1975). Lead isotope relations in oceanic ridge basalts from the Juan de Fuca–Gorda ridge area, N.E. Pacific Ocean. *Contr. Miner. Petrol.*, **53**, 253.
- Cleverly, R.W., Betton, P.J., and Bristow, J.W. (1984). Geochemistry and petrogenesis of the Lebombo rhyolites. *Spec. Publ. geol. Soc. S. Afr.*, **13**, 171–194 (this volume).
- Cohen, R.S., Evensen, N.M., Hamilton, P.J., and O’Nions, R.K. (1980). U–Pb, Sm–Nd and Rb–Sr systematics of mid-ocean ridge basalt glasses. *Nature*, **283**, 149–153.
- Cox, K.G. (1978). Flood basalts, subduction and the break-up of Gondwanaland. *Nature*, **274**, 47–49.
- (1980). A model for flood basalt vulcanism. *J. Petrology*, **21**, 629–650.
- (1983). The Karoo Province of Southern Africa: origin of trace element enrichment patterns, 139–157. In: Hawkesworth, C.J., and Norry, M.J., Eds., *Continental basalts and mantle xenoliths*. Shiva, UK, 272 pp.
- , and Bell, J.D. (1972). A crystal fractionation model for the basaltic rocks of the New Georgia Group, British Solomon Islands. *Contr. Miner. Petrol.*, **37**, 1–13.
- , and Bristow, J.W. (1984). The Sabie river basalt formation of the Lebombo monocline and south-east Zimbabwe. *Spec.*

- Publ. geol. Soc. S. Afr.*, **13**, 125–147 (this volume).
- , Duncan, A.R., Bristow, J.W., Taylor, S.R., and Erlank, A.J. (1984). Petrogenesis of the basic rocks of the Lebombo. *Spec. Publ. geol. Soc. S. Afr.*, **13**, 149–169 (this volume).
- Dalziel, I.W.D. (1981). Back-arc extension in the southern Andes: a review and critical appraisal. *Phil. Trans. R. Soc. Lond.*, **A300**, 319–335.
- De Beer, J.H., Van Zijl, J.S.V., and Gough, D.I. (1982). The southern Cape conductive belt (South Africa): its composition, origin and tectonic significance. *Tectonophysics*, **83**, 205–225.
- DePaolo, D.J. (1981). Trace element and isotopic effects of combined wallrock assimilation and fractional crystallization. *Earth Planet. Sci. Lett.*, **53**, 189–202.
- Dooley, R.E., and Wampler, J.M. (1978). Low temperature release of excess ^{40}Ar from Georgia Dolerites. *U.S. geol. Surv. Open File Rep.*, **78-701**, 94–96.
- Duncan, A.R., Erlank, A.J., and Marsh, J.S. (1984). Regional geochemistry of the Karoo igneous province. *Spec. Publ. geol. Soc. S. Afr.*, **13**, 355–388 (this volume).
- Duncan, R.A. (1981). Hotspots in the southern oceans—an absolute frame of reference for motion of the Gondwana continents. *Tectonophysics*, **74**, 29–42.
- Dupré, B., and Allègre, C.J. (1980). Pb–Sr–Nd isotopic correlation and the chemistry of the North Atlantic mantle. *Nature*, **286**, 17–22.
- Du Toit, A.L. (1937). *Our wandering continents*. Oliver and Boyd, Edinburgh, 366 pp.
- Eales, H.V., and Marsh, J.S. (1984). The Karoo igneous province: an introduction. *Spec. Publ. geol. Soc. S. Afr.*, **13**, 1–26 (this volume).
- Erlank, A.J. (1971). *Studies of the distribution of potassium and some geochemically related elements*. Ph.D. thesis (unpubl.), Univ. Cape Town, 190 pp.
- , Allsopp, H.L., Duncan, A.R., and Bristow, J.W. (1980). Mantle heterogeneity beneath southern Africa: evidence from the volcanic record. *Phil. Trans. R. Soc. Lond.*, **A297**, 295–307.
- , ---, Hawkesworth, C.J., and Menzies, M.A. (1982). Chemical and isotopic characterization of upper mantle metasomatism in peridotite nodules from the Bultfontein kimberlite. *Terra Cognita*, **2**, 261–263.
- , and Kable, E.J.D. (1976). The significance of incompatible elements in mid-Atlantic ridge basalts from 45°N with particular reference to Zr/Nb. *Contr. Miner. Petrol.*, **54**, 281–291.
- , and Shimizu, N. (1977). Strontium and strontium isotope distributions in some kimberlite nodules and minerals. *Extnd. Abstr., Second Int. Kimberlite Conf., New Mexico, USA*.
- Faure, G., Bowman, J.R., Elliot, D.H., and Jones, L.M. (1974). Sr-isotope composition and petrogenesis of the Kirkpatrick basalts, Queen Alexandra Range, Antarctica. *Contr. Miner. Petrol.*, **48**, 153–159.
- Fitch, F.J., and Miller, J.A. (1971). Potassium-argon radioages of Karoo volcanic rocks from Lesotho. *Bull. volcan.*, **35**, 64–84.
- , and --- (1984). Dating Karoo igneous rocks by the conventional K–Ar and $^{40}\text{Ar}/^{39}\text{Ar}$ age spectrum methods. *Spec. Publ. geol. Soc. S. Afr.*, **13**, 247–266 (this volume).
- Fitton, J.G. (1983). Active versus passive continental rifting: evidence from the west African Rift System. *Tectonophysics*, **94**, 473–481.
- Frets, D.C. (1969). *Geology and structure of the Huab–Welwitschia area, South West Africa*. Precambrian Res. Unit, Bull. 5, Univ. Cape Town, 235 pp.
- Gidskehaug, A. (1975). *Analytical methods in rock magnetism and palaeomagnetism and their applications to Mesozoic igneous rocks from South West Africa*. Ph.D. thesis (unpubl.), Geophys. Inst., Univ. Bergen, 142 pp.
- , Creer, K.M., and Mitchell, J.G. (1975). Palaeomagnetism and K–Ar ages of the South-West African basalts and their bearing on the time of initial rifting of the South Atlantic Ocean. *Geophys. J. R. astr. Soc.*, **42**, 1–20.
- Girdler, R.W. (1983). Processes of planetary rifting as seen in the rifting and breakup of Africa. *Tectonophysics*, **94**, 241–252.
- Haack, U., Hoefs, J., and Gohn, E. (1982). Constraints on the origin of Damaran granites by Rb/Sr and $\delta^{18}\text{O}$ data. *Contr. Miner. Petrol.*, **79**, 279–289.
- Haggerty, S.E., Smyth, J.R., Erlank, A.J., Rickard, R.S., and Danchin, R.V. (1983). Lindsleyite (Ba) and mathiasite (K): Two new chromium titanates in the crichtonite series from the upper mantle. *Am. Miner.*, **68**, 494–505.
- Harland, W.B., Cox, A., Llewellyn, P.G., Pickton, C.A.G., Smith, A.G., and Walters, R. (1982). *A geologic time scale*. Cambridge Univ. Press, Cambridge, 131 pp.
- Hawkesworth, C.J., Gledhill, A.R., Roddick, J.C., Miller, R.McG., and Kröner, A. (1983). Rb–Sr and $^{40}\text{Ar}/^{39}\text{Ar}$ studies bearing on models for the thermal evolution of the Damara belt, Namibia. *Spec. Publ. geol. Soc. S. Afr.*, **11**, 323–338.
- , Kramers, J.D., and Miller, R.McG. (1981). Old model Nd ages in Namibian Pan-African rocks. *Nature*, **289**, 278–282.
- , Marsh, J.S., Duncan, A.R., Erlank, A.J., and Norry, M.J. (1984). The role of continental lithosphere in the generation of the Karoo volcanic rocks: evidence from combined Nd- and Sr-isotope studies. *Spec. Publ. geol. Soc. S. Afr.*, **13**, 341–354 (this volume).
- Hildreth, W. (1981). Gradients in silicic magma chambers: implications for lithospheric magmatism. *J. geophys. Res.*, **86**, 10153–10192.
- Hodgson, F.D.I., and Botha, B.J.V. (1975). Notes on the Cretaceous Volcanism in the area north-west of the Doros Complex, South West Africa. *Ann. geol. Surv. Dep. Min. S. Afr.*, **11**, 135–136.
- Hoefs, J., Faure, G., and Elliot, D.H. (1980). Correlation of $\delta^{18}\text{O}$ -initial $^{87}\text{Sr}/^{86}\text{Sr}$ ratios in Kirkpatrick basalts on Mt. Falla, Transantarctic Mountain. *Contr. Miner. Petrol.*, **75**, 199–204.
- Hofmann, A.W., and White, W.M. (1982). Mantle plumes from ancient oceanic crust. *Earth Planet. Sci. Lett.*, **57**, 421–436.
- Iddings, J.P. (1913). *Igneous Rocks* Vol. II. John Wiley and Sons, New York, 685 pp.
- Johannsen, A.J. (1937). *A descriptive petrography of the Igneous Rocks*. Vol. III, Univ. Chicago Press, Chicago, 360 pp.
- Keen, C.E., and Barrett, D.L. (1981). Thinned and subsided continental crust on the rifted margin of eastern Canada: crustal structure, thermal evolution and subsidence history. *Geophys. J. R. astr. Soc.*, **65**, 443–465.
- Korn, H., and Martin, H. (1954). The Messum Igneous Complex in South West Africa. *Trans. geol. Soc. S. Afr.*, **57**, 83–124.
- Kouchi, A., and Sunagawa, I. (1983). Mixing basaltic and dacitic magmas by forced correction. *Nature*, **304**, 527–528.
- Kramers, J.D. (1977). Lead and strontium isotopes in Cretaceous kimberlites and mantle derived xenoliths from southern Africa. *Earth Planet. Sci. Lett.*, **34**, 419–431.
- Kröner, A., Halpern, M., and Jacob, R.E. (1978). Rb–Sr geochronology in favour of polymetamorphism in the Pan African Damara belt of Namibia (South West Africa). *Geol. Rdsch.*, **67**, 688–705.
- Kyle, P.R., Pankhurst, R.J., and Bowman, J.R. (1983). Isotopic and chemical variations in Kirkpatrick Basalt Group rocks from south Victoria Land, 234–237. In: Oliver, R.L., James, P.R., and Jago, J.B., Eds., *Antarctic Earth Science*. Australian Acad. Science, Canberra, 697 pp.
- Langmuir, C.J., Vocke, R.D., Hanson, G.N., and Hart, S.R. (1978). A general mixing equation with applications to Icelandic basalts. *Earth Planet. Sci. Lett.*, **37**, 380–392.
- Lanphere, M.A., and Dalrymple, G.B. (1977). Identification of excess $^{40}\text{Ar}/^{39}\text{Ar}$ age spectra technique. *Earth Planet. Sci. Lett.*, **32**, 141–148.
- Le Pichon, X., Angelier, J., and Sibuet, J.-C. (1982). Plate boundaries and extensional tectonics. *Tectonophysics*, **81**, 239–256.
- Le Roex, A.P. (1980). *Geochemistry and mineralogy of Selected Atlantic Ocean Basalts*. Ph.D. thesis (unpubl.), Univ. Cape Town, 281 pp.
- , Dick, H.J.B., Erlank, A.J., Reid, A.M., Frey, F.A., and Hart, S.R. (1983). Geochemistry, mineralogy and petrogenesis of lavas erupted along the southwest Indian ridge between the Bouvet triple junction and 11 degrees east. *J. Petrology*, **24**, 267–318.
- , ---, Reid, A.M., and Erlank, A.J. (1982). Ferrobasalts from the Spiess Ridge segment of the South-West Indian Ridge. *Earth Planet. Sci. Lett.*, **60**, 437–451.
- , Erlank, A.J., and Needham, H.D. (1981). Geochemical and mineralogical evidence for the occurrence of at least three distinct magma types in the “Famous” region. *Contr. Miner. Petrol.*, **77**, 24–37.
- Lowrie, W. (1982). A revised magnetic polarity timescale for the Cretaceous and Cainozoic. *Phil. Trans. R. Soc. Lond.*, **A306**, 129–136.
- MacKenzie, D.E., and Chappell, B.W. (1972). Shoshonitic and calc-alkaline lavas from the highlands of Papua New Guinea. *Contr. Miner. Petrol.*, **35**, 50–62.
- Mahoney, J., MacDougall, J.D., Lugmair, G.W., Murali, A.V.,

- Sankar Das, M., and Goplan, K. (1982). Origin of the Deccan Trap flows at Mahabaleshwar inferred from Nd and Sr isotopic and chemical evidence. *Earth Planet. Sci. Lett.*, **60**, 47–60.
- Manton, W.I., and Siedner, G. (1967). Age of the Paresis Complex, South West Africa. *Nature*, **216**, 1197–1198.
- Marsh, J.S., and Eales, H.V. (1984). The chemistry and petrogenesis of igneous rocks of the Karoo central area, Southern Africa. *Spec. Publ. geol. Soc. S. Afr.*, **13**, 27–67 (this volume).
- Martin, H. (1961). The hypothesis of continental drift in the light of recent advances of geological knowledge in Brazil and in South West Africa. *Du Toit mem. Lect. No. 7, Annex. to Trans. geol. Soc. S. Afr.*, **64**, 1–47.
- (1975). Structural and palaeogeographical evidence for an upper Palaeozoic sea between southern Africa and South America, 37–51. In: Campbell, K.S.W., Ed., *Gondwana Geology*. Australian National Univ. Press, Canberra, 705 pp.
- , Mathias, M., and Simpson, E.S.W. (1960). The Damaraland sub-volcanic ring complexes in South West Africa. *Rep. Int. geol. cong. XXI Sess.*, **13**, 156–174.
- McDougall, I. (1963). Potassium-Argon age measurements on dolerites from Antarctica and South Africa. *J. geophys. Res.*, **68**, 1535–1545.
- Melfi, A.J. (1967). Potassium-Argon ages for core samples of basaltic rocks from southern Brazil. *Geochim. cosmochim. Acta*, **31**, 1079–1089.
- Mensing, T.M., Faure, G., Jones, L.M., Bowman, J.R., and Hoefs, J. (1984). Petrogenesis of the Kirkpatrick Basalt, Solo Nunatak, Northern Victoria Land, Antarctica, based on isotopic compositions of strontium, oxygen and sulfur. *Contr. Miner. Petrol.*, **87**, 101–108.
- Menzies, M., and Rama Murthy, V. (1980). Enriched mantle: Nd and Sr isotopes in diopsides from kimberlite nodules. *Nature*, **283**, 634–636.
- Miller, R.McG. (1973). Geological map of sheet 2013, Cape Cross. *Geol. Surv. S. Afr.* (unpubl.).
- (1983). The Pan-African Damara Orogen of South West Africa/Namibia. *Spec. Publ. geol. Soc. S. Afr.*, **11**, 431–515.
- Moorbath, S., and Thompson, R.N. (1980). Strontium isotope geochemistry and petrogenesis of the early Tertiary lava pile of the Isle of Skye, Scotland, and other basic rocks of the British Tertiary Province: an example of magma-crust interaction. *J. Petrology*, **21**, 295–321.
- Morgan, P., and Baker, B.H. (1983). Introduction: processes of continental rifting. *Tectonophysics*, **94**, 1–10.
- Morgan, W.J. (1983). Hotspot tracks and the early rifting of the Atlantic. *Tectonophysics*, **94**, 123–139.
- Nathan, H.D., and Van Kirk, C.K. (1978). A model of magmatic crystallization. *J. Petrology*, **19**, 66–94.
- Nelson, D.O. (1983). Implications of oxygen isotope data and the trace-element modelling for a large scale mixing-model for the Columbia River Basalt. *Geology*, **2**, 248–251.
- Nicholls, J., and Stout, M.Z. (1982). Heat effects of assimilation, crystallization and vesiculation in magmas. *Contr. Miner. Petrol.*, **81**, 328–339.
- Nixon, P.H., Rogers, N.W., Gibson, I.L., and Grey, A. (1981). Depleted and fertile mantle xenoliths from southern African kimberlites. *Ann. Rev. Earth Planet. Sci. Lett.*, **9**, 285–309.
- Pearce, J.A. (1983). Role of the sub-continental lithosphere in magma genesis at active continental margins, 230–249. In: Hawkesworth, C.J., and Norry, M.J., Eds., *Continental basalts and mantle xenoliths*. Shiva, UK, 272 pp.
- , and Cann, J.R. (1973). Tectonic setting of basic volcanic rocks determined using trace element analyses. *Earth Planet. Sci. Lett.*, **19**, 290–300.
- Peccerillo, A., and Taylor, S.R. (1976). Geochemistry of Eocene calc-alkaline volcanic rocks from the Kastamonu area, northern Turkey. *Contr. Miner. Petrol.*, **58**, 63–81.
- Reid, D.L. (1977). *Geochemistry of Precambrian igneous rocks in the lower Orange River region*. Precambrian Res. Unit, Bull. 22, Univ. Cape Town, 394 pp.
- , and Erlank, A.J. (1979). Chemical characterization of a Precambrian mobile belt in southern Africa. *Abstr. IAVCEI-IUGG XVII Gen. Ass.*, Canberra, Australia.
- Reuning, E. (1929). Differentiation der Karoo-Eruptiva im südlichen Kaokofeld, Südwestafrika. *Cmpte Rendu, Int. Geol. Congr.*, Vol. II, **15**, 28–35.
- , and Martin, H. (1957). Die Par-Karoo-Landschaft, die Karoo-sedimente und Karoo-Eruptivgesteine des südlichen Kaokofeldes im Südwestafrika. *Neues Jb. Miner. Geol. Palaont.*, **91**, 193–212.
- Richardson, S.H. (1979). Chemical variation induced by flow differentiation in an extensive Karoo dolerite sheet, southern Namibia. *Geochim. cosmochim. Acta*, **43**, 1433–1441.
- (1984). Sr, Nd and O isotope variation in an extensive Karoo dolerite sheet, Southern Namibia. *Spec. Publ. geol. Soc. S. Afr.*, **13**, 289–293 (this volume).
- , Erlank, A.J., Duncan, A.R., and Reid, D.L. (1982). Correlated Nd, Sr and Pb isotope variation in the Walvis Ridge basalts and implications for the evolution of their mantle source. *Earth Planet. Sci. Lett.*, **59**, 327–342.
- , Gurney, J.J., Erlank, A.J., Harris, J.W. (1984). Origin of diamonds in old enriched mantle. *Nature*, **310**, 198–202.
- Roddick, J.C., Cliff, R.A., and Rex, D.C. (1980). The evaluation of excess argon in Alpine biotites — A ⁴⁰Ar/³⁹Ar analysis. *Earth Planet. Sci. Lett.*, **48**, 185–208.
- Roeder, P.L., and Emslie, R.F. (1970). Olivine-liquid equilibrium. *Contr. Miner. Petrol.*, **29**, 275–289.
- Rogers, N.W. (1979). *Trace element analysis of kimberlites and associated rocks and xenoliths*. Ph.D. thesis (unpubl.), Univ. Lond., 266 pp.
- , and Hawkesworth, C.J. (1982). Proterozoic age and cumulate origin for granulite xenoliths, Lesotho. *Nature*, **299**, 409–413.
- Ruegg, N.R. (1976). Características de distribuicao e teor de elementos principais em Rochas basálticas de Bacia do Paraná. *Boletim IG. Instituto de Geociencias U.S.P.*, **7**, 81–106.
- , and Amaral, G. (1976). Variacao regional da composicao quimica das rochas basálticas da bacia do Paraná. *Boletim IG. Instituto de Geociencias U.S.P.*, **7**, 131–147.
- Shimizu, N. (1983). Interface Kinetics and Trace Element distribution between phenocrysts and magma, 175–195. In: Augustithus, A.A., Ed., *The Significance of Trace Elements in solving petrographic problems and controversies*. Theophrastus Publ., Greece, 910 pp.
- Siedner, G., and Miller, J.A. (1968). K–Ar age determination on basaltic rocks from South West Africa, and their bearing on continental drift. *Earth Planet. Sci. Lett.*, **4**, 451–458.
- , and Mitchell, J.G. (1976). Episodic Mesozoic volcanism in Namibia and Brazil: A K–Ar isochron study bearing on the opening of the South Atlantic. *Earth Planet. Sci. Lett.*, **30**, 292–302.
- South African Committee for Stratigraphy (SACS) (1980). *Stratigraphy of South Africa. Part 1 (comp. L.E. Kent). Lithostratigraphy of the Republic of South Africa, South West Africa/Namibia, and the Republics of Bophuthatswana, Transkei and Venda. Handbk. geol. Surv. S. Afr.*, **8**, 690 pp.
- Steiger, R.H., and Jäger, E. (1977). Subcommission on geochronology: convention on the use of decay constants in geo- and cosmochronology. *Earth Planet. Sci. Lett.*, **36**, 359–362.
- Sun, S.-S. (1980). Lead isotope study of young volcanic rocks from mid-ocean ridges, ocean islands and island arcs. *Phil. Trans. R. Soc. Lond.*, **A297**, 409–445.
- , and Hanson, G.N. (1975). Origin of Ross Island basanitoids and limitations upon the heterogeneity of mantle sources for alkali basalts and nephelinites. *Contr. Miner. Petrol.*, **52**, 77–106.
- Tatsumoto, M. (1978). Isotopic composition of lead in oceanic basalt and its implications to mantle evolution. *Earth Planet. Sci. Lett.*, **38**, 63–87.
- Taylor, H.P. (1980). The effects of assimilation of country rocks by magmas on ¹⁸O/¹⁶O and ⁸⁷Sr/⁸⁶Sr systematics in igneous rocks. *Earth Planet. Sci. Lett.*, **47**, 243–254.
- Taylor, S.R. (1964). Abundance of chemical elements in the continental crust: a new table. *Geochim. cosmochim. Acta*, **28**, 1273–1286.
- Thompson, R.N., Dickin, A.P., Gibson, I.L., and Morrison, M.A. (1982). Elemental fingerprints of isotopic contamination of Hebridean Palaeocene mantle-derived magmas by Archaean sial. *Contr. Miner. Petrol.*, **79**, 159–168.
- , Morrison, M.A., Dickin, A.P., and Hendry, G.L. (1983). Continental flood basalts . . . Arachnids Rule OK?, 158–185. In: Hawkesworth, C.J., and Norry, M.J., Eds., *Continental basalt and mantle xenoliths*. Shiva, UK, 272 pp.
- Turcotte, D.L., and Emmerman, S.H. (1983). Mechanisms of active and passive rifting. *Tectonophysics*, **94**, 39–50.
- Ulbrich, H.H.G.J., and Gomes, C.B. (1981). Alkaline rocks from continental Brazil. *Earth Sci. Rev.*, **17**, 135–154.

- Van Zyl, J.S.V., and De Beer, J.H. (1983). Electrical structure of the Damara Orogen and its tectonic significance. *Spec. Publ. geol. Soc. S. Afr.*, **11**, 369–379.
- Weaver, B.L., and Tarney, J. (1984). Major and trace element compositions of the continental lithosphere. *Phys. Chem. Earth*, **15**, 39–68.
- White, W.M., and Hofmann, A.W. (1982). Sr and Nd isotope geochemistry of oceanic basalts and mantle evolution. *Nature*, **296**, 821–825.
- A.J. Erlank and A.R. Duncan,
Department of Geochemistry,
University of Cape Town,
7700 Rondebosch,
South Africa.
- J.S. Marsh,
Department of Geology,
Rhodes University,
6140 Grahamstown,
South Africa.
- R.McG. Miller,
Geological Survey,
P.O. Box 2168,
9000 Windhoek,
SWA/Namibia.
- C.J. Hawkesworth,
Department of Earth Sciences,
The Open University,
Milton Keynes MK7 6AA,
UK.
- P.J. Betton,*
Department of Geology,
University of Cape Town,
7700 Rondebosch,
South Africa.
- D.C. Rex,
Department of Earth Sciences,
The University,
Leeds LS2 9JT,
UK.

*Deceased